Organocatalytic Synthesis of End-functionalized Poly(methyl methacrylate)s Using Group Transfer Polymerization

A Dissertation for the Degree of Doctor of Philosophy

ERIC OFOSU-TWUM

Hokkaido University

September, 2017

Acknowledgement

The study presented in this dissertation has been carried out under the direction of Prof. T. Kakuchi, Assoc. Prof. S. Sato, Assoc. Prof. T. Yamamoto and Assist. Prof. Y.-G. Chen, Division of Biotechnology and Macromolecular Chemistry, Faculty of Engineering, Hokkaido University, during the period of October 2014 – September 2017.

The author wishes to express his profound gratitude to the Almighty God for giving him this great opportunity and life to be able to carry out this study. The author also wishes to express his sincere appreciation to Prof. T. Kakuchi for his kind instruction during the course of this work.

The author is deeply grateful to Assoc. Prof. S. Sato and Assoc. Prof. T. Yamamoto for their helpful suggestions throughout this work. The author is also deeply indebted to Assist. Prof. Y.-G. Chen for his practical guidance and valuable contributions to this work. The author is also very grateful to Prof. T. Satoh for his helpful advice and instruction.

The author enjoyed working with colleagues because the friendship and good humor of the members in the laboratory created a pleasant and stimulating environment in which to do this work. The author thanks all members and ex-members of Prof. Kakuchi's group, Assoc. Prof. Sato's group and Assoc. Prof Yamamoto`s group; Messrs. K. Takada, Y. Takagi, S. Tsuchida, T. Ito, K. Kitano, M. Jin, K. Miyachi, J. Quinsaat, S. Kikuchi, E. Ichinohe, T. Satoh, S. Mizutani, M. Hosokawa, S. Yoshino, M. Nakamura and Y. Miyata.

Finally, the author wishes to express his deepest gratitude to his family. He owes the achievement of this study to their support and encouragement throughout his study in Japan

September, 2017 *Ofosu-Twum Eric*

Contents

Chapter 1

General Introduction

1.1 Organocatalysts

1.1.1 Introduction of Organocatalysts

An organocatalyst is referred as an organic compound that functions as a metal-free catalyst to promote an organic reaction. An organocatalyst is defined as an organic compound consisting of non-metallic elements, such as carbon, hydrogen, nitrogen, phosphorus, and sulfur, having catalytic activity. The concept of organocatalysis was proposed by MacMillan et al. in 2000 when they reported the metal-free and enantioselective Diels–Alder reaction using an imidazolidinone derivative as the catalyst.[1] List et al. reported a metal-free and asymmetric aldol reaction catalyzed by L-proline in the same year.[2] Organocatalysts are considered to have the following advantages in comparison to conventional organometallics catalysts; (1) higher tolerance toward moisture and oxygen; (2) more tunable catalytic activity by changing the catalyst structure; (3) lower toxicity; and (4) easier immobilization onto carriers, such as polymer substrates. Thus, organocatalysts are being considered as a promising replacement for metallic catalysts. Organocatalysts have been recognized as third generation catalysts following enzymes and transition metal catalysts. Since their emergence, the field of organocatalysis has undergone rapid growth through the development of the following reactions: the alkylation reaction using the Maruoka catalyst,[3] the Mannich reaction catalyzed by proline derivatives,[4,5] the Friedel–Crafts reaction catalyzed by chiral phosphoric acid,[6] the Mukaiyama aldol reaction catalyzed by oxazaborolidinone,[7] etc.

Generally organocatalysts can be classified into two categories, Lewis base catalysts and Lewis acid catalysts, according to their interaction with an electron pair. However recently, List et al. introduced a system of classification of most organocatalysts into four

categories, namely, Lewis bases, Lewis acids, Brønsted bases, and Brønsted acids, based on the mechanism of the catalysis.[8]

1.1.2 Organocatalysts for Polymer Chemistry

Just after the proposal of organocatalysis, Hedrick et al. introduced the concept into polymer synthesis and reported the controlled ring-opening polymerization (ROP) of L-lactide catalyzed by 4-dimethylaminopyridine, which produced a breakthrough in polymer chemistry.[9] Organocatalytic polymerization has not only emerged as a promising alternative of organometalcatalyzed polymerizations, but also refined conventional polymerization methods.[10,11] Although most of the effort on organocatalytic polymerization has been devoted only to ROP, Taton and Gnanou et al. and Waymouth et al. reported in 2007–2008 that *N*-heterocyclic carbene (NHC), one of the organocatalysts, is capable of efficiently catalyzing the GTP of both MMA and *tert*-butyl acrylate in a controlled/living fashion.[12,13]

Although many organocatalysts had been used in the ROPs of cyclic monomers in the past decade, the applications of organocatalysts in other polymerization systems such as the polymerizations of vinyl monomers have been rarely reported. Thus, the development of novel polymerization systems using organocatalysts is of significant importance. In this thesis, the establishment of an effective organocatalyzed group transfer polymerization (GTP) synthesis of end-functionalized poly(methyl methacrylate)s (a type of vinyl monomer) is the objective of the author.

1.2. Group Transfer Polymerization (GTP)

1.2.1 Introduction of Group Transfer Polymerization

Group transfer polymerization (GTP), one of the important living polymerization methods, was for the first time proposed in 1983. The GTP of an acrylic monomer proceeds through numerous iterations of the Mukaiyama-Michael featuring a recombination-free nature reaction between the propagating polymer chain end and the monomer in polymerization system.[14] It uses a silyl enolate as the initiator and a Lewis base or acid as the catalyst (Scheme 1.3). It was initially proposed that the trialkylsilyl group transferred to the coming monomer when it added to the polymer chain ends, which was thus the name "group transfer polymerization" though it has since been shown not to be comprehensive according to the studies for the GTP mechanisms. The relatively mature associative and dissociative mechanisms for GTP were proposed by Webster et al.,[15] Müller et al.,[16] Seebach et al.,[17] and Quirk et al.[18] The GTPs of (meth)acrylates can be carried out at room temperature or above, which is the main reason why the DuPont company developed this polymerization process to reduce the high cost of low-temperature devices used in the anionic polymerization of (meth)acrylates. The GTP method enables the polymerization of (meth)acrylates with an excellent control over the molecular weights and polydispersities. The living nature of GTP not only allows the syntheses of linear homopolymers, but is also applicable for preparing complicated macromolecular architectures, such as block copolymers, hyperbranched and star-shaped polymers.

Scheme 1.1 A general illustration of group transfer polymerization

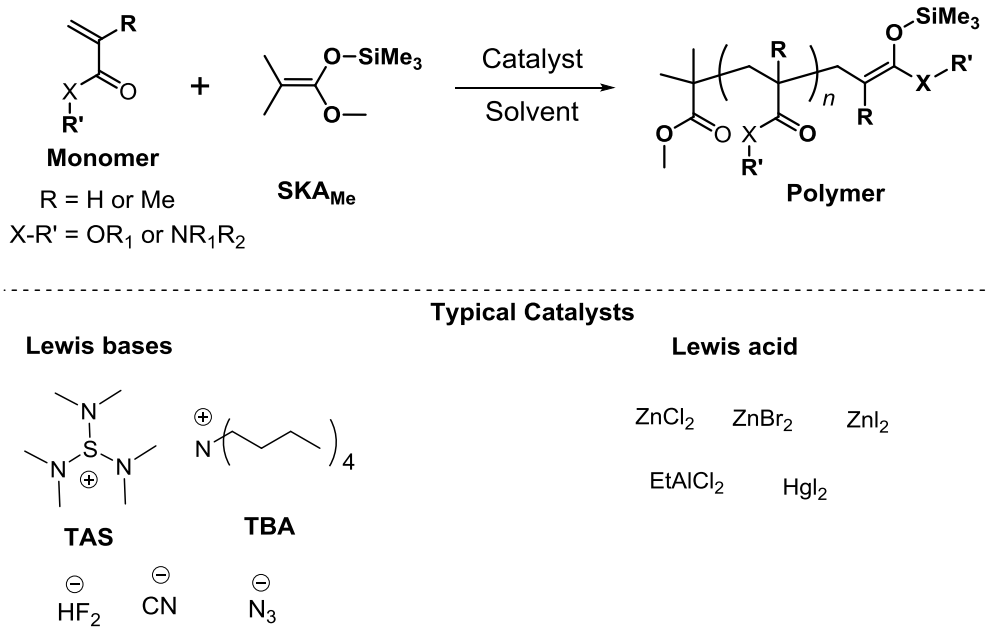

1.2.2 Organocatalysts for Group Transfer Polymerization

The application of organocatalysis in GTP has demonstrated an organocatalytic vinyl polymerization. Besides, organocatalysts have been found to work as versatile catalysts for GTP beyond the limitations of conventional GTP in terms of catalytic activity, polymerizable monomers, molecular weight control, and polymer structures that can be synthesized. Following are the Lewis base and Lewis acid organocatalysts already employed in GTP: NHCs, organic strong bases, phosphines, tris(pentafluorophenyl)borane ($B(C_6F_5)_3$) with a silylating agent, triphenylmethyl salts, and organic strong Brønsted acids. Scheme 1.1 summarizes the catalysts that have been employed so far and the monomers that have been polymerized in a controlled/living fashion by the GTP using the Lewis base organocatalysts. The employed catalysts are electronically neutral and much less nucleophilic than the conventional Lewis base

catalysts, thus suppressing side-reactions between the catalysts and a monomer or a solvent to increase the livingness of the polymerization. In particular, NHCs were revealed to be capable of efficiently catalyzing the GTPs of alkyl acrylates, *N*,*N*-dimethylacrylamide (DMAA), and methacrylonitrile (MAN) in addition to alkyl methacrylates, though conventional Lewis base catalysts were only suitable for the polymerization of methacrylates. The Lewis base organocatalysts are regularly used at a ratio of ca. 0.5–20 mol% relative to the initiator used to obtain polymers with polydispersity index (M_w/M_n) narrower than 1.20.[19]

Scheme 1.2 Catalysts and monomers employed in the GTP using Lewis base organocatalysts.

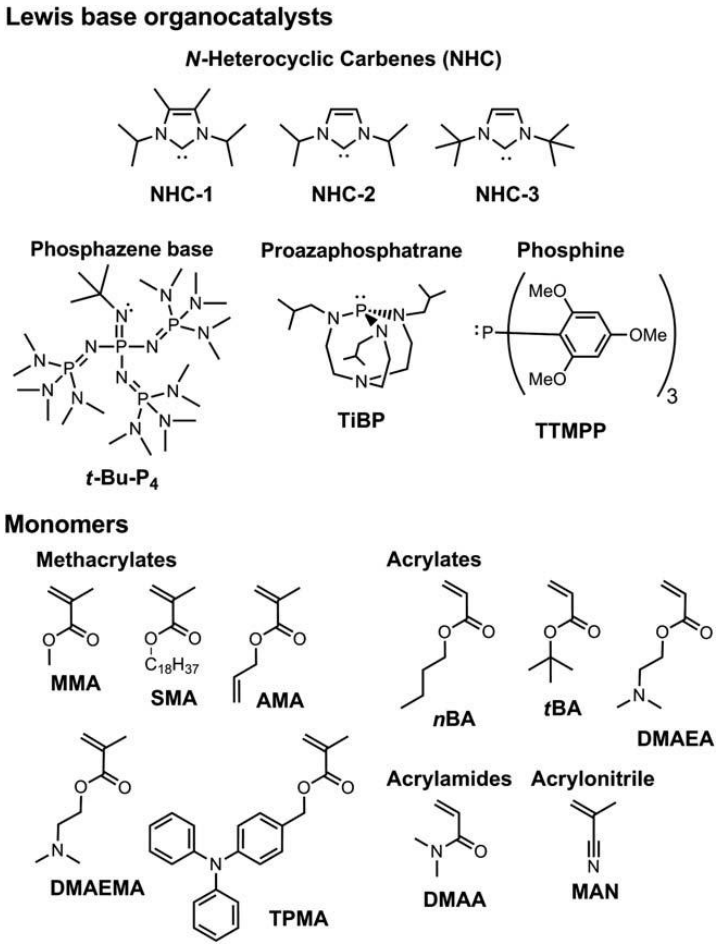

Lewis-acid-catalyzed GTP is considered to proceed with the activation of a monomer by the Lewis acid. Conventional Lewis acid catalysts, such as zinc halides and alkyl aluminums, are only suitable for the polymerization of acrylates because of their low catalytic activity, i.e., weak Lewis acidity. 10–20 mol% of the Lewis acids based on the amount of the monomer was required for the controlled polymerization.[20] However, the emergence of highly Lewis acidic non-metallic catalysts has broken this limitation of conventional Lewis-acid-catalyzed GTPs. Scheme 1.2 summarizes the monomers, initiators, and (pre)catalysts used in the GTP catalyzed by Lewis acid organocatalysts.

The GTPs of alkyl methacrylates, DMAA, α-methylenebutyrolactone (MBL), and γ-methyl-α-methylenebutyrolactone (MMBL), have been newly achieved with the Lewis acid organocatalysts, such as tris-(pentafluorophenyl)borane ($B(C_6F_5)_3$) with a silylating agent, triphenylmethyl salts, and strong organic Brønsted acids. The Lewis acid organocatalysts are regularly used at a ratio of ca. 1–50 mol% relative to the initiator used to obtain polymers with M_w/M_n narrower than 1.15.

The potential of organic strong bases, which have a low nucleophilicity and high basicity has also been investigated.[21] The following bases were employed in the GTP of MMA using 1-methoxy-1-(trimethylsiloxy)-2-methylprop-1-ene (SKA_{Me}) in THF or toluene at 25 °C: 1,8-diazabicyclo[5.4.0]undec-7-ene (DBU); proazaphosphatrane bases, i.e., 2,8,9-trimethyl-2,5,8,9-tetraaza-1-phosphabicyclo[3.3.3]undecane (TMP) and 2,8,9-triisobutyl-2,5,8,9-tetraaza-1-phosphabicyclo[3.3.3]undecane (TiBP); phosphazene bases, i.e., 1-*tert*-butyl-2,2,4,4,4-pentakis(dimethylamino)-2Λ^5, 4Λ^5-catenadi(phosphazene) (*t*-Bu-P_2), and 1-*tert*-butyl-4,4,4-tris(dimethylamino)-2,2-bis[tris(dimethylamino)-phosphoranylidenamino]- 2Λ^5, 4Λ^5-catenadi(phosphazene) (*t*-Bu-P_4). The polymerization

using TiBP or *t*-Bu-P_4 rapidly proceeded with a small amount of catalyst (1 mol% relative to the initiator), which afforded PMMA with M_n of 6.5–55.9 kg mol^{-1} and 6.5–109.6 kg mol^{-1} while the narrow M_w/M_n is retained in the range of 1.05–1.14 and 1.15–1.32. Importantly, the *t*-Bu-P_4-catalyzed GTP also afforded PMMAs with M_n values of greater than 100 kg mol^{-1}.

Scheme 1.3 Catalysts, monomers, and initiators employed in GTP catalyzed by Lewis acid organocatalysts.

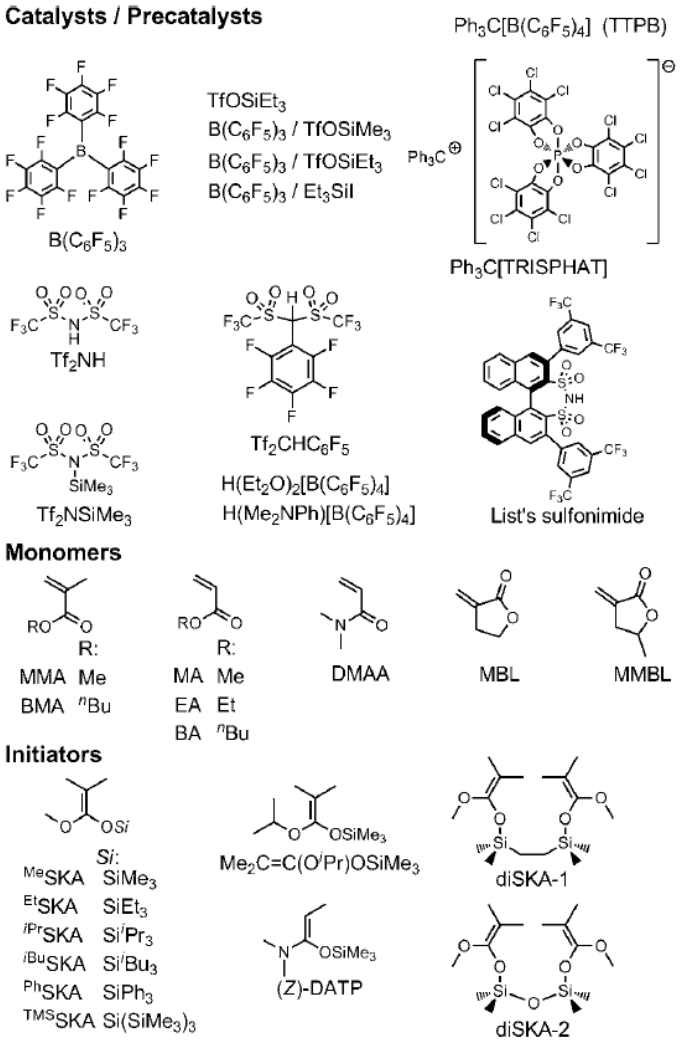

Brønsted acids have also been found to be effective for GTP. Kakuchi et al. first paid attention to the potential of strong Brønsted acids and applied them to the GTP.[22] In advance of the series of this study, Yamamoto et al. reported that trifluoromethanesulfonimide (Tf_2NH), one of the strong Brønsted acids, could efficiently promote the Mukaiyama aldol reaction of which the reaction mechanism is similar to the propagation reaction of GTP.[23,24] List et al. achieved the asymmetric Mukaiyama aldol reaction promoted by a chiral strong Brønsted acid, which showed high reactivity and high enantioselectivity.[25] In these reactions, a strong Brønsted acid was considered to first react with a silyl enolate to form a silicon Lewis acid as the actual catalyst with an extremely high Lewis acidity. The GTP of MMA was carried out using Tf_2NH and SKA_{Me} in CH_2Cl_2 at 27 °C under the condition of $[MMA]_0/[SKA_{Me}]_0/[Tf_2NH]_0$. 100/1/0.05 to produce PMMA with M_n of 13.5 kg mol^{-1} and M_w/M_n of 1.04 within 24 h.[17]

1.2.3 Brief history of organocatalysts usage in group transfer polymerization

In recent times, metal-free catalysts, known as organocatalysts, have received much attention for catalyzing GTP and have been widely developed because organocatalyzed-GTP can afford metal-free well-defined polymers. Taton et al. and Waymouth et al. first reported the *N*-heterocyclic carbene-catalyzed GTPs of MMA and *t*-butyl acrylate (*t*BA) using SKA_{Me}, which produced well-defined homopolymers and block copolymers with well-controlled molar mass and dispersities, as shown in Scheme 1.4.[12,26]

Scheme 1.4 The GTP of various monomers using *N*-heterocyclic carbene as a catalyst

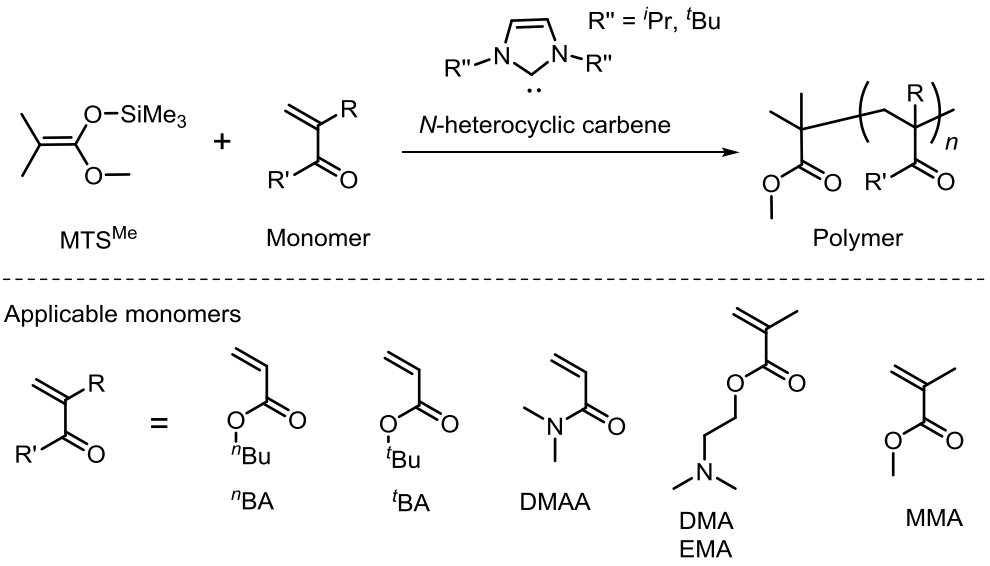

Kakuchi et al. have also been developing organocatalyzed GTP. We reported that the phosphazene base, 1-*tert*-butyl-4,4,4-tris(dimethylamino)-2,2-bis[tris(dimethylamino)-phosphoranylidenamino]-2Λ^5,4Λ^5-catenadi(phosphazene) (*t*-Bu-P_4), a very strong organic base, was extremely efficient for the syntheses of the PMMAs and 3-, 4-, and 6-armed star-shaped PMMAs, as shown Scheme 1.5.[27,28] We have particularly been endeavoring to develop organocatalyzed GTP using acid catalysts. For instance, we used trifluoromethanesulfonimide ($HNTf_2$), a highly strong Brønsted acid, to promote the GTP of MMA using SKA_{Me}, which proceeded in a living manner and afforded well-defined syndiotactic PMMAs without any obvious side reactions.[17] Furthermore, by designing suitable initiator for GTP of *N*,*N'*-dimethylacrylamide (DMAA) and GTP of methyl acrylate (MA) using highly strong Brønsted acid, poly(*N*,*N'*-dimethylacrylamide) (PDMAA) and poly(methyl acrylate) (PMA) with a low dispersity (M_w/M_n) could be readily synthesized, as shown in Scheme 1.5.[29]

Scheme 1.5 Organoacid catalyzed-GTP of MMA, MA, and DMAA using designed initiators

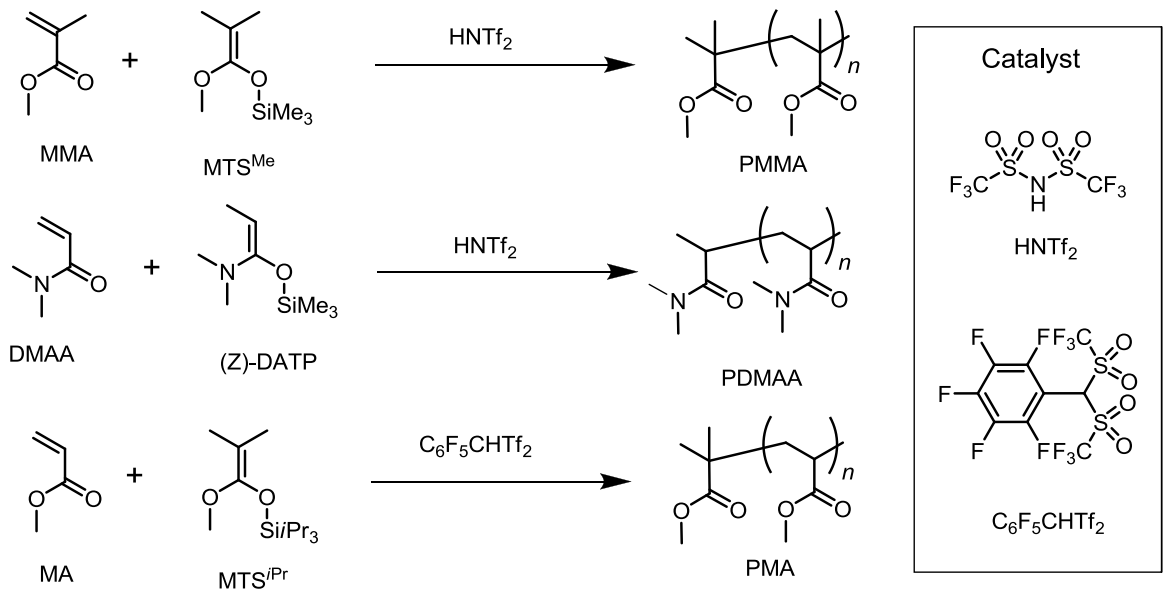

In addition to the afore discussed strong Brønsted acids, tris(pentafluorophenyl)borane ($B(C_6F_5)_3$), one of the organic Lewis acids with high acidity, is also employed as catalyst for the GTP because it catalyzes the Mukaiyama-Michael reaction that corresponds to the propagation reaction of the GTP. Indeed, Ute et al. preliminary reported the GTP of ethyl acrylate using 10 mol% of $B(C_6F_5)_3$ as the catalyst relative to 1-methoxy-1-triethylsiloxy-2-methyl-1-propene (SKA_{Et}) as the initiator, which produced poly(ethyl acrylate) with the number averaged molecular weight (M_n) of 7.5-12.6 kg mol^{-1} and the polydispersity (M_w/M_n) of 1.13-1.52. Recently, our group brushed up the $B(C_6F_5)_3$-catalyzed GTP of *n*BA and DEAA using SKA_{Et}, affording well-defined P*n*BA and PDEAA with narrow M_w/M_n (1.07), respectively (scheme 1.6).

Scheme 1.6 $B(C_6F_5)_3$-catalyzed GTP of *n*BA and DEAA using SKA^{Et} as an initiator

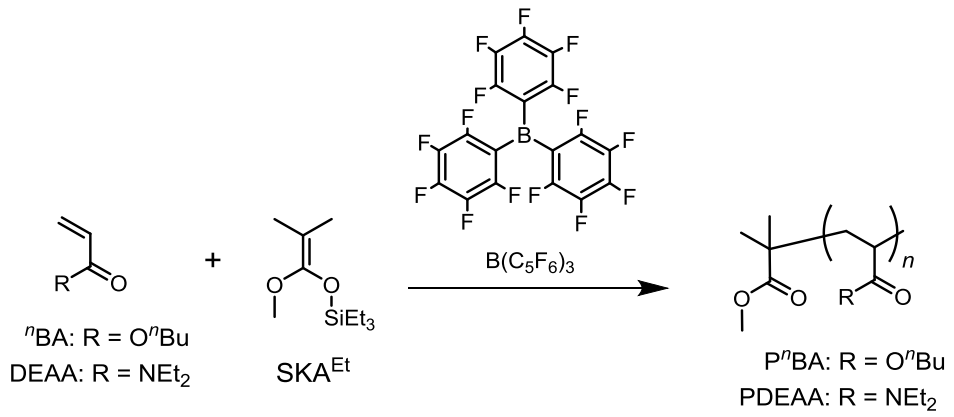

1.2.4 End-functionalization by group transfer polymerization

The synthesis of end functionalized polymers by controlled/living polymerization can be achieved using either functional initiators or terminators, or both. This study aims at the synthesis of end-functionalized poly(methyl methacrylate) (PMMA) by the organocatalyzed GTP method. During the GTP process, a silyl ketene acetal (SKA) group as the propagating end is one of the typical reactants for the Mukaiyama-Michael reaction with α,β-unsaturated ketones and the Mukaiyama aldol reaction with aldehydes. The α-end-functionalization by the GTP was reported using functional initiators that generally required the protection of the functional groups due to their high reactivity toward the SKA end groups of the polymers. For instance, α-end-functionalized poly(meth)acrylates with hydroxyl, carboxylic acid, cyanide,[30,31] alkylthio, triphenylphosphonium,[32,33] and phenol [34] groups were prepared by the GTP using appropriately protected initiators.

On the contrary, the ω-end-functionalization by the GTP has not been sufficiently realized even though various types of terminators have been examined. For example, Sogah et al.

synthesized end-functionalized PMMAs with the bromo and vinylphenyl groups by the termination reaction using bromine/*N*-bromosuccinimide and 4-(bromomethyl)styrene, respectively.[35-37] Webster et al. reported the synthesis of the ω-end-functionalized PMMAs with the Phosphonate group using diethyl vinylphosphonate and bis(trymethylilyl) vinylphosphonate as terminating agents.[38] Quirk et al. and Sivaram et al. reported the synthesis of the ω-end-functionalized PMMAs with the hydroxyl and amino groups using methyl-2-phenylpropenoate and benzaldehyde derivatives, respectively.[39,40] Nevertheless, these GTPs using conventional catalysts were hardly controlled to produce well defined polymers, resulting in the fact that their ω-end-functionalization efficiency turned out to be poor because these catalysts gives a low cyclic fraction due to back-biting reactions and needed to be improved. The recent utilization of organocatalysts for GTP has made significant progress in the improvement of the livingness of polymerization.[41-50] The living nature of organocatalyzed GTP is advantageous for ω-end-functionalization; for example, we recently reported the quantitative ω-end-functionalization of poly(*n*-butyl acrylate) and PMMA by organic Lewis acid-catalyzed GTP using α-phenyacrylate derivatives as the terminators.[47,48]

1.2.5 Star-shaped polymers by group transfer polymerization

The synthetic methodology of a star-shaped polymer dates back to the 1960s with the arm-first procedure based on the coupling reaction between the living polystyryllithium species and multifunctional linking reagents, such as 1,2,4-tris(chloromethyl)benzene and silicon tetrachloride.[51] Since the initial studies, anionic polymerization using the arm-first method has been used to prepare star-shaped polybutadiene,[52] polyisoprene,[53] and PMMA.[54] The core-first method utilizes the polymerization of the respective monomer(s) on a core formed from molecules having a well-defined number of initiating centers or a multifunctional core with branched and/or cross-linked structure. Although both synthesis methods provide excellent routes for the synthesis of star-shaped polymers, both synthesis methods have drawbacks. For example, for the arm-first method, severe reaction conditions and complex purification processes have been generally indispensable because it is difficult to achieve the complete coupling and linking reactions between the propagating polymers and multifunctional linking reagents. On the other hand, the core-first synthesis of star-shaped polymers using living radical polymerizations has essentially involved certain difficulties, such as the polymerization should be stopped at an earlier stage to avoid any radical recombination among propagating ends, which causes low monomer conversion.[55]

The living nature of GTP was used to prepare complicated macromolecular architectures, such as block copolymers,[56-68] a hyperbranched polymer,[69] and a star-shaped polymer, using a Lewis acid or base as a catalyst. For star-shaped polymers, Webster and Sogah first reported the core-first synthesis of three- and four-armed star-shaped poly(ethyl acrylate)s,[56] Wnek et al. reported the core-first synthesis of the four-armed star-shaped

PMMA,[70] and Patrickios et al. reported the arm-first synthesis of various star-shaped poly(methacrylate)s using a bifunctional monomer as a linking agent.[71-78] However, these star-shaped poly(methacrylate)s were insufficient for controlling the molecular weights and their distributions. Thus, the precise synthesis of star-shaped PMMAs still remains as a challenging task from the viewpoint of polymer science. Our group recently reported a preliminary result for the core-first synthesis of a three-armed star-shaped polymer by the *t*-Bu-P_4-catalyzed GTP of 4-(diphenylamino)benzyl methacrylate.[79] This study has ensured that the *t*-Bu-P_4-catalyzed GTP is applicable for the core-first synthesis of star-shaped poly(methacrylate)s. In this study, the author aims to describe the precisely synthesize star-shaped PMMAs with different arm numbers carrying hydroxyl functional groups by the GTP based on the core-first method as well as the arm-first method

Scheme 1.7 Synthesis of star-shaped PMMA by GTP using multi-functional initiators

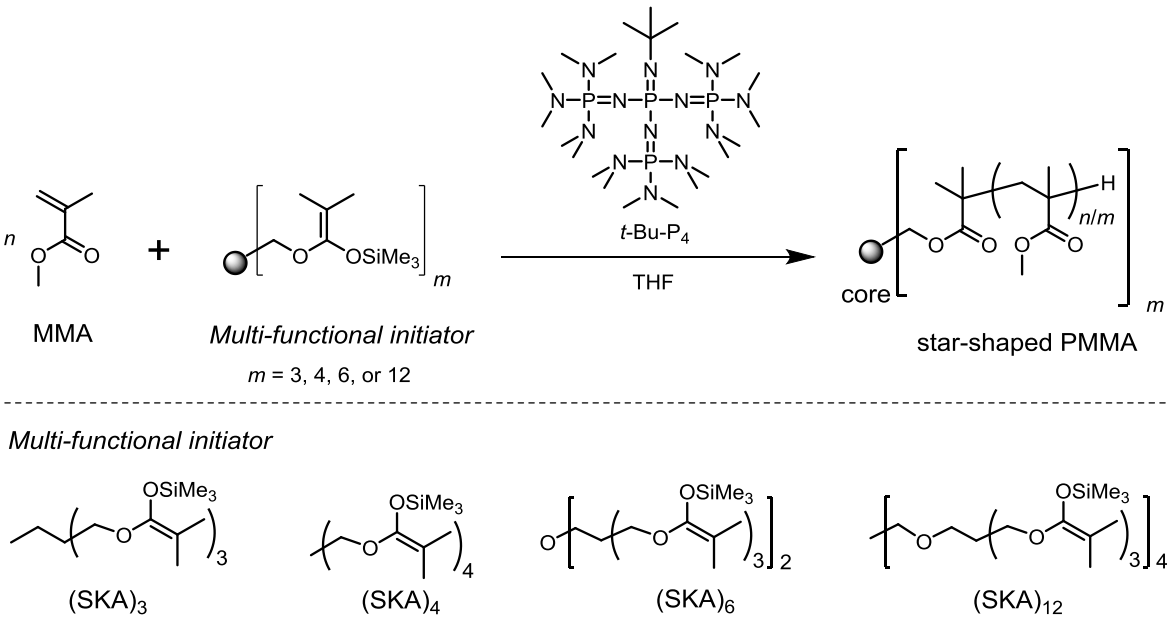

1.3 Poly(methyl methacrylate)

In this thesis, the author elucidates the synthesis method to modify PMMA through end-functionalization. It has been established that a polymer`s composition, molecular weight and architecture affects its physical properties. So it is aim of the author to investigate how end-functional groups affect the properties of PMMA. PMMA a kind of transparent thermoplastic, has been extensively used as an optical material with an extremely wide range of applications in everyday life, as shown in Figure 1.1 Generally, the molecular weight, its distribution, and the stereoregularity of main chain significantly affect the physical properties of the PMMA, such as transparency, mechanical strength, and glass transition temperature. In addition, well-defined macromolecular structures, such as graft, cyclic, dendritic, and star-shaped ones, are related to the respective properties, which differ from those of the linear polymers.[80] Thus, the stereospecific polymerization of methyl methacrylate (MMA) through living polymerization processes has been developed in order to construct well-defined PMMA architectures.

For the anionic polymerization of MMA, Fox et al. and Miller et al. were pioneers in reporting the preparation of stereoregular PMMAs in 1958.[81,82] Anderson et al. then reported the precise synthesis of a syndiotactic PMMA using alkyllithium in a polar solvent at a low temperature.[83] In contrast, Hatada et al. primarily reported the synthesis of an isotactic PMMA (*mm* > 95%) with a narrow molecular weight distribution by anionic polymerization using *tert*-butylmagnesium bromide prepared in diethyl ether,[84] and developed anionic catalyst systems by combining alkyllithium with bulky organoaluminum compounds.[85,86] For the radical polymerization, Okamoto et al. reported the stereospecific synthesis of PMMA by free-radical polymerizations using $Sc(OTf)_3$ or

fluoroalcohols at low temperature.[87–91] Matyjaszewski and coworkers revealed stereospecific systems, such as the reversible addition-fragmentation chain transfer polymerization and the copper(I)-catalyzed atom transfer radical polymerization (ATRP) of MMA.[92] Additionally, the simultaneous control of the molecular weight and tacticity of PMMA by the ATRP of MMA in a fluoroalcohol has been reported.[93] For coordination polymerization, Abe et al. reported that the polymerization of MMA using $TiCl_4/Al(CH_2CH_3)_3$ at low temperature produced a PMMA with the high syndiotacticity of *rr* >92%.[94] Yasuda et al. reported that organolanthanides were efficient for the stereospecific living polymerization of MMA at low temperature to afford a PMMA with *rr* >90%.[95–97] However, these stereospecific anionic, radical, and coordination polymerizations are limited to producing only linear stereospecific PMMA architectures.

For the synthesis of complex structures, such as stereospecific star-shaped PMMAs, the arm-first method was typically applied to preparing the end-functionalized arm, which was followed by a reaction with a linking agent. For example, Hatada et al. initially reported the preparation of a uniform syndiotactic and isotactic 3-armed star-shaped PMMA by reacting hydroxyl-terminated syndiotactic and isotactic PMMAs with a coupling agent, benzene-1,3,5-tricarbonyl trichloride, and also succeeded in the synthesis of stereo-complex 3-armed star-shaped PMMAs by the same method.[98-100] Moreover, Kitayama and coworkers reported the synthesis of stereoregular 4- and 6-armed star-shaped PMMAs by coupling the stereoregular living PMMA with tetrakis- and hexakis-functional linking agents, that is, tetrakis- and hexakis (bromomethyl)benzene,respectively.[101,102] Furthermore, the preparation of star-shaped PMMA micro gels with multiple stereoregular PMMA arms was also realized by

coupling the living stereoregular PMMA with core-forming monomers, such as ethylene glycol dimethacrylate and butane-1,4-diol dimethacrylate.[103]

PMMA is often used as a light weight or shatter-resistant alternative to glass. It is often used as a substitute for glass in products such as shatter proof windows, skylights, illuminated signs, and aircraft canopies. Although it is not technically a type of glass, the substance has sometimes historically been called acrylic glass.

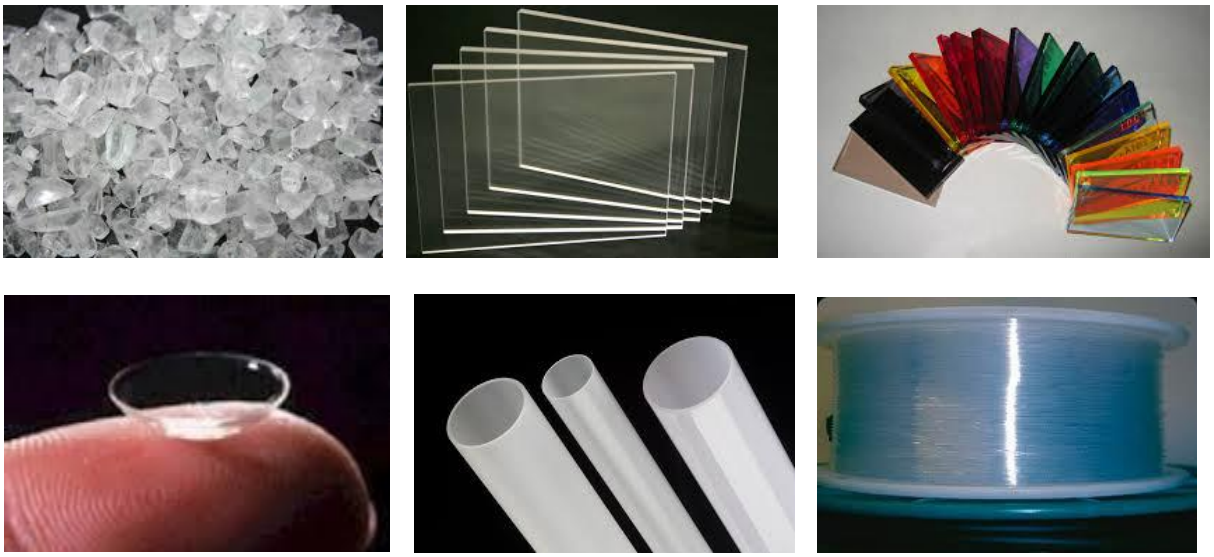

Figure 1.1. Various applications of commercial PMMA in daily life, such as applications for transparent and color glasses, pipes, fibers, and lens.

1.4 Objectives and outline of the thesis

As previously stated, end-functionalized polymers are receiving much attention in recent times, due to their wide applications in chemistry, medicine, and material science. In polymer chemistry, they are also very useful precursors for preparing polymers of interesting architectures like block, graft, and star-shaped copolymers and network structures. On the other hand, synthesis methods for quantitatively end-functionalized PMMA have few reports and there is even no report of synthesis of hydroxyl functionalized star-shaped PMMA with defined arm number and uniform length to the best knowledge of the author, because precise synthesis of hydroxyl end-functionalized polymers is less-developed in comparison with other functionalized polymers due to the difficulty to achieve total functionalization and also control the high reactivity of the hydroxyl end group. To overcome these problems, the author employed organocatalyzed GTP which has advantages as follow; (1) well-controlled PMMA is synthesized with minimum back-biting side reactions, (2) complete functionalization can be easily tailored by utilizing its livingness with an appropriate functionalized initiator or terminator, and (3) star-shaped polymer with defined arm number and uniform length can be synthesized using arm-first method by terminating living PMMA with appropriate terminators as well as the core-first method by using multi-functional initiators to synthesize star polymers which can then be functionalized by terminating the living arm ends with appropriate terminators.

The following is the outline of this thesis;

Chapter 2 describes the precise syntheses of α-end-functionalized PMMAs by Me_3SiNTf_2- and *t*-Bu-P_4-catalyzed GTP using various functional trimethyl SKA initiators and ω-end-functionalized PMMAs using functional α-phenylacrylate terminators. The ω-end-functionalization of PMMAs with a hydroxyl group is also reported. A detailed study of the termination reaction of the living chain ends of PMMA prepared by the *t*-BuP_4-catalyzed GTP method with benzaldehydes as terminators to synthesize hydroxyl group ω-end-functionalized PMMAs is described. Me_3SiNTf_2 and *t*-Bu-P_4 were effective catalysts for the α- and ω-end-functionalization of PMMA, and could easily produce PMMAs with predictable molecular weights and narrow polydispersities and quantitative functionalization efficiencies. The characterization of the obtained end-functional PMMA by size exclusion chromatography (SEC), ^{1}H NMR measurements, and MALDI-TOF MS measurements strongly suggested that the side reactions had been avoided and defect-free α- and ω-end-functionalized PMMAs had been obtained.

Chapter 3 describes the core-first synthesis of well-defined star-shaped poly(methyl methacrylate)s functionalized with hydroxyl groups by the *t*-Bu-P_4-catalyzed GTP for the first time. Based on the elementary study described in Chapter 2, *t*-Bu-P_4 was found to be a powerful catalyst for the hydroxyl end-functionalization of PMMA. For the core-first synthesis of the star-shaped PMMAs by GTP, the previously designed initiators possessing multiple numbers of silyl enolate groups $(SKA)_3$, $(SKA)_6$ and $(SKA)_{12}$, were used as the cores respectively. The star-shaped PMMAs were then terminated by benzaldehydes terminators to synthesize three-, six- and twelve-armed PMMAs carrying three, six and 12 hydroxyl groups respectively at their chain ends as shown in Figure 1.2.

The arm-first synthesis of hydroxyl functionalized two-armed and three-armed star-shaped PMMAs is also described. As the name suggests linear PMMAs were first synthesized as arms and then their reactive ends terminated electrophilically with multi-aldehydic terminators terephthaldehyde and benzene-1, 3, 5- tricarbaldehyde to synthesize hydroxyl functionalized two-armed and three-armed star-shaped PMMAs as shown in Figure 1.4.

Scheme 1.8 α- and ω-end-functionalization of PMMA by Me_3SiNTf_2 and *t*-Bu-P_4 catalyzed GTP

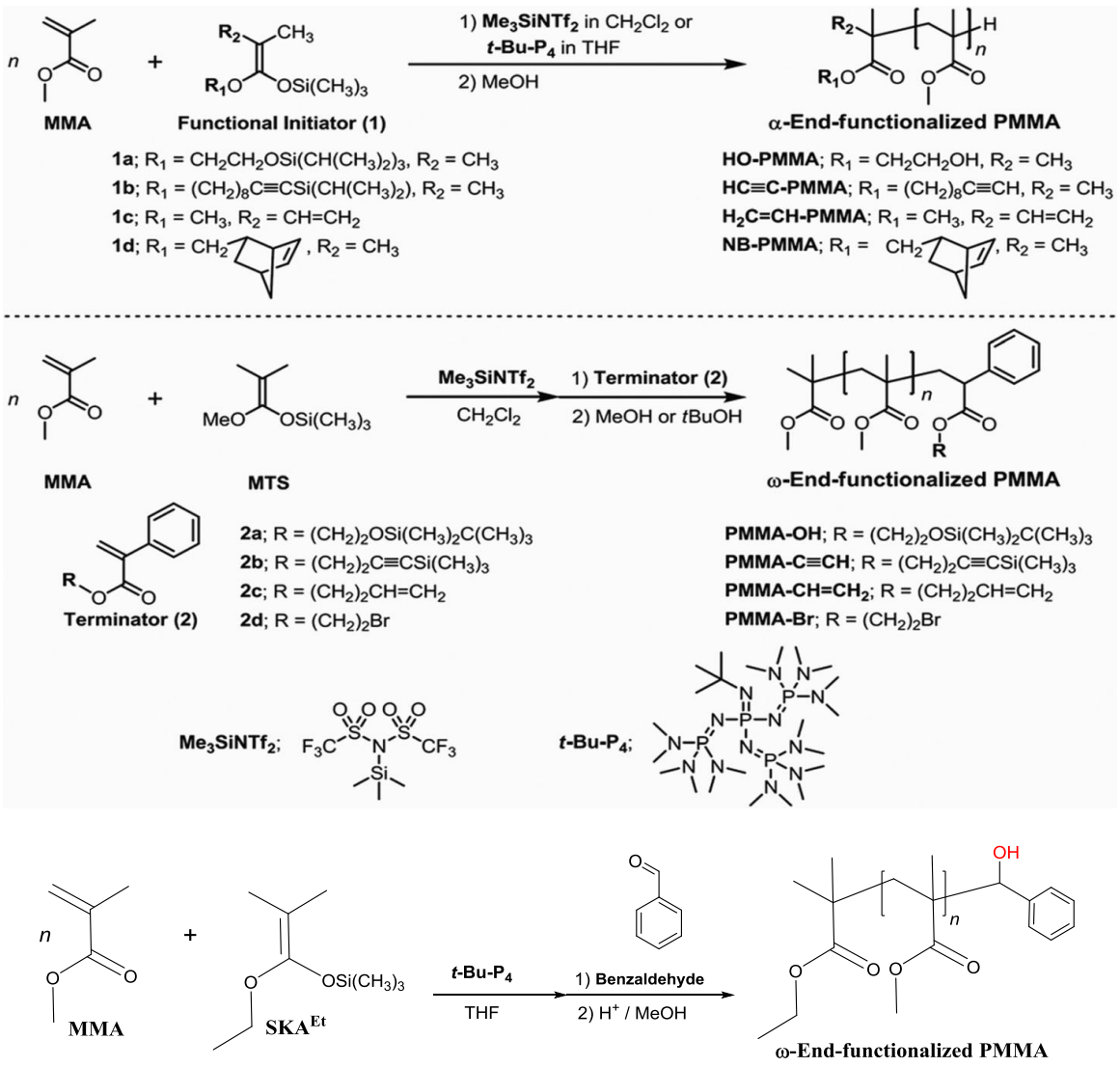

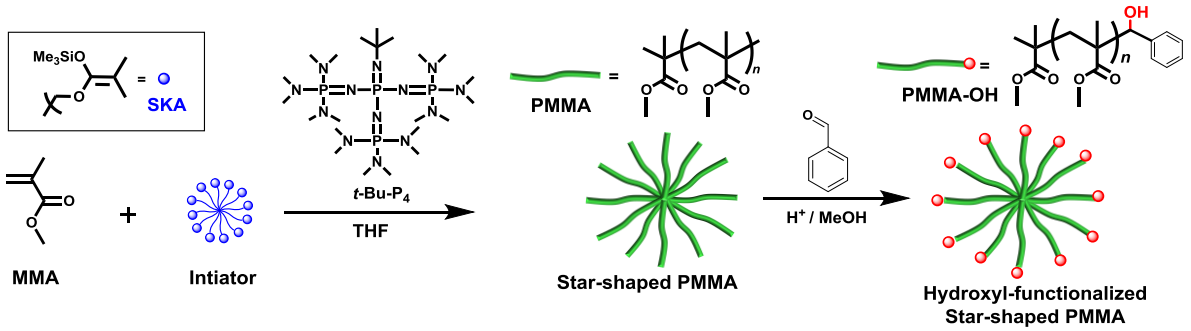

Figure 1.2 Star-shaped of PMMAs functionalized with hydroxyl groups by core-first *t*-Bu-P_4 catalyzed GTP

Chapter 4 describes the organocatalytic synthesis of star block copolymers and miktoarm star polymers using the hydroxyl-functionalized whose synthesis was reported in Chapter 3 as the macroinitiators. Star block copolymers were obtained when the hydroxyl-functionalized star-shaped PMMAs obtained by the core-first method was used as macroinitiators to initiate the ring opening polymerization ROP of L-Lactide as shown in Figure 1.3. Miktoarm star polymers were obtained when the hydroxyl-functionalized star-shaped PMMAs obtained by the arm-first method was used as macroinitiators to initiate the ring opening polymerization ROP of L-Lactide as shown in Figure 1.4. The ^{1}H NMR measurements of the star block copolymers and miktoarm star polymers showed proton signals for the PMMA chain and PLLA chain simultaneously giving evidence that star block and miktoarm copolymers containing two chemically different polymer arms in the same molecule was obtained. The thermal properties of the obtained star block and miktoarm star polymers were also investigated through their glass transition temperature (T_g).

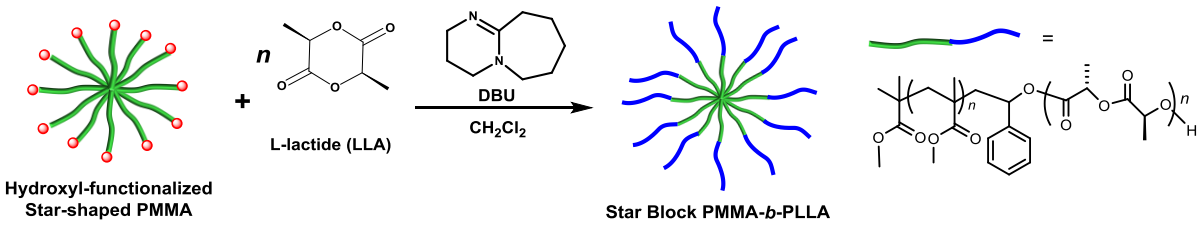

Figure 1.3. Synthesis of star block copolymers with arms consisting of blocks of PMMA and PLLA

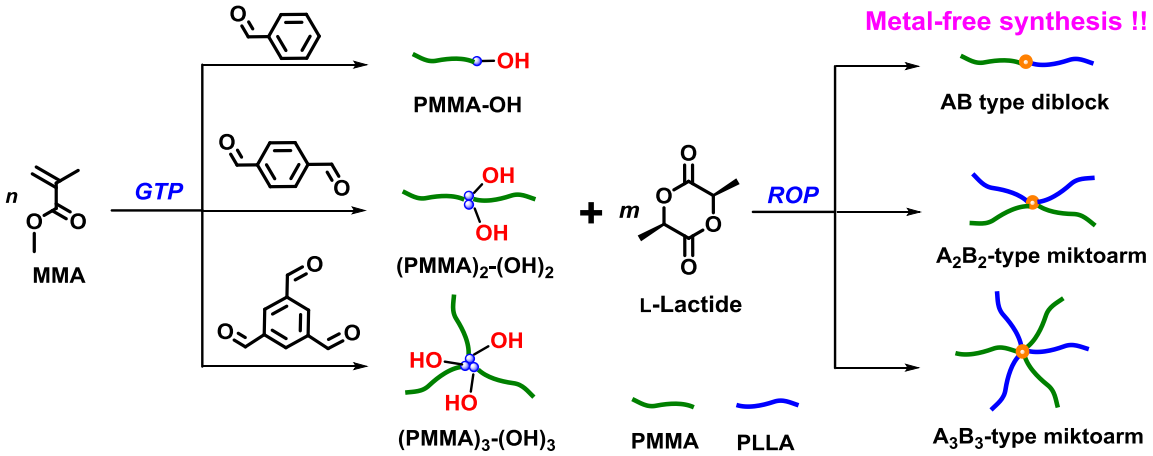

Figure 1.4. Synthesis of miktoarm star polymers with PMMA and PLLA arms using star-shaped hydroxyl-functionalized PMMA prepared by the arm-first method

Chapter 5 listed the overall conclusions of this thesis.

1.5 References and Notes

1. K. A. Ahrendt, C. J. Borths and D. W. C. MacMillan, *J. Am. Chem. Soc.*, **2000**, *122*, 4243-4244.
2. B. List, R. A. Lerner and C. F. Barbas, *J. Am. Chem. Soc.*, **2000**, *122*, 2395-2396.
3. T. Ooi, M. Taniguchi, M. Kameda and K. Maruoka, *J. Am.Chem. Soc.*, **2000**, *122*, 5228-5229.
4. B. List, *J. Am. Chem. Soc.*, **2000**, *122*, 9336-9337.
5. J.-W. Tang, C. Chander, M. Stadler, D. Kampen and B. List, Nature, **2008**, *452*, 453-455.
6. D. Enders, M. Seppelt and T. Beck, *Adv. Synth. Catal.*, **2010**, *352*, 1413-1418.
7. S. Adachi and T. Harada, *Org. Lett.*, **2008**, *10*, 4999-5001.
8. J. Seayad and B. List, *Org. Biomol. Chem.* **2005**, *3*, 719-724.
9. F. Nederberg, E. F. Connor, M. M¨oller, T. Glauser and J. L. Hedrick, *Angew. Chem., Int. Ed.*, **2001**, *40*, 2712-2715.
10. N. E. Kamber, W. H. Jeong, R. M. Waymouth, R. C. Pratt, B. G. G. Lohmeijer and J. L. Hedrick, *Chem. Rev.*, **2007**, *107*, 5813-5840.
11. M. K. Kiesewetter, E. J. Shin, J. L. Hedrick and R. M. Waymouth, *Macromolecules*, **2010**, *43*, 2093-2107.
12. M. D. Sholten, J.L. Hedrick and R.M Waymouth, *Macromolecules* **2008,** *41*, 7399-7404.
13. Raynaud, A. Ciolino, A. Baceiredo, M. Destarac, F. Bonnette, T. Kato, Y. Gnanou and D. Taton, *Angew. Chem., Int. Ed.*, **2008**, *47*, 5390-5393.
14. T. Mukaiyama, *Angew. Chem. Int. Ed.* **2004**, *43*, 5590-5614.

15. O. W. Webster, W. R. Hertler, D. Y. Sogah, W. B. Farnham and T. V.Rajanbabu, *J. Am. Chem. Soc.* **1983**, *105*, 5706-5708.

16. A. H. E. Müller, G. Litvinenko and D-Y. Yan, *Macromolecules* **1996**, *29*, 2346-2353.

*17. D. Seebach, Angew. Chem. Int. Ed. Engl. **1988**, 27, 1624-1654.*

18. R. P. Quirk and G. P. Bidinger, *Polym. Bull.* **1989**, *22*, 63-70.

19. K. Fuchise, Y. Chen, T. Satoh and T. Kakuchi, *Polym. Chem.* **2013**, *4*, 4278-4291.

20. W. R. Hertler, D. Y. Sogah and O. W. Webster, *Macromolecules*, **1984**, *17*, 1415-1417.

21. T. Kakuchi, Y. Chen, J. Kitakado, K. Mori, K. Fuchise and T. Satoh, *Macromolecules*, **2011**, *44*, 4641-4647.

22. R. Kakuchi, K. Chiba, K. Fuchise, R. Sakai, T. Satoh, T. Kakuchi, *Macromolecules* **2009**, *42*, 8747–8750.

23. K. Ishihara, Y. Hiraiwa and H. Yamamoto, *Synlett*, **2001**,1851.

24. M. B. Boxer and H.Yamamoto, *J. Am. Chem. Soc.*, **2006**, *128*, 48.

25. P. García-García, F. Lay, C. Rabalakos and B. List, *Angew. Chem., Int. Ed.*, **2009**, *48*, 4363.

26. J. Raynaud, Y. Gnanou, D. Taton, *Macromolecules* **2009,** *42*, 5996-4000.

27. Y. Chen, K. Takada, K. Fuchise, T. Satoh and T. Kakuchi, J. *Polym. Sci., Part A: Polym. Chem.*, **2012**, *50*, 3277–3285.

28. Y. Chen, K. Fuchise, A. Narumi, S. Kawaguchi, T. Satoh and T. Kakuchi, *Macromolecules* **2011**, *44*, 9091–9098.

29. K. Fuchise, R. Sakai, T. Satoh, S. Sato, A. Narumi, S. Kawaguchi and T. Kakuchi, *Macromolecules 2010, 43*, 5589–5594.

30. D. Sogah, W. Hertler and O. Webster, G. Cohen, *Macromolecules* **1987**, *20*, 1473-1486

31. D. Sogah and O. Webster, *J. Polym. Sci. Polym. Lett. Ed.*, **1983**, *21*, 927-931.

32. M. T. Reetz, R. Ostarek, K. E. Piejko, D. Arlt and B. Bömer, *Angew. Chem. Int. Ed. Engl. Ed.*, **1986**, *25*, 1108-1109.

33. W. P. Shen, W. D. Zhu, M. F. Yang and L. Wang, *Makromol. Chem.*, **1989**, *190*, 3061-3066.

34. W. R. Hertler, *J. Polym. Sci., Part A: Polym. Chem.*, **1991**, *29*, 869-873.

35. R. Asami, Y. Kondo and M. Takaki, *ACS Polym. Prepr.*, **1986**, *27*, 186-187.

36. G. M. Cohen, *ACS Polym. Prepr.*, **1988**, *29*, 46.

37. W. R. Hertler, D. Y. Sogah and F. P. Boettcher, *Macromolecules* **1990**, *23*, 1264-1268.

38. O. Webster, W. R. Hertler, D. Y. Sogah, W. B. Farnham and T. V. RajanBabu, *J. Am. Chem. Soc.*, **1983**, *105*, 5706-5708.

39. R. Gnaneshwar and S. Sivaram, *J. Polym. Sci., Part A: Polym. Chem.*, **2007**, *45*, 2514-2531.

40. R. Quirk and J. Ren, *Polym. Int.* **1993**, *32*, 205-212.

41. J. Raynaud, Y. Gnanou, D. Taton, *Macromolecules* **2009,** *42*, 5996-4000.

42. M. D. Sholten, J. L. Hedrick, R. M. Waymouth, *Macromolecules* **2008,** *41*, 7399-7404.

43. Y. Zhang, E. Y.-X. Chen, *Macromolecules* **2008**, *41*, 36-42

44. Y.-G. Chen, K. Fuchise, A. Narumi, S. Kawaguchi, T. Satoh, T. Kakuchi, *Macromolecules* **2011**, *44*, 9091-9098.

45. Y.-G. Chen, K. Takada, K. Fuchise, T. Satoh, T. Kakuchi, *J. Polym. Sci., Part A: Polym. Chem.*, **2012**, *50*, 3277-3285.

46. T. Kakuchi, Y.-G. Chen, J. Kitakado, K. Mori, K. Fuchise, T. Satoh, *Macromolecules* **2011**, *44*, 4641-4647.

47. K. Takada, K. Fuchise, Y.-G. Chen, T. Satoh, and T. Kakuchi, *J. Polym. Sci., Part A: Polym. Chem.*, **2012**, *50*, 3560-3566.

48. R. Kakuchi, K. Chiba, K. Fuchise, R. Sakai, T. Satoh, T. Kakuchi, *Macromolecules* **2009**, *42*, 8747-8750.

49. Y.-G. Chen, K. Takada, N. Kubota, O. T. Eric, T. Ito, T. Isono, T. Satoh, T, Kakuchi. *Polym. Chem.* **2015**, *5*, **1830-1837**.

50. K. Takada, K. Fuchise, N. Kubota, T. Ito, Y.-G. Chen, T. Satoh, T. Kakuchi, *Macromolecules* **2014**, *47*, **5514-5525**.

51. T. A. Orofino and F. Wenger, *J. Phys. Chem*. **1963**, *67*, 566-575

52. J. Roovers, P. Toporowski, and J. Martin, *Macromolecules* **1989**, *22*, 1897-1903

53. D. J Lunn, E. H. Discekici, J. R. de Alaniz, W. R. Gutekunst and C. J Hawker, *J. Polym. Sci., Part A: Polym. Chem.*, **2017**, 55, 808-819.

54. F. Lo Verso and C. N. Likos, *Polymer* **2008**, *49*, 1425–1434.

55. R. A. Sperling and W. J. Parak, *Philos. Trans. R. Soc. A Math. Phys. Eng. Sci.* **2010**, *368*, 1333–1383

56. Y. Mai and A. Eisenberg, *Chem. Soc. Rev.* **2012**, *41*, 5969–5985.

57. M. Beija, M.-T. Charreyre and J. M. G. Martinho, *Prog. Polym. Sci*. **2011**, *36*, 568–602.

58. S. Dehn, R. Chapman and K. A. Jolliffe, S. Perrier, *Polym. Rev.* **2011**, *51*, 214–234.

59. Miasnikova, A. Laschewsky, *J. Polym. Sci. Part A Polym. Chem.* **2012**, *50*, 3313–3323.

60. B. J. Kim, S. Given-Beck, J. Bang, C. J. Hawker and E. J. Kramer, *Macromolecules* **2007**, *40*, 1796–1798.

61. T. D. Michl, K. E. S. Locock, N. E. Stevens, J. D. Hayball, K. Vasilev, A. Postma, Y. Qu, A. Traven, M. Haeussler, L. Meagher and H. J. Griesser, *Polym. Chem.* **2014**, *5*, 5813–5822.

62. J. Du, H. Willcock, J. P. Patterson, I. Portman and R. K. O'Reilly, *Small* **2011**, *7*, 2070–2080.

63. M.-H. Wei, B. Li, R. L. A. David, S. C. Jones, V. Sarohia, J. A. Schmitigal and J. A. Kornfield, *Science* **2015**, *350*, 72–75.

64. U. Koldemir, S. R. Puniredd, M. Wagner, S. Tongay, T. D. McCarley, G. D. Kamenov, K. Mullen, W. Pisula and J. R. Reynolds, *Macromolecules* **2015**, *48*, 6369–6377.

65. J. Kuwabara, T. Yasuda, N. Takase and T. Kanbara, *ACS Appl. Mater. Interfaces* **2016**, *8*, 1752–1758.

66. C.-M. Chen, T.-H. Jen and S.-A. Chen, *ACS Appl. Mater. Interfaces* **2015**, *7*, 20548–20555.

67. G. Gody, C. Rossner, J. Moraes, P. Vana, T. Maschmeyer and S. Perrier, *J. Am. Chem. Soc.*, **2012**, *134*, 12596−12603.

68. R. Gnaneshwar and S. Sivaram**,** *J. Polym. Sci., Part A: Polym. Chem.*, **2007**, *45*, 2514-2531.

69. K. Y. Baek, M. Kamigaito and M. Sawamoto, *J. Polym. Sci.: Part A: Polym. Chem.*, **2002**, *40*, 1937–1944

70. D. Sogah and O. Webster, *J. Polym. Sci. Polym. Lett. Ed.*, **1983**, *21*, 927-931

71. W. R. Hertler, *J. Polym. Sci., Part A: Polym. Chem.*, **1991**, *29*, 869-873.

72. M. K. Mishra and S. Kobayashi, *Plast. Eng. (N.Y)*, **1999,** *53*, 350-376.

73. Y. Chen, K. Takada, K. Fuchise, T. Satoh and T. Kakuchi, J. *Polym. Sci., Part A: Polym. Chem.*, **2012**, *50*, 3277–3285.

74. T.G Fox, S. Garrett, W. E. Goode, S. Gratch, J.F. Kincaid, A. Spell and J. D. Stroupe, *J. Am. Chem. Soc.* **1958**, *80*, 1768–1769.

75. R. G. Miller, B. Mills, P. A. Small, J. A. Turner and D. G. M. Wood, *Chem. Ind.* **1958**, 1323-1324 .

76. B. C. Anderson, G. D. Andrews, J. P. Arthur, H. W. Jacobson, L. R. Melby, A. J. Playtis and W. H. Sharkey, *Macromolecules* **1981**, *14*, 1599-1601

77. K. Hatada, K. Ute, K. Tanaka, T. Kitayama and Y. Okamoto, *Polym. J.* **1985**, *17*, 977–980.

78. T. Kitayama, T. Shinozaki, E. Masuda, M. Yamamoto and K. Hatada, *Polym. Bull.* **1988**, *20*, 505–510.

79. T. Kitayama, T. Shinozaki, T. Sakamoto, M. Yamamoto and K. Hatada, *Makromol. Chem.* **1989**, *15*, 167–185.

80. Y. Chen, K. Takada, K. Fuchise, T. Satoh and T. Kakuchi, J. *Polym. Sci., Part A: Polym. Chem.*, **2012**, *50*, 3277–3285.

81. T.G Fox, S. Garrett, W. E. Goode, S. Gratch, J.F. Kincaid, A. Spell and J. D. Stroupe, *J. Am. Chem. Soc.* **1958**, *80*, 1768–1769.

82. R. G. Miller, B. Mills, P. A. Small, J. A. Turner and D. G. M. Wood, *Chem. Ind.* **1958**, 1323-1324 .

83. B. C. Anderson, G. D. Andrews, J. P. Arthur, H. W. Jacobson, L. R. Melby, A. J. Playtis and W. H. Sharkey, *Macromolecules* **1981**, *14*, 1599-1601

84. K. Hatada, K. Ute, K. Tanaka, T. Kitayama and Y. Okamoto, *Polym. J.* **1985**, *17*, 977–980.

85. T. Kitayama, T. Shinozaki, E. Masuda, M. Yamamoto and K. Hatada, *Polym. Bull.* **1988**, *20*, 505–510.

86. T. Kitayama, T. Shinozaki, T. Sakamoto, M. Yamamoto and K. Hatada, *Makromol. Chem.* **1989**, *15*, 167–185.

87. K. Satoh and M. Kamigaito, *Chem. Rev.* **2009**, *109*, 5120–5156.

88. G. M. Miyake and Y. X Chen, *Polym. Chem.* **2011**, *2*, 2462–2480.

89. Y. Isobe, K. Yamada, T. Nakano and Y. Okamoto, *Macromolecules* **1999**, *32*, 5979–5981.

90. Y. Isobe, K. Yamada, T. Nakano and Y. Okamoto, J. *Polym. Sci. Part A: Polym. Chem.* **2000**, *38*, 4693–4703.

91. Y. Isobe, K. Yamada, T. Nakano and Y. Okamoto, *J. Polym. Sci. Part A: Polym. Chem.* **2001**, *39*, 1463–1471.

92. J.-F. Lutz, W. Jakubowski and K. Matyjaszewski, *Macromol. Chem. Rapid Commun* **2004**, *25*, 486–492.

93. Y. Miura, T. Satoh, A. Narumi, O. Nishizawa, Y. Okamoto and T. Kakuchi, *J. Polym. Sci. Part A: Polym. Chem.* **2006**, *44*, 1436–1446.

94. H. Abe, K. Imai and M. Matsumoto, *J. Polym. Sci. Part B: Polym. Lett.* **1965**, *3*, 1053–1058.

95. H. Yasuda, H. Yamamoto, K. Yokota, S. Miyake and A. Nakamura, *A. J. Am. Chem. Soc.* **1992**, *114*, 4908–4910.

96. H. Yasuda and E.; Ihara, *Adv. Polym. Sci.*, **1997**, *133*, 53–101.

97. H. Yasuda, *J. Polym. Sci. Part A: Polym. Chem.*, **2001**, *39*, 1955–1959.

98. K. Hatada, T. Nishiura, T. Kitayama and M. Tsubota, *Polym. Bull.* **1996**, *36*, 399–405.

99. T. Kitayama, T. Nishiura, M. Tsubota, H. Nakanishi and K. Hatada, *Polym. J.* **1999**, *31*, 1001–1003.

100. T. Nishiura, Y. Abe and T. Kitayama, *Polym. J.* **2010**, *42*, 868–874.

101. M. Lazzari, T. Kitayama, M. Jančo and K. Hatada, *Macromolecules* **2001**, **34**, 5734–5736.

102. M. Lazzari, T. Kitayama, M. Jančo and K. Hatada, *Macromol. Rapid Commun.* **2003**, *24*, 1019–1023.

103. K. Hatada, T. Kitayama, N. Fujimoto, T. Fukuoka, O. Nakagawa and T. Nishiura, *J. Macromol. Sci.* **2002**, *39*, 801–814.

Chapter 2

Organocatalytic Synthesis of α- and ω-End-functionalized Poly(methyl methacrylate)s by Group Transfer Polymerization using Functional Initiators and Terminators

2.1 Introduction

The development of "controlled" and "living" chain-growth polymerization strategies has revolutionized the design and preparation of functional polymers. These polymerizations have allowed access to materials with low dispersity and high chain-end fidelity.[1] In particular, the potential to control the chain-end functionality has transformed chemists' view of polymers from ill-defined structures to a versatile building block for the preparation of more complex materials.[2] This has led to a wide range of new applications for polymers, including surface/particle functionalization,[3] self-assembly,[4] molecular labelling,[5] and bioconjugation.[6] Furthermore, the importance and influence of polymer chain-ends on physical properties has emerged as an important consideration in a range of applications.[7–9] For example, chain-ends have been shown to have a significant effect on polymer self-assembly,[10,11] dictating structural ordering, charge transport and overall performance of organic semiconductors.[12–14] As a result, the incorporation of new functionality or removal of unwanted chain-end reactivity is a major theme and essential tool for polymer researchers. The increasing number of studies examining the synthesis and the influence of the end groups on the overall performance of the polymer reflect the growing prominence of end-functionalized polymers.

Three main strategies exist for the functionalization of polymer chain-ends (Figure. 1.1); the use of a functional initiator, use of a reactive terminator to end-cap a growing polymer chain, or the post-polymerization functionalization of pre-existing chain ends. In all of these cases, the scope of end-groups that can be introduced is dependent on their compatibility with the polymerization process and chemical composition of the polymer. For the majority of polymerizations, the active species is not isolatable and requires

termination after polymerization. In the case of controlled radical polymerization (CRP), these terminations are intrinsically coupled to the mechanism and post-polymerization functionalization becomes the dominant strategy. For all of these approaches, researchers can draw inspiration from decades of small molecule organic methodology, where conditions have been reported for the transformation of a myriad of functional groups (FG).

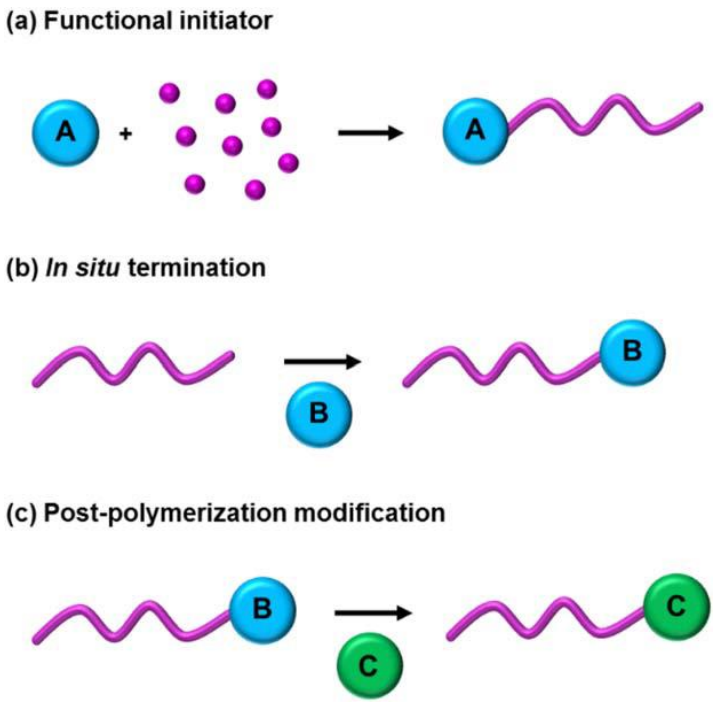

Figure 2.1. Schematic representations of available strategies for the modification of polymer chain-ends; (a) initiation using a functional initiator, (b) in situ termination using an appropriate quenching reagent, and (c) post-polymerization modification of the acquired chain-end functionality. Note that the chain-end moiety to be transformed via strategy (c) can be located at either the α or ω polymer chain end.

The most significant advances in polymer chemistry has been based on employing organic chemistry concepts and tools to control the structure of polymeric architectures at the molecular level.[15] Synthesis of new materials with improved properties and applications is still an intense and challenging area for scientists and the advent of modern synthetic methods has paved the way for new opportunities in the preparation of well-defined materials based on polymeric macromolecules. Among these materials, end-functionalized polymers are receiving considerable attention, due to their wide applications in chemistry, medicine, and material science.

End-functional polymers are useful in a wide range of applications, such as compatibilizing agents for polymer processing, macromolecular surfactants, and modification of surfaces. End-functionalized polymers are also useful precursors for preparing block, graft, and star-shaped copolymers and network structures (Figure 2.2).[16] Synthesis of end-functionalized polymers can be achieved in almost all of the living/controlled polymerizations like atom transfer radical polymerization (ATRP), reversible addition fragmentation transfer (RAFT) polymerization and living anionic polymerization (LAP), by introducing end functionalities either using a functional initiator or a functional terminator from its α or ω end, or using both. Although living ionic polymerizations provide a wide variety of such polymers, the functional groups in the initiators or the terminators should be protected to avoid side reactions to which the ionic growing ends are usually susceptible.[17] For example, group transfer polymerization (GTP), a type of anionic polymerization, in most situations needs to use protected initiators or terminators for synthesizing end-functionalized polymers. In more detail, for instance, a functionalized silyl ketene acetal (SKA) initiator bearing a hydroxyl group

protected by a silyl group was used to synthesize hydroxyl end-functionalized polymers.[18]End-functionalization of polymers using terminating agents in GTP for example is based on the electrophilic addition of the SKA at the propagating polymer chain end, with nucleophiles. Various types of terminators have been used depending on the desired end-functional group. For example, bromine end-functionalized PMMA was synthesized by the termination of living PMMA using *N*-brominesuccinamide.[19] Phosphonate end-functionalized PMMA was obtained by tris(dimethy1amino)sulfonium bifluoride-catalyzed GTP using diethyl vinylphosphonate and bis(trymethylilyl) vinylphosphonate as terminating agents.[20]

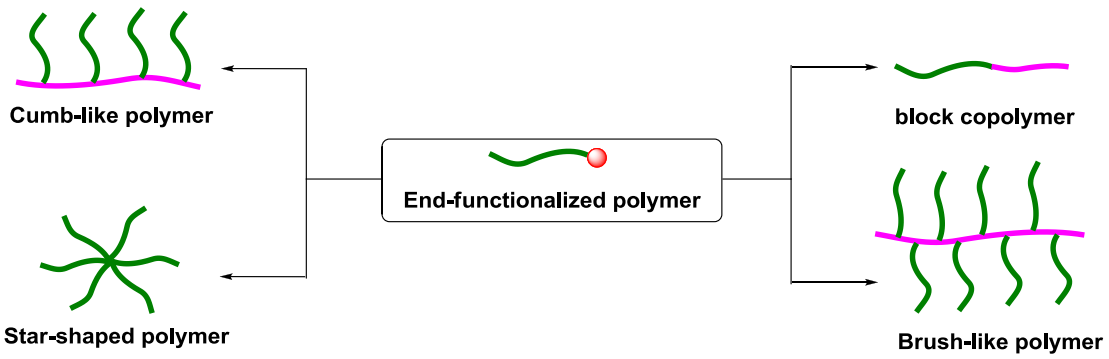

Figure 2.2. Applications of end-functionalized polymer in architectural synthesis

Group transfer polymerization can be used for the synthesis of end-functionalized polymers with two approaches: the use of functional initiators or the termination of the living chain by a suitable electrophile (or a radical precursor) bearing the functional group. Both methods have merits and demerits. The nature of the polymer and the functional group required to be introduced will determine the specific choice of the synthetic method. Additionally, to obtain high efficiencies of functionalization, each

method has to be carefully optimized in terms of the choice of the initiator and the polymerization conditions. The use of functional initiators in GTP ensures that each polymer chain contains one functional group. However, initiators of this type are not easily accessible. Furthermore, such initiators generally require the protection of the functional group because groups such as hydroxyl, amino, and carbonyl groups are not compatible with the chain ends of living polymers. The protection of reactive functional groups is resorted to in and GTP.[21-26] Hydroxyl, carboxylic acid,[25] and phenol end-functional poly(methyl methacrylate) (PMMA)[26] has been prepared by GTP with appropriately protected initiators.

On the contrary, the ω-end-functionalization by the GTP has not been sufficiently realized even though various types of terminators have been examined. For example, Sogah et al. synthesized end-functionalized PMMAs with the bromo and vinylphenyl groups by the termination reaction using bromine/*N*-bromosuccinimide and 4-(bromomethyl)styrene, respectively.[27-29] Webster et al. reported the synthesis of ω-end-functionalized PMMAs with the Phosphonate group using diethyl vinylphosphonate and bis(trimethylsilyl)vinylphosphonate as terminating agents.[21] Quirk et al. and Sivaram et al. reported the synthesis of ω-end-functionalized PMMAs with hydroxyl and amino groups using methyl-2-phenylpropenoate and benzaldehyde derivatives, respectively.[30,16] Nevertheless, these GTPs using conventional catalysts were hardly controlled to produce well defined polymers, resulting in the fact that their ω-end-functionalization efficiency turned out to be poor because these catalysts give a low cyclic fraction due to backbiting reactions and needed to be improved in terms of the precise polymer synthesis and end-functionalization efficiency (%F). The work reported by the author in this thesis is to

address these problems. Recently, we reported that α- and ω-end-functionalized poly(*n*-butyl acrylate)s (P*n*BAs) were precisely synthesized by Me_3SiNTf_2-catalyzed GTP using functional triisopropyl SKA initiators and α-phenylacrylate terminators,[31] which afforded quantitative %Fs. Some functionalities, such as the ethynyl and norbornenyl groups, were for the first time introduced to the α and ω-ends of P*n*BA in the GTP field.

Scheme 2.1 Synthesis of ω-end-functionalized poly (methyl methacrylate) by organocatalytic GTP using functional silyl ketene acetal initiators and α-phenylacrylate terminators.

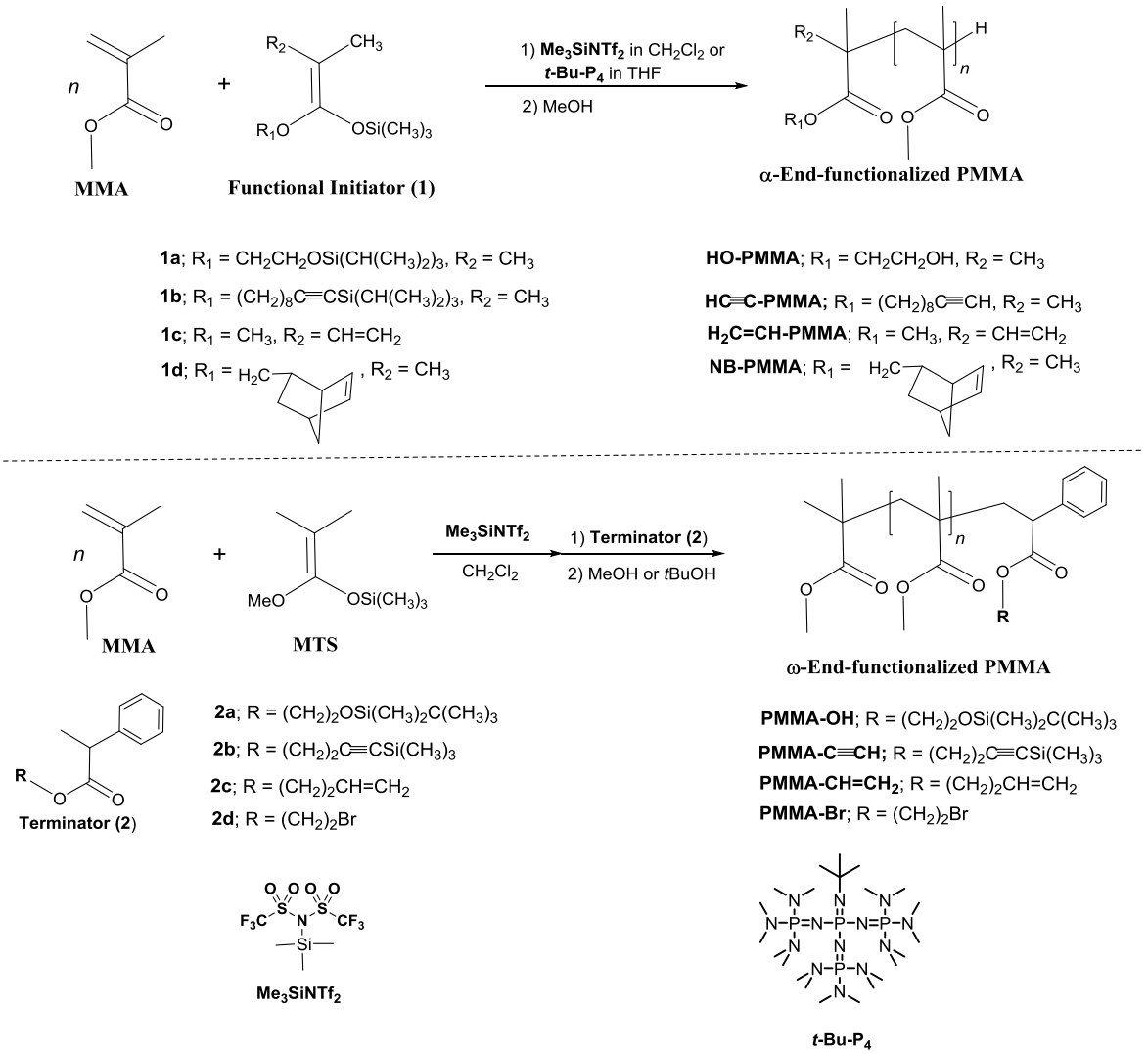

In this chapter, the author describes the precise syntheses of α-end functionalized PMMAs by Me_3SiNTf_2- and *t*-Bu-P_4-catalyzed GTP using various functional trimethyl SKA initiators (1a–1d) and ω-end-functionalized PMMAs using functional α-phenylacrylate terminators (2a–2d) and aldehydic terminators. It should be strongly emphasized that the end-functionalization of PMMA is rather different from that of previously reported P*n*BA because the designed trimethyl SKA initiators for PMMA synthesis have much higher reactivity than those of triisopropyl SKA initiators for P*n*BA synthesis and they are inappropriate for acrylic polymer synthesis; on the other hand, for ω-end-functionalization, the reactivity of the living center at the PMMA ω-end is low and totally different from that of living polyacrylate end which would change the possibility and efficiency of ω-end-functionalization.

Scheme 2.2 Synthesis of ω-end-functionalized poly (methyl methacrylate) by organocatalytic GTP using benzaldehyde terminators.

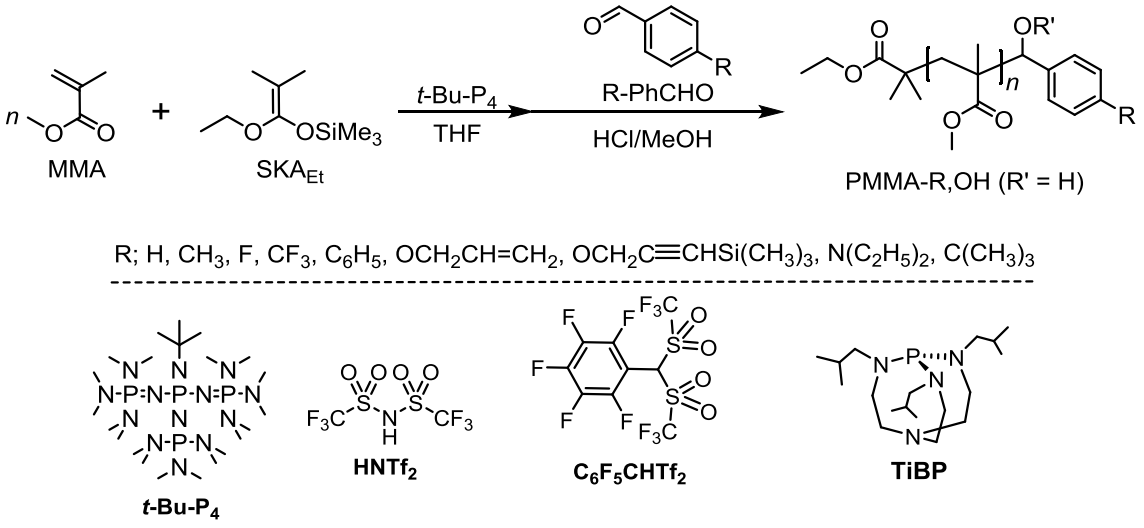

2.2 Experimental Section

Materials

Dichloromethane (CH_2Cl_2, >99.5%; water content, <0.001%), toluene (>99.5%; water content, <0.001%), tetrahydrofuran (THF, >99.5%; water content, <0.001%), *n*-butyllithium (*n*-BuLi, 1.6 mol L^{-1} in *n*-hexane), imidazole (>98.0%), and triethylamine (>99.0%) were purchased from Kanto Chemicals Co., Inc. Methyl methacrylate (MMA, >99.8%), *N*-(trimethylsilyl)bis(trifluoromethanesulfonyl)imide (Me_3SiNTf_2, >95.0%), isobutyryl chloride (>98.0%), methyl tiglate (>98.0%), 9-decyn-1-ol (>94.0%), *tert*-butyldimethylsilyl chloride (*t*-$BuMe_2SiCl$), 4-(dimethylamino)pyridine (DMAP, >99.0%), diisopropylamine (DIPA, >99.0%), chlorotriisopropylsilane ($^{i}Pr_3SiCl$, >98.0%), chlorotrimethylsilane (Me_3SiCl, >98.0%), and sodium hydride (55 wt%, dispersion in liquid paraffin) were purchased from Tokyo Kasei Kogyo Co., Ltd. (1*R*,2*S*,4*R*)-5-Norbornene-2-carboxylic acid (97%), tetrabutyl-ammonium fluoride (TBAF, 1.0 mol L^{-1} in THF), sodium trifluoroacetate (98%), and DowEX® marathon® MSC (H) ion exchange resin were purchased from the Sigma-Aldrich Chemicals Co. MMA, methyl tiglate, DIPA, and CH_2Cl_2 were distilled over CaH_2 and degassed by three freeze–pump–thaw cycles prior to use. Me_3SiCl was distilled without using any drying agent and degassed by three freeze–pump–thaw cycles prior to use. Toluene and THF were distilled from sodium benzophenone ketyl. The functional initiators, 1-(2-triisopropylsiloxyethoxy)-1-trimethylsiloxy-2-methyl-1-propene (**1a**), 1-(10-trimethylsilyldec-9-yn-1-yloxy)-1-trimethylsiloxy-2-methyl-1-propene (**1b**), 1-methoxy-1-trimethylsiloxy-2-methyl-1,3-butadiene (**1c**), and 1-((1S,4S)-norborn-5-en-2-ylmethoxy)-1-trimethylsiloxy-2-metylprop-1-ene (**1d**), were synthesized according to a previously reported procedure.[34]

1-Ethoxy-1-(trimethylsiloxy)-2-methylprop-1-ene (SKA_{Et}) was synthesized according to a previously reported procedure.[34] The functional terminators, 2-(*tert*-butyldimethylsiloxy)-ethyl 2-phenylacrylate (**2a**), 4-trimethylsilyl-3-butynyl 2-phenylacrylate (**2b**), 3-butenyl 2-phenylacrylate (**2c**), and 2-bromoethyl 2-phenylacrylate (**2d**) were used as reported.[34] 4-(3-(Trimethylsilyl)prop-2-ynyloxy)benzaldehydes (*p*-$Me_3SiC{\equiv}CCH_2O$-PhCHO) was prepared according to a reported procedure.[35-38] All other chemicals were purchased from available suppliers and used without further purification.

Measurements

The ^1H (400 MHz) and ^{13}C NMR (100 MHz) spectra were recorded using a JEOL JNM-A400II. The polymerization solution was prepared in an MBRAUN stainless steel glove-box equipped with a gas purification system (molecular sieves and copper catalyst) in a dry argon atmosphere (H_2O, O_2 <1 ppm). The moisture and oxygen contents in the glove-box were monitored by an MB-MO-SE 1 and an MB-OX-SE 1, respectively. Size exclusion chromatography (SEC) measurements for the end functionalized PMMAs were performed at 40 °C using a Jasco GPC-900 system equipped with a reflective index (RI) detector and two Shodex KF-804 L columns (linear, 8 mm × 300 mm) in THF at a flow rate of 1.0 mL min^{-1}. The molar mass ($M_{n,SEC}$) and dispersity (M_w/M_n) of the resulting PMMA were determined using SEC based on PMMA standards with M_w (M_w/M_n) values of 1.25×10^3 kg mol^{-1} (1.07), 6.59×10^2 kg mol^{-1} (1.02), 3.003×10^2 kg mol^{-1} (1.02), 1.385×10^2 kg mol^{-1} (1.05), 60.15 kg mol^{-1} (1.03), 30.53 kg mol^{-1} (1.02), and 11.55 kg mol^{-1} (1.04), 4.90 kg mol^{-1} (1.10), 2.87 kg mol^{-1} (1.06), and 1.43 kg mol^{-1} (1.15). The matrix-assisted laser desorption/ionization time-of-flight mass spectrometry (MALDI-

TOF MS) measurements were performed using an Applied Biosystems Voyager-DE STR-H mass spectrometer with a 25 kV acceleration voltage. The positive ions were detected in the reflector mode (25 kV). A nitrogen laser (337 nm, 3 ns pulse width, 106–107 W cm^{-2}) operating at 3 Hz was used to produce the laser desorption, and 200–500 shots were summed. The spectra were externally calibrated using narrow-dispersed polystyrene as a linear calibration. Samples for the MALDI-TOF MS measurements of the end-functionalized PMMAs were prepared by mixing the polymer (10 mg mL^{-1}, 30 μL), the matrix (1,8-dihydroxy-9-(10H)-anthracenone (20 mg mL^{-1}, 90 μL), and the cationizing agent (sodium trifluoroacetate, 10 mg mL^{-1}, 30 μL) in THF.

Synthesis of functional trimethyl SKA initiators

2-Triisopropylsiloxyethyl isobutyrate (**a**) and (1*S*, 4*S*)-norborn-5-en-2-ylmethyl isobutyrate (**d**) were used as described in our previous report.[32] Methyl tiglate (**c**) was commercially available from Tokyo Kasei Kogyo Co., Ltd.

Synthesis of dec-9-yn-1-yl isobutyrate (b).

Isobutyryl chloride (4.75 mL, 45.0 mmol) was dropwise added to a solution of 9-decyn-1-ol (5.00 g, 32.4 mmol), triethylamine (5.40 mL, 36.0 mmol), and DMAP (190 mg, 1.56 mmol) in $CHCl_2$ (100 mL) under a nitrogen atmosphere at 0 ºC. After 22 h of stirring at room temperature, the reaction mixture was filtered and washed with conc. aq. $NaHCO_3$ (50 mL × 3) and distilled water (50 mL × 3). The organic layer was then dried over Na_2SO_4. The obtained crude product was purified by column chromatography using CH_2Cl_2/*n*-hexane = 2/3 (v/v) to give dec-9-yn-1-yl isobutyrate as a colorless liquid. Yield, 7.01 g (96%). ^{1}H NMR (400 MHz, $CDCl_3$): δ (ppm) 4.05 (t, 2H, *J* = 6.8 Hz, -COOC*H*$_2$-),

2.54 (sep, J = 7.0 Hz, 1H, $(CH_3)_2CH$-), 2.18 (dt, ^4J = 2.4 Hz and ^3J = 7.0 Hz, 2H, $CH{\equiv}CCH_2$-), 1.94 (t, J = 2.4 Hz, 1H, $CH{\equiv}C$-), 1.62 (m, 2H, - $COOCH_2CH_2$-), 1.53 (m, 2H, $\equiv CCH_2CH_2$-), 1.46-1.24 (m, 8H, -$COOCH_2CH_2(CH_2)_4$-), 1.16 (d, J= 7.0 Hz, 6H, $(CH_3)_2CH$-). ^{13}C NMR (100 MHz, $CDCl_3$): δ (ppm) 177.1 (-*C*OO-), 84.6 (HC≡*C*-), 68.1 (H*C*≡C-), 64.2 (-COO*C*H_2-), 34.0 ($(CH_3)_2CH$-), 29.0-28.3 (-$COOCH_2CH_2CH_2(CH_2)_4$-), 25.8 (-$COOCH_2CH_2CH_2$-), 18.9 ($(CH_3)_2CH$-), 18.3 ($CH{\equiv}CCH_2$-). Anal. Calcd for $C_{14}H_{24}O_2$ (224.33): C, 74.95; H, 10.78. Found: C, 74.97; H, 10.94.

Synthesis of 1-(2-triisopropylsiloxyethoxy)-1-trimethylsiloxy-2-methyl-1-propene (1a)

Method A: *n*-BuLi (18.1 mL, 1.62 mol L^{-1} in *n*-hexane, 29.1 mmol) was dropwise added to a solution of DIPA (5.31 mL, 29.1 mmol) in THF (40 mL) at 0 °C under an argon atmosphere, then the mixture was stirred for 30 min to produce lithium diisopropylamide (LDA). 2-Triisopropylsiloxyethyl isobutyrate (8.00 g, 27.7 mmol) was added to the LDA solution and the mixture was stirred for 30 min at 0 °C. Me_3SiCl (5.05 mL, 30.5 mmol) was then added to the reaction mixture at 0 °C. After stirring for 5 h at room temperature, the reaction mixture was directly distilled from the reaction container under reduced pressure to give **1a** as a colorless liquid. Yield, 7.10 g (71 %). b.p., 117 °C / 0.08 mmHg. ^{1}H NMR (400 MHz, $CDCl_3$): δ (ppm) 3.85 (t, J = 5.2 Hz, 2H, =C-OCH_2-), 3.78 (t, J = 5.2 Hz, 2H, -CH_2-OSi-), 1.59 (s, 3H, =C(^{Z}CH_3)(^{E}CH_3)), 1.52 (s, 3H, =C(^{Z}CH_3)(^{E}CH_3)), 1.02−1.18 (m, 21H, -OSi[C*H*(CH_3)$_2$]$_3$), 0.20 (s, 9H, -OSi(CH_3)$_3$). ^{13}C NMR (100 MHz, $CDCl_3$): δ (ppm) 148.3, 91.9, 70.3, 62.3, 18.1, 17.1, 16.4, 12.1, 0.2.

Synthesis of 1-(10-trimethylsilyldec-9-yn-1-yloxy)-1-trimethylsiloxy-2-methyl-1-propene (1b).

Method A was applied to *n*-BuLi (20.9 mL, 1.62 mol L^{-1} in *n*-hexane, 33.8 mmol), DIPA (4.74 mL, 33.8 mmol), THF (50 mL), 9-yn-1-yl isobutyrate (3.58 g, 16.0 mmol), and Me_3SiCl (7.60 mL, 60.0 mmol) to give **1b** as a pale yellow liquid. Yield, 2.87 g (49 %). b.p., 115 °C / 0.06 mmHg. ^{1}H NMR (400 MHz, CDCl3): δ (ppm) 3.68 (t, *J* = 4.0 Hz, 2H, -OC*H*$_2$-), 2.21 (t, *J* = 7.0 Hz, 2H, -C≡CC*H*$_2$), 1.54 (s, 3H, =C(^{E}C*H*$_3$)(^{Z}CH$_3$)), 1.52 (s, 3H, =C(^{E}CH$_3$)(^{Z}C*H*$_3$)), 1.68-1.24 (m, 12H, -OCH$_2$(C*H*$_2$)$_6$-), 0.20 (s, 9H, -OSi(C*H*$_3$)$_3$), 0.15 (s, 9H, -C≡C(C*H*$_3$)$_3$). ^{13}C NMR (100 MHz, $CDCl_3$): δ (ppm) 148.44 (-*C*=C(CH$_3$)$_2$), 107.85 (≡*C*-Si(CH$_3$)$_3$), 91.56 (=*C*(CH$_3$)$_2$), 84.40 (-*C*≡CSi(CH$_3$)$_3$), 69.13 (-O*C*H$_2$-), 29.62, 29.45, 29.17, 28.89, 28.75, 26.23, 19.99 (≡C*C*H$_2$-), 17.10 (^{Z}CH$_3$C(^{E}*C*H$_3$)=), 16.50 (^{Z}*C*H$_3$C(^{E}CH$_3$)=), 0.34 (-OSi (*C*H$_3$)$_3$), 0.22 (≡CSi(*C*H$_3$)$_3$).

Synthesis of 1-methoxy-1-trimethylsiloxy-2-methyl-1,3-butadiene (1c).

Method A was applied to *n*-BuLi (42.2 mL, 1.62 mol L^{-1} in *n*-hexane, 67.5 mmol), DIPA (9.48 mL, 67.5 mmol), THF (70 mL), methyl tiglate (7.00 g, 61.3 mmol), and Me_3SiCl (8.60 mL, 67.5 mmol) to give **1c** as a colorless liquid. Yield, 4.23 g (37 %). b.p., 55 °C / 7.50 mmHg. ^{1}H NMR (400 MHz, $CDCl_3$): δ (ppm) 6.71 (ddd, ^{3}*J-cis* = 10 Hz, ^{3}*J-trans* = 17.0 Hz, ^{3}*J-cis* = 10 Hz), 4.85 (dd, ^{3}*J-trans* = 17.0 Hz, ^{2}*J* =1.8 Hz), 4.78 (dd, ^{3}*J-cis* = 10 Hz, ^{2}*J* = 1.8 Hz, 4-H), 3.57 (s, 3H, -OC*H*$_3$), 1.63 (s, 3H, =CC*H*$_3$), 0.25 (s, 9H, -C≡C(C*H*$_3$)$_3$). ^{13}C NMR (100 MHz, $CDCl_3$): δ (ppm) 152.32 (-*C*=CCH$_3$CH=CH$_2$), 134.83 (-*C*H=CH$_2$), 107.45 (-CH=*C*H$_2$), 97.43 (-C=*C*CH$_3$CH=CH$_2$), 57.62 (-O*C*H$_3$), 18.12 (-C=C*C*H$_3$CH=CH$_2$), 0.20 (-OSi (*C*H$_3$)$_3$).

Synthesis of 1-((1*S*, 4*S*)-norborn-5-en-2-ylmethoxy)-1-trimethylsiloxy-2-metylprop-1-ene (1d).

Method A was applied to *n*-BuLi (11.5 mL, 1.64 mol L^{-1} in *n*-hexane, 18.9 mmol), DIPA (2.66 mL, 18.9 mmol), THF (20.0 mL), (1*S*, 4*S*)-norborn-5-en-2-ylmethyl isobutyrate (3.50 g, 18.0 mmol), and Me_3SiCl (2.53 mL, 19.8 mmol) to give **1d** as a yellow liquid. Yield, 3.52 g (73 %). b.p.,77 °C / 0.08 mmHg. ^{1}H NMR (400 MHz, $CDCl_3$): δ (ppm) 6.00-6.17 (m, 2H, -C*H*=C*H*-), 3.75 (dd, *J* = 6.0 Hz, *J* = 9.6 Hz, 1H, -OCH_2-), 3.65 (dd, *J* = 8.8 Hz, *J* = 9.6 Hz, 1H, -OCH_2-), 2.80 (br s, 2H, -C*H*-CH=CHC*H-),* 1.70 (m, 1H, -CH-C*H*-CH_2-), 1.14-1.66 (m, 4H, bridgehead and -CH-CH-CH_2-), 1.60 (s, 3H, =C(^{E}CH_3)(^{Z}CH_3)), 1.52 (s, 3H, =C(^{E}CH_3)(^{Z}CH_3)), 0.20 (s, 9H, -OSi(CH_3)$_3$). ^{13}C NMR (100 MHz, $CDCl_3$): δ (ppm) 148.29 (-*C*=C$(CH_3)_2$), 136.65, 136.48, 91.47 (=*C*$(CH_3)_2$), 73.36 (-O*C*H_2-), 44.99, 43.81, 41.55, 33.60, 29.78, 16.98 (^{Z}CH_3C(^{E}*C*H_3)=), 16.38 (^{Z}*C*H_3C(^{E}CH_3)=), 0.09 (-OSi(*C*H_3)$_3$).

Synthesis of 1-ethoxy-1-(trimethylsiloxy)-2-methylprop-1-ene (SKA_{Et}).

Diisopropylamine (11.5 ml, 94.7 mmol) and THF (ca. 50 mL) were added into a 100-mL cock-attached Schlenk flask under an argon atmosphere. The mixture was cooled to -78 °C and *n*-butyl lithium (59.5 ml, 94.7 mmol, 1.6 M in *n*-hexane) was added. The mixture was then allowed to react for 30 min, after which ethyl isobutyrate (11.5 ml, 86.1 mmol) was added and the reaction was allowed to proceed further for 30 min at -78 °C. Trimethylsilyl chloride (13.1 ml, 0.103 mol) was finally added and the reaction was allowed to proceed at -78 °C for 30 min. It was then allowed to react further for 6 hours at room temperature. At the end of the reaction, solvent was removed at reduced pressure

and product purified by vacuum distillation (58-59 ^{o}C, ca. 2.0 kPa) to give SKA_{Et} as a colorless liquid. Yield, 4.10 g (25.3%).

Scheme 2.3. Synthesis of 1-ethoxy-1-(trimethylsiloxy)-2-methylprop-1-ene (SKA_{Et}) Initiator

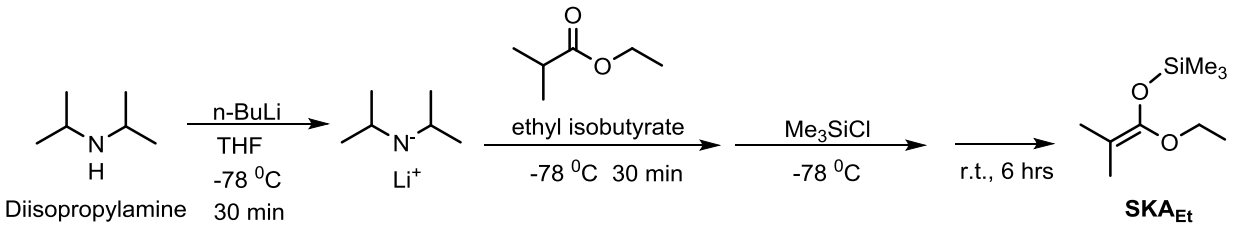

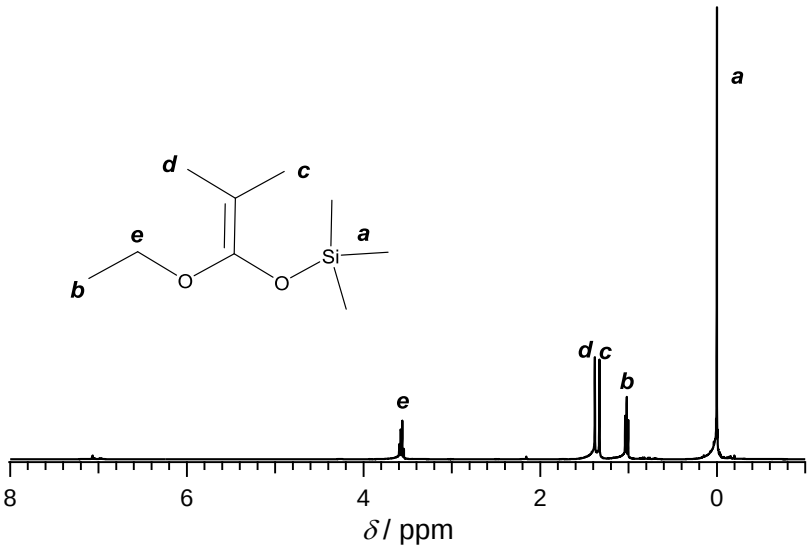

Figure 2.3. ^{1}H NMR spectra of 1-ethoxy-1-(trimethylsiloxy)-2-methylprop-1-ene (SKA_{Et}) in $CDCl_3$

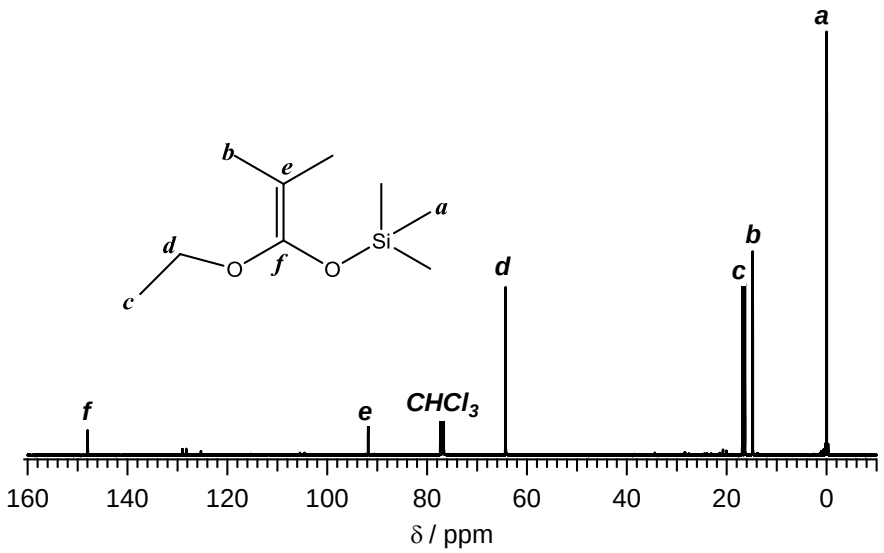

Figure 2.4. ^{13}C NMR spectra of 1-ethoxy-1-(trimethylsiloxy)-2-methylprop-1-ene (SKA_{Et}) in $CDCl_3$

Synthesis of 4-(3-(Trimethylsilyl)prop-2-ynyloxy)benzaldehyde.

The protected alkyne functionalized benzaldehyde was synthesized according to previously reported procedure [35-38] as follows; A 300 mL round bottom flask equipped with a magnetic stir bar was charged with 4-hydroxybenzaldehyde (5.00 g, 40.9 mmol), potassium carbonate (22.63 g, 0.164 mol), propargyl bromide (19.48 g, 0.164 mol), and acetone (250 mL). The heterogeneous mixture was heated to reflux for 4 h and cooled to room temperature. After addition of water, the mixture was extracted twice with dichloromethane and the combined organic layers were dried over $MgSO_4$. The solvent was removed under reduced pressure to afford the crude product as pale yellow solid. The crude was then purified twice by column chromatography using a mobile phase mixture of hexane: ethyl acetate; 2:1 to afford 2.55 g (39% yield) of pure product. To a two-neck 100mL round-bottom flask that contained the aldehyde (2.55 g, 15.9 mmol) and silver

chloride (0.46 g, 3.18 mmol) was first added 50 mL of dry dichloromethane followed by 1,8-diazabicyclo[5.4.0]undec-7-ene (DBU 4.75 mL, 4.85 g, 31.8 mmol). The reaction mixture was then heated under reflux at 40 °C and chlorotrimethylsilane (6.1 mL, 5.2 g, 47.7 mmol) added drop wise, and the contents were stirred for 2 days. The mixture was allowed to cool to ambient temperature and diluted with 150 mL of *n*-hexane. The organic phase was subsequently washed successively with aqueous $NaHCO_3$, 2M HCl, and water before being dried over anhydrous $MgSO_4$, filtered, and concentrated under high vacuum. Beige solids were recovered (2.37 g, 24.9% yield from the original aldehyde) and the product was used in the next step without further purification.

Scheme 2.4. Synthesis of 4-(3-(Trimethylsilyl)prop-2-ynyloxy)benzaldehydes

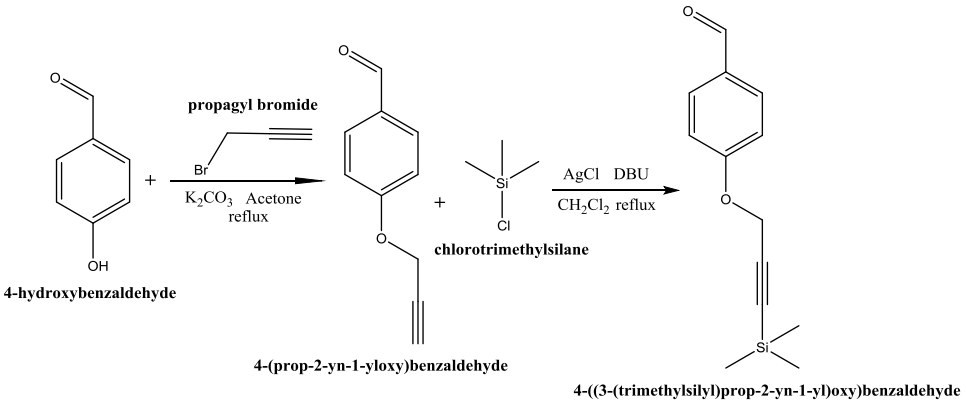

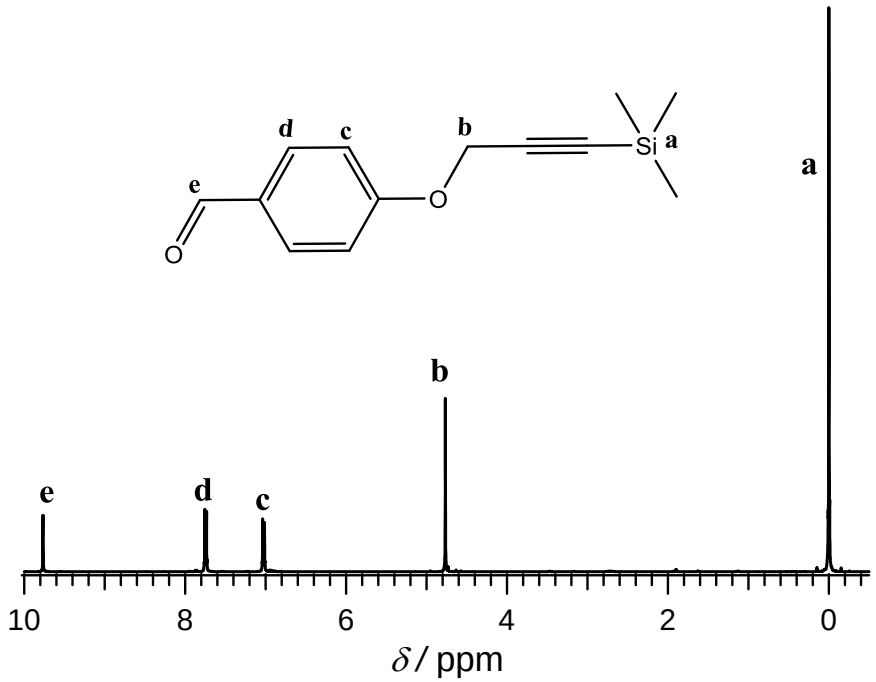

Figure 2.5. ^{1}H NMR spectrum of 4-(3-(Trimethylsilyl)prop-2-ynyloxy)benzaldehyde terminator in Acetone-d_6 (400 MHz)

Synthesis of α-end-functionalized PMMA by Me_3SiNTf_2-catalyzed GTP of MMA using functional initiators (1a–1d)

A typical procedure was as follows: a stock solution of Me_3SiNTf_2 (20 μL, 2.0 μmol, 0.10 mol L^{-1}) was added to the mixture of MMA (200 mg, 2.00 mmol) and 1a (16.0 μL, 40.0 μmol) in CH_2Cl_2 (1.75 mL) under an argon atmosphere at room temperature. After stirring for 4 h, a small amount of methanol was added to quench the polymerization. The crude product was purified by reprecipitation into *n*-hexane to give $^{i}Pr_3SiO$-PMMA as a white solid. The deprotection of the triisopropylsilyl group was implemented for 2 days at room temperature by adding TBAF (0.80 mL (0.80 mmol), 1.0 mol L^{-1} in THF) to a solution of $^{i}Pr_3SiO$-PMMA (180 mg (28.1 μmol), $M_{n,SEC}$ = 6400 g mol^{-1}, and M_w/M_n = 1.04) in THF (4.0 mL) and methanol (0.1 mL). The mixture was then diluted with THF

and passed through a short column of silica gel. The polymer was purified by reprecipitation into n-hexane to give HO-PMMA as a white solid; yield, 130 mg (72%). $M_{n,SEC}$ = 5900 g mol^{-1}, and M_w/M_n = 1.04. The GTPs of MMA using 1b–1d were carried out by a similar method.

Synthesis of ω-end-functionalized PMMA by Me_3SiNTf_2-catalyzed GTP of MMA using functional terminators (2a–2d)

The above described polymerization procedure was applied to the mixture of MMA (0.200 g, 2.00 mmol), SKA_{Me} (16.2 μl, 80.0 μmol), and Me_3SiNTf_2 (40.0 μl (4.00 μmol), 0.100 mol L^{-1}in CH_2Cl_2) in CH_2Cl_2 (1.73 mL). After 2 h polymerization, **2a** (109 mg, 0.4 mmol) was added and the entire mixture was further stirred for 24 h. The polymer was purified by reprecipitation into *n*-hexane to give the PMMA-$CuCSiMe_3$ as a white solid; yield, 190 mg (95%), $M_{n,SEC}$ = 3460 g mol^{-1}, and M_w/M_n = 1.07. The GTPs of MMA using **2b–2d** as terminators were carried out by the same method.

Synthesis of ω-end-functionalized PMMA with a hydroxyl group using benzaldehyde as the terminator

A typical procedure for the synthesis of ω-end-functionalized PMMA with a hydroxyl group (PMMA-OH) is described as follows: SKA_{Et} (160 μL, 80 μmol; 0.50 mol L^{-1} in toluene), a *t*-Bu-P_4 stock solution (16 μL, 0.80 μmol; 0.05 mol L^{-1} in THF), and THF (0.50 mL) were added to a test tube at room temperature under an argon atmosphere, followed by the drop wise addition of MMA (213 μL, 2.0 mmol) in THF (2.0 mL). The polymerization was terminated by adding benzaldehydes (82 μL, 0.80 mmol) to the

polymerization solution immediately afterwards and the ω-end-functionalization reaction was allowed to proceed for 6 h. Aliquots were taken out from the reaction mixture before termination to determine the conversion of MMA by ^{1}H NMR measurements. The polymer product was purified by precipitation in n-hexane after quenching the reaction with methanol to give a white solid powder. Yield, 172 mg (86%); $M_{n,SEC}$ = 2.9 kg mol^{-1}, M_w/M_n = 1.15; $M_{n,NMR}$ = 2.7 kg mol^{-1}. A deprotection reaction was then carried out to remove the trimethylsilyl group by reacting the polymer with 1 N HCl in MeOH/THF for 30 minutes to quantitatively obtain PMMA-OH. The synthesis of PMMA-OHs with other functional groups was carried out using a similar procedure with functional terminators.

2.3 Results and Discussion

2.3.1 Synthesis of hydroxyl, ethynyl, vinyl, and norbornenyl α-end-functionalized PMMA

The functional trimethylsilyl ketene acetals (**1a–1d**) were synthesized by a conventional method using lithium diisopropylamide (LDA). Their synthetic details are rather similar to those for synthesizing functional triisopropylsilyl ketene acetals in our previous study.[34] **1a, 1b,** and **1d** were prepared by reacting precursors of the functional isobutyrates with LDA followed by Me_3SiCl, while **1c** was synthesized by treating methyl tiglate with LDA and then Me_3SiCl. All the functional initiators were purified by distillation under reduced pressure and stored under an argon atmosphere prior to use. The group transfer polymerization (GTP) of methyl methacrylate (MMA) using **1a, 1b, 1c,** and **1d** as initiators was carried out to synthesize the hydroxyl, ethynyl, vinyl, and norbornenyl α-end-functionalized poly(methyl methacrylate)s (HO-PMMA, HC≡C-PMMA, H_2C=CH-PMMA, and NB-PMMA), respectively. We previously reported that Me_3SiNTf_2 was a significant catalyst for the synthesis of low molar mass PMMA,[18] while *t*-Bu-P_4 was more favorable for the synthesis of the high molar mass PMMA.[22] Me_3SiNTf_2 and *t*-Bu-P_4 were thus correspondingly utilized in this study to realize the synthesis of both the low and high molar mass α-end-functionalized PMMAs. Table 1 summarizes the results of the polymerizations. All the polymerizations of MMA, either using Me_3SiNTf_2 or *t*-Bu-P_4, proceeded in a quantitative manner (monomer conversion) within the fixed polymerization time. The α-end-functionalized PMMAs prepared with 1a and 1b were treated by tetra-*n*-butylammonium fluoride (TBAF) in order to remove the trialkylsilyl protection moieties. The Me_3SiNTf_2-catalyzed GTPs of MMA at the low

initial $[MMA]_0/[I]_0$ ratios of 25, 50, and 100 (Runs 1–3, 6–8, 11–13, and 16–18) were well controlled no matter which initiator was used, i.e., the molar mass of each α-end-functionalized PMMA estimated using SEC ($M_{n,SEC}$) was in good agreement with its calculated value ($M_{n,calcd}$), all the dispersities (M_w/M_n) were narrower than 1.08, and the SEC traces of all polymer products in Figure 2.4 were unimodal and had extremely narrow dispersities. On the other hand, the *t*-Bu-P_4-catalyzed GTPs of MMA at the relatively high initial $[MMA]_0/[I]_0$ ratios of 200 and 400 (Runs 4–5, 9–10, 14–15, and 19–20) produced α-end-functionalized PMMAs with $M_{n,SEC}$ values ranging from 20 000 to 50 000 g mol^{-1} though the M_w/M_n values were slightly greater than those prepared using Me_3SiNTf_2.

Scheme 2.5. Synthesis of functional trimethyl SKA initiators (**1a-1d**)

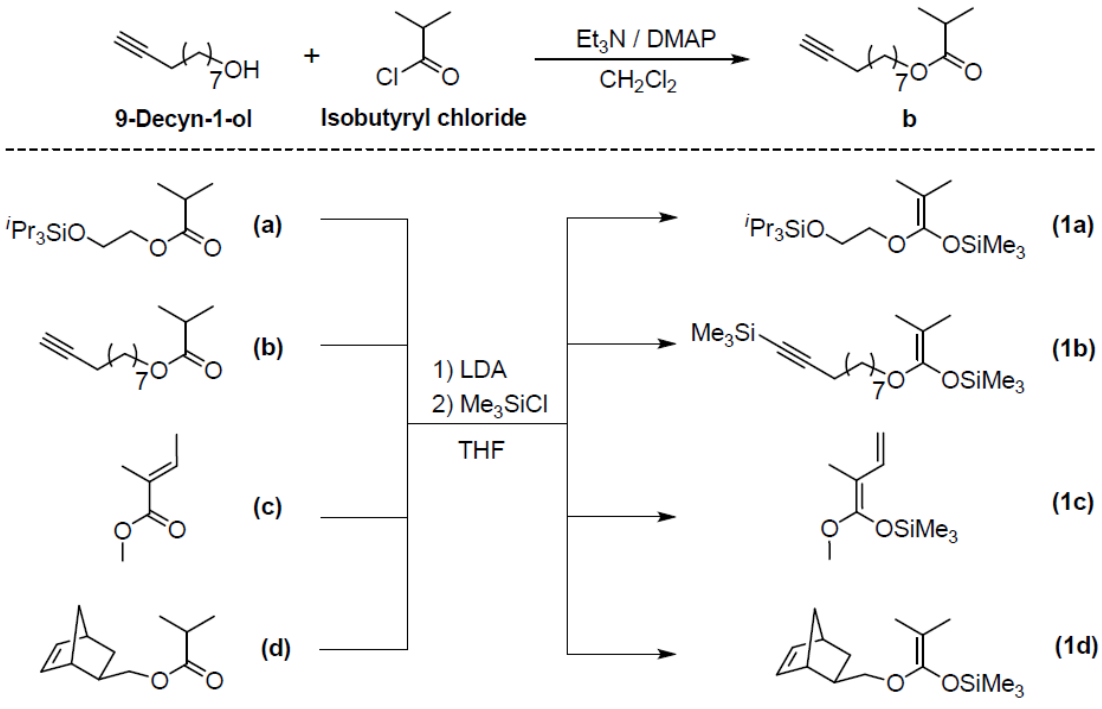

DMAP, 4-dimethylaminopyridine; LDA, lithium diisopropylamide; ^{i}Pr, *iso*-propyl group.

The introduction of hydroxyl, ethynyl, vinyl, and norbornenyl functionalities to the α-end of PMMA was initially investigated using ^{1}H NMR measurements, as shown in Figure 2.5. Characteristic signals were clearly observed around 3.80–4.30 ppm due to the –CH_2O_2C– protons of the residues of **1a, 1b**, and **1d** at the α-ends of PMMAs, while characteristic signals appeared at 4.95–5.15 ppm and 5.75–6.15 ppm for the vinyl protons derived from the residue of **1c**, together with those from the PMMA main chain at 3.62 ppm, 2.10–1.75 ppm, and 1.02 ppm. In order to clarify the chemical composition of the resulting α-end-functionalized PMMAs, matrix-assisted laser desorption/ionization time-of-flight mass spectrometry (MALDI-TOF MS) measurements for each type of α-end-functionalized PMMA were implemented using a low molar mass polymer, as shown in Figure 2.6(a)–(d). For each of the MALDI-TOF MS spectra of (a) HO-PMMA, (b) HC≡C-PMMA, and (c) H_2C=CH-PMMA, only one population of molecular ion peaks was observed. The interval between two neighboring molecular ion peaks was ca. 100.02, which was very consistent with the exact molar mass of the repeating MMA unit (M.W. = 100.05). In addition, the *m/z* values of the observed molecular ion peaks for each α-end-functionalized PMMA corresponded to their calculated molar masses when the α-end possessed an initiator residue; for example, the observed values of 2656.71 (a), 2748.01 (b), and 2638.14 (c) agreed with the calculated values of 2656.38, 2748.48, and 2638.37 for the sodium-cationized 25-mer structures of $[HO(CH_2)_2O_2CCMe_2\text{-}(MMA)_{25}\text{-}H + Na]^+$, $[HC{\equiv}C(CH_2)_8O_2CCMe_2\text{-}(MMA)_{25}\text{-}H + Na]^+$, and $[MeO_2CCMe(HC{=}CH_2)\text{-}(MMA)_{25}\text{-}H + Na]^+$, respectively. On the contrary, the MALDI-TOF MS spectrum of NB-PMMA showed two populations of molecular ion peaks. The values of the molecular ion peaks in the main population corresponded to the calculated molar mass values of the sodium-

cationized NB-PMMA, $[NBCH_2O_2CCMe_2\text{-}(MMA)_n\text{-}H + Na]^+$. Those of the sub population, on the other hand, were assigned to the sodium-cationized structure of $[H_2C{=}CHCH_2O_2CCMe_2\text{-}(MMA)_n\text{-}H + Na]^+$, which was regenerated during the cationization process due to the retro Diels–Alder reaction. The α-end-functionalization efficiency (%F) of the obtained PMMAs, which was directly estimated from the MALDI-TOF MS measurements, was determined to be quantitative (>99%), which indicated the quantitative introduction of functionalities to the α-end of PMMA using the functional initiators.

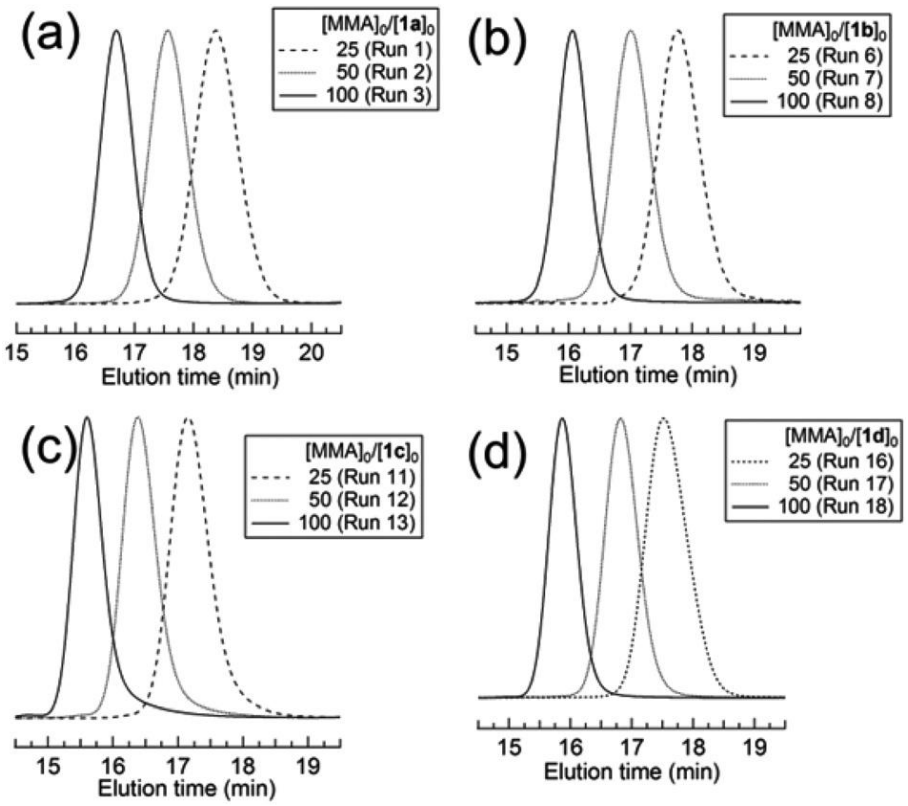

Figure 2.6. SEC traces of (a) HO-PMMA (Runs 1–3), (b) HC≡C-PMMA (Runs 6–8), (c) $H_2C{=}CH$-PMMA (Runs 11–13), and (d) NB-PMMA (Runs 16–18) synthesized by Me_3SiNTf_2-catalyzed GTP.

Table 2.1. Synthesis of hydroxyl, ethynyl, vinyl, and norbornenyl α-end-functionalized PMMAs using **1a, 1b, 1c**, and **1d** [a]

Run	Initiator (I)	Catalyst	$[MMA]_0/[I]_0$	Time (h)	$M_{n,calcd}$ [b] (g mol^{-1})	$M_{n,SEC}$ [c] (g mol^{-1})	M_w/M_n [c]
1	1a	Me_3SiNTf_2	25	2	2700	3300	1.08
2	1a	Me_3SiNTf_2	50	4	5100	5900	1.04
3	1a	Me_3SiNTf_2	100	16	10100	10200	1.03
4	1a	*t*-Bu-P_4	200	1	20300	22300	1.07
5	1a	*t*-Bu-P_4	400	1	40300	48400	1.18
6	1b	Me_3SiNTf_2	25	2	2700	3800	1.07
7	1b	Me_3SiNTf_2	50	5	5200	6500	1.04
8	1b	Me_3SiNTf_2	100	18	10200	11900	1.02
9	1b	*t*-Bu-P_4	200	1	20100	22300	1.07
10	1b	*t*-Bu-P_4	400	1	40300	49200	1.12
11	1c	Me_3SiNTf_2	25	4	2600	4500	1.08
12	1c	Me_3SiNTf_2	50	17	5100	7800	1.06
13	1c	Me_3SiNTf_2	100	19	10000	13900	1.05
14	1c	*t*-Bu-P_4	200	1	20100	25100	1.14
15	1c	*t*-Bu-P_4	400	1	40100	42200	1.22
16	1d	Me_3SiNTf_2	25	2	2700	3400	1.08
17	1d	Me_3SiNTf_2	50	5	5200	6000	1.04
18	1d	Me_3SiNTf_2	100	18	10200	11800	1.03
19	1d	*t*-Bu-P_4	200	1	20200	20300	1.05
20	1d	*t*-Bu-P_4	400	1	40200	40700	1.13

[a] Argon atmosphere; solvent, CH_2Cl_2 (Me_3SiNTf_2) or THF (*t*-Bu-P_4); $[MMA]_0$ = 1.0 mol L^{-1}; $[Me_3SiNTf_2]_0/[I]_0$ = 0.05 or $[t\text{-Bu-}P_4]_0/[I]_0$ = 0.01; temperature, room temp.; monomer conversion determined by ^{1}H NMR in $CDCl_3$, >99%. [b] Calculated using $[MMA]_0/[I]_0$ × conv. × (M.W. of MMA: 100.12) + (M.W. of initiator residue: 1a = 132.16, 1b = 224.34, 1c = 114.14, and 1d = 194.27). [c] Determined via SEC in THF using PMMA standards

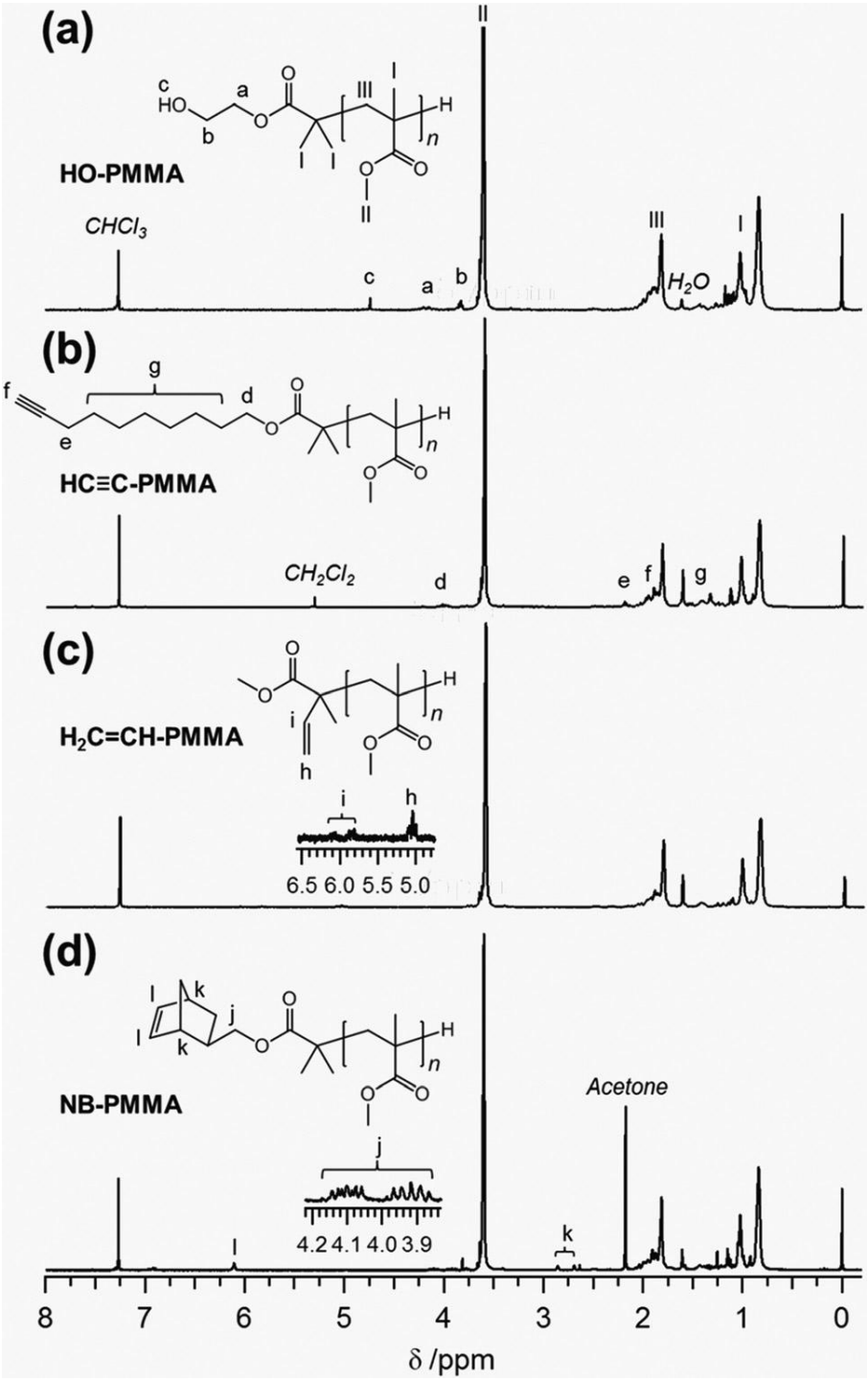

Figure. 2.7. ^{1}H NMR spectra of (a) HO-PMMA (Run 1, $M_{n,SEC}$ = 3300 g mol^{-1}, M_w/M_n = 1.08), (b) HC≡C-PMMA (Run 6, $M_{n,SEC}$ = 3800 g mol^{-1}, M_w/M_n = 1.07), (c) H_2C=C-PMMA, (Run 11, $M_{n,SEC}$ = 4500 g mol^{-1}, M_w/M_n = 1.08), and (d) NB-PMMA, (Run 16, $M_{n,SEC}$ = 3400 g mol^{-1}, M_w/M_n = 1.08).

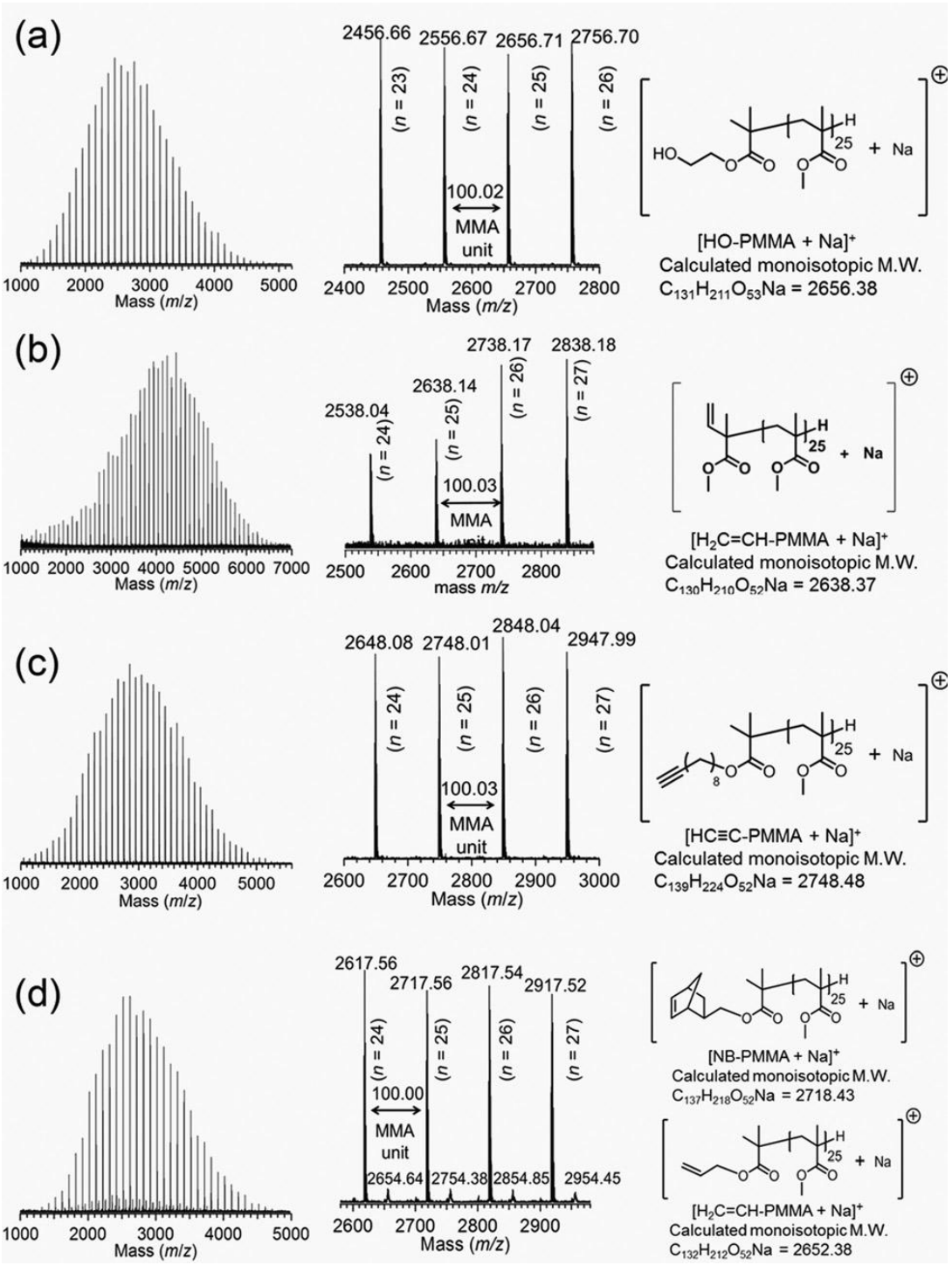

Figure. 2.8. MALDI-TOF MS spectra of (a) HO-PMMA (Run 1, $M_{n,SEC}$ = 3300 g mol^{-1}, M_w/M_n = 1.08), (b) H_2C=CH-PMMA, (Run 11, $M_{n,SEC}$ = 4500 g mol^{-1}, M_w/M_n = 1.08) (c) HC≡C-PMMA (Run 6, $M_{n,SEC}$ = 3800 g mol^{-1}, M_w/M_n = 1.07), and (d) NB-PMMA, (Run 16, $M_{n,SEC}$ = 3400 g mol^{-1}, M_w/M_n = 1.08).

2.3.2 Synthesis of hydroxyl, ethynyl, vinyl, and bromo ω-end-functionalized PMMA

In addition to the α-end-functionalization, the ω-end functionalization of PMMA by Me_3SiNTf_2-catalyzed GTP using functional terminators was also attempted. In order to find a suitable terminator, five potential candidates, methyl α-phenylacrylate (α-PhA-Me), dimethyl itaconate (DMI), benzaldehydes (BA), ethyl ethylacrylate (EEA), and *N*,*N*-dimethyl methacrylamide (DMMAm), were initially used to investigate their suitability, as shown in Scheme 2.6

Scheme 2.6 Potential Terminators for Me_3SiNTf_2-catalyzed GTP of MMA

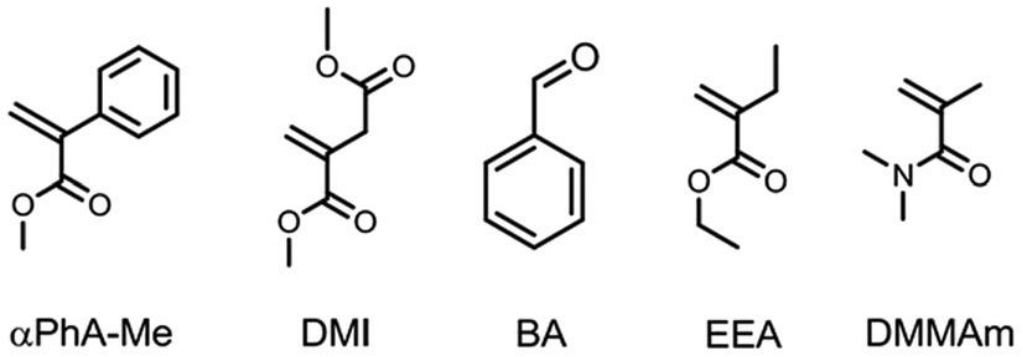

Following the quantitative polymerization of 25 equiv. MMA, the termination reaction was carried out for 24 h with the addition of an excessive quantity of terminator. Table 2.2 summarizes the polymerizations and ω-end-functionalization results. All the polymerizations (Runs 21–25) produced well-defined PMMAs with the targeted molar mass and extremely narrow dispersity. For the %F, a quantitative value (>99%) was only achieved when α-PhA-Me was used (Run 21). High %F values of 92.1% and 78.6% were also attained with DMI (Run 22) and BA (Run 23), respectively.

Table 2.2. Termination reaction using αPhA-Me, DMI, BA, EEA, and DMMAm subsequent to Me_3SiNTf_2-catalyzed GTP of MMA[a]

Run	Terminator (T)	$[T]_0/[I]_0$	$M_{n,SEC}$[b]	M_w/M_n[b]	%F[c]
21	α-PhA-Me	5	3470	1.07	>99
22	DMI	5	3350	1.07	92.1
23	BA	5	3440	1.09	78.6
24	EEA	10	3540	1.07	46.9
25	DMMAm	5	3100	1.08	0

[a] Ar atmosphere; $[M]_0$ = 1.0 mol L^{-1}; initiator, MTS; catalyst, Me_3SiNTf_2; $[M]_0/[I]_0/[Cat.]_0$ = 25/1/0.05; solvent, CH_2Cl_2; polymerization time, 2 h; termination time, 24 h; polymerization temperature, room temp.; MMA conversion determined using ^1H NMR in $CDCl_3$, >99%. [b] Determined via SEC in THF using PMMA standards. [c] End-functionalization efficiency estimated using intensity of ion peaks in MALDI-TOF MS spectrum.

On the contrary, a moderate %F of only 46.9% was obtained using EEA (Run 24) and absolutely no end-functionalized product was obtained using DMMAm (Run 25). The termination behavior using these potential terminators was further investigated by MALDI-TOF MS measurements, as shown in Figure 2.4. The MALDI-TOF MS spectrum of the α-PhA-Me terminated PMMA only showed one population of molecular ion peaks. In addition, the value of each ion peak could be perfectly assigned to a PMMA possessing a MTS residue at the α-end, a specified degree of polymerization (DP) of MMA, and a reacted α-PhA-Me residue at the ω-end, strongly suggesting the quantitative ω-end-functionalization by α-PhA-Me. When using DMI, the MALDI-TOF MS spectrum exhibited three populations of molecular ion peaks. The two main populations of ion peaks corresponded to the ω-end-functionalized products with DMI, in which one population was attributed to the desilylated DMI ω-end-functionalized products and the

other was the silylated ones.

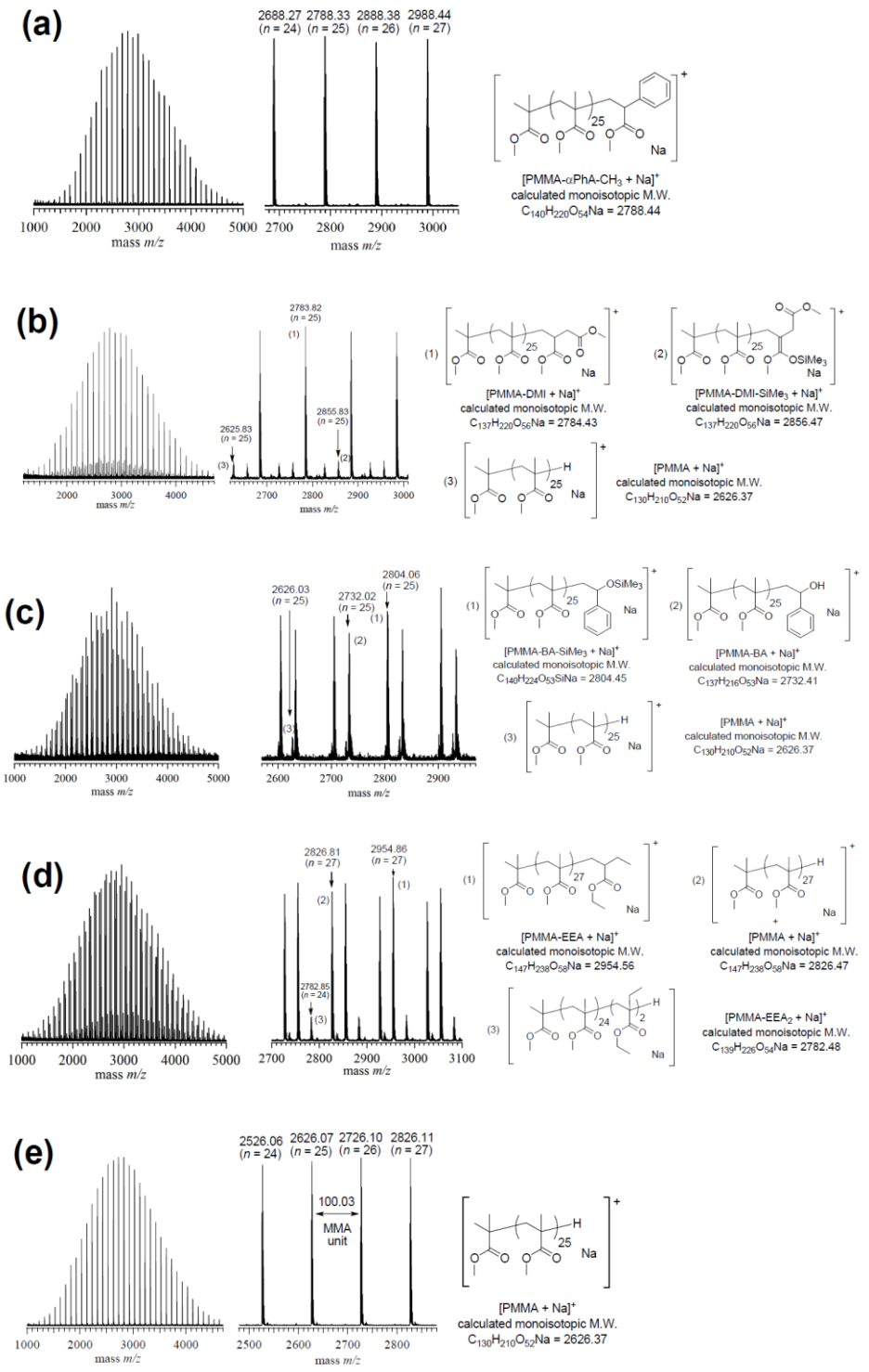

Figure 2.9. MALDI-TOF MS spectra of PMMAs terminated by (a) α-PhA-Me, (b) DMI, (c) BA, (d)EEA, and (e) DMMAm.

The sub ion peaks were assigned to the hydrogen ω-end-functionalized PMMA products, which were obtained after quenching with alcohol. Obviously, no DMI functionality was bonded to their ω-ends at all for the PMMA products due to the sub ion peaks. When using BA, a similar ion peak distribution to that of DMI was observed in its MALDI-TOF MS spectrum. Unlike DMI and BA, termination using EEA resulted in three types of products, i.e., the products with the ω-end-functionalized with EEA, two EEAs, and hydrogen. The targeted product with the ω-end-functionalized with EEA only had a 46.9% content. In the case using DMMAm, only the ion peaks of the hydrogen ω-end-functionalized PMMAs were observed in its MALDI-TOF MS spectrum, indicating that DMMAm could not react with the living propagation end of PMMA at all. It seems that the %F was significantly dependent on the chemical structure of the terminator used. For instance, α-PhA-Me with an electron-delocalized phenyl group at the α position was highly favorable for the electrophilic reaction with the living PMMA chain end of a SKA moiety as the active center. DMI and EEA with electron-donating alkyl groups at the α position, on the other hand, showed a less efficient electrophilicity toward the SKA group at the PMMA chain end. DMMAm with low monomer reactivity did not react with the SKA group at all. Since α-PhA-Me was the most efficient terminator for the Me_3SiNTf_2-catalyzed GTP of MMA, four functional α-phenylacrylates, **2a–2d**, were correspondingly used for synthesizing the ethynyl, hydroxyl, vinyl, and bromo ω-end-functionalized PMMAs (PMMA-C≡CH, PMMA-OH, PMMA-CH=CH_2, and PMMA-Br). After a 2 h polymerization of MMA in CH_2Cl_2, the termination reaction was further carried out for 24 h by adding an excessive amount of a terminator to the polymerization mixture. All the polymerizations (Runs 26–29) had a quantitative monomer conversion and produced

PMMAs with a targeted molar mass around 3000 g mol^{-1} and dispersity narrower than 1.07, as shown in Table 2.3.

Table 2.3. Synthesis of ω-end-functionalized PMMAs via Me_3SiNTf_2-catalyzed GTP of MMA using functional α-phenylacrylates (2a–2d)[a]

Run	Terminator (T)	$M_{n,cald.}$[b]	$M_{n,SEC}$[c]	M_w/M_n[c]	%F[d]
26	2a	2900	3460	1.07	>99
27[e]	2b	2930	3250	1.06	>99
28	2c	2830	3730	1.07	>99
29	2d	2880	3690	1.07	>99

[a] Ar atmosphere; $[M]_0$ = 1.0 mol L^{-1}; $[MMA]_0/[MTS]_0/[Me_3SiNTf_2]_0$ = 25/1/0.05; $[T]_0/[MTS]_0$ = 5; solvent, CH_2Cl_2; polymerization temperature, room temp.; polymerization time, 2 h; termination time, 24 h; MMA conversion (conv.) determined using ^{1}H NMR in $CDCl_3$, > 99%. [b] Calculated using $M_{n,cald} = [MMA]_0/[I]_0 \times$ conv. × (M.W. of MMA: 100.12) + (M.W. of initiator residue: 101.12) + (M.W. of terminator residue: 2a = 272.41, 2b = 306.47, 2c = 202.25, and 2d = 255.11) × %F. [c] Determined via SEC in THF using PMMA standards. [d] End-functionalization efficiency determined using ^{1}H NMR in acetone-d_6. [e] Terminated using ^{t}BuOH instead of MeOH.

The %F, as estimated using the ^{1}H NMR measurements, was >99% no matter which functional α-phenylacrylate was used. The existence of these functionalities at the ω-end of PMMA was confirmed by ^{1}H NMR and MALDI-TOF MS measurements.

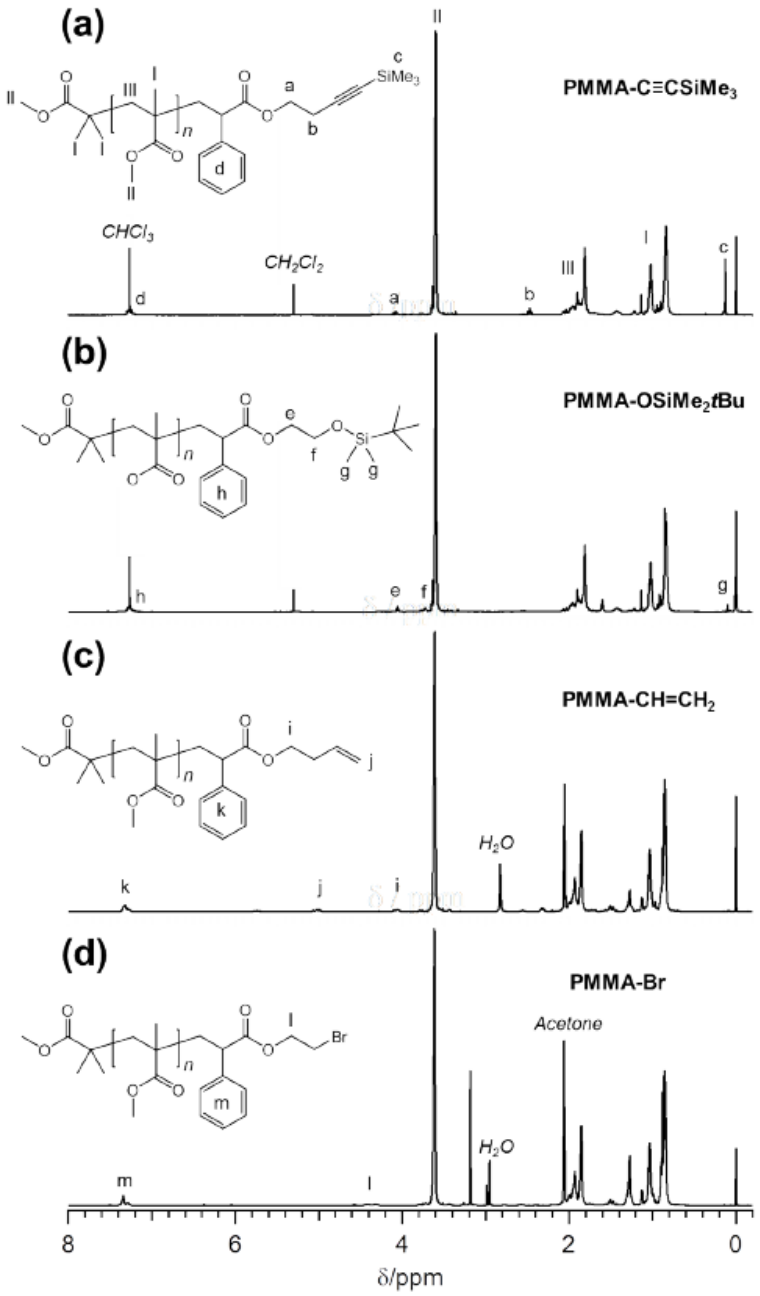

Figure 2.10. ^{1}H NMR spectra of (a) PMMA-C≡CSiMe$_3$ (Run 26, $M_{n,SEC}$= 3,460; M_w/M_n= 1.07) in CDCl$_3$, (b) PMMA-OSiMe$_2$^{t}Bu (Run 27, $M_{n,SEC}$= 3,250; M_w/M_n= 1.06) in CDCl$_3$, (c) PMMACH=CH$_2$ (Run 28, $M_{n,SEC}$= 3,730; M_w/M_n= 1.07) in acetone-d_6, and (d) PMMA-Br (Run 29, $M_{n,SEC}$= 3,690; M_w/M_n= 1.07) in acetone-d_6.

As shown in the ^{1}H NMR spectra Figure. 2.5, the characteristic signals belonging to the

residues of **2a–2d** were simultaneously observed at 0.11–0.15, 4.01–4.15, and 7.18–7.33 ppm due to the $Si(CH_3)_3$, $–CH_2O_2C–$, and aromatic H of 2a, at 4.03–4.08 and 7.17–7.32 ppm due to the $–CH_2O_2C–$ and aromatic H of 2b, at 3.99–4.15, 5.65–5.82, 4.94–5.10, and 7.22–7.42 ppm due to the $–CH_2O_2C–$, $–CH=CH_2$, $–CH=CH_2$, and aromatic H of 2c, and at 4.26–4.47 and 7.23–7.40 ppm due to the $–CH_2O_2C–$, and aromatic H of 2d, respectively, together with the proton signals of the PMMA main chain at 0.77–1.25, 1.76–2.09, and 3.54–3.69 ppm.

In the MALDI-TOF MS spectra shown in Figure. 2.6, each of the spectra showed only one population of ion peaks with the interval between two neighboring ion peaks being around 100.05 (exact molar mass of MMA unit). In addition, no matter which functional α-phenylacrylate was used, the *m*/*z* value of each ion peak perfectly corresponded to the polymer product which was composed of an MTS residue at the α-end, specified MMA units in the main chain, and a reacted residue of a functional α-phenylacrylate at the ω-end. For instance, the determined m/z values of the sodium-cationized 25-mer PMMA-$C{\equiv}CSiMe_3$, PMMA-$OSiMe_2$*t*Bu, PMMA-$C=CH_2$, and PMMA-Br were 2898.80, 2932.26, 2827.83, and 2879.75, respectively, which agreed closely with their theoretical monoisotopic molar masses of 2898.49, 2932.53, 2828.47, and 2880.36, respectively, when they had the predicted sodium cationized 25-mer structures of $[MeO_2CCMe_2\text{-}MMA_{25}\text{-}CH_2CHPhCCO_2(CH_2)_2C{\equiv}CSiMe_3 + Na]^+$, $[MeO_2CCMe_2\text{-}MMA_{25}\text{-}CH_2CHPhCCO_2(CH_2)_2OSiMe_2tBu + Na]^+$, $[MeO_2CCMe_2\text{-}MMA_{25}\text{-}CH_2CHPhCCO_2(CH_2)_2CH=CH_2 + Na]^+$, and $[MeO_2CCMe_2\text{-}MMA_{25}\text{-}CH_2CHPhCCO_2(CH_2)_2Br + Na]+$, respectively. These results provided definitive proof to support the fact that the functional α-phenylacrylate was stoichiometrically bonded to the

PMMA ω-end after the termination reaction.

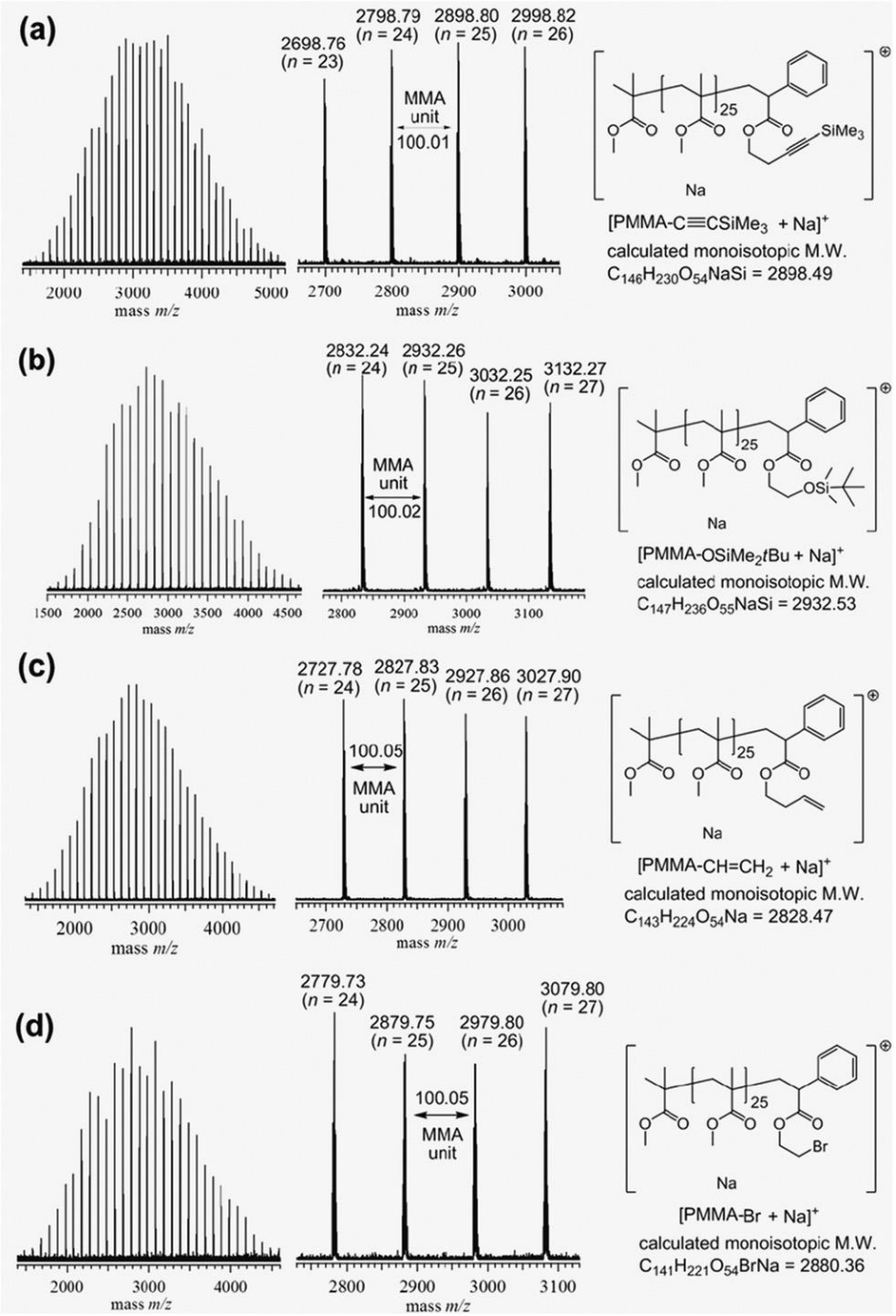

Figure.2.11. MALDI-TOF MS spectra of (a) PMMA-C≡CSiMe$_3$ (Run 26, $M_{n,SEC}$ = 3460; M_w/M_n = 1.07), (b) PMMA-OSiMe$_2$^{t}Bu (Run 27, $M_{n,SEC}$ = 3250; M_w/M_n = 1.06), (c) PMMA-CH=CH$_2$ (Run 28, $M_{n,SEC}$ = 3730; M_w/M_n = 1.07), and (d) PMMA-Br (Run 29, $M_{n,SEC}$ = 3690; M_w/M_n = 1.07).

2.3.3 Synthesis of ω-end-functionalized PMMA with a hydroxyl group by *t*-Bu-P_4-catalyzed GTP using benzaldehydes

After failing to achieve quantitative ω-end-functionalization of hydroxyl group by Me_3SiNTf_2 catalyzed GTP the author proceeded to attempt achieving quantitative ω-end-functionalization of hydroxyl group by *t*-Bu-P_4 catalyzed GTP. In this study, the newly prepared 1-ethoxy-1-(trimethylsiloxy)-2-methylprop-1-ene (SKA_{Et}) was used as the initiator instead of the common silyl ketene acetal (SKA) of 1-methoxy-1-(trimethylsiloxy)-2-methylprop-1-ene (SKA_{Me}) to provide an indicative α-end for the estimation of the ω-end-functionalization efficiency (%F), which is described later. For the synthesis of ω-end-functionalized PMMA with a hydroxyl group (PMMA-OH) by *t*-Bu-P_4-GTP, benzaldehyde (PhCHO) and various *p*-substituted benzaldehydes (*p*-R-PhCHO) were used as terminators due to their ability to promote the Mukaiyama aldol reaction with the reactive SKA group at the ω-end of PMMA, as shown in Scheme 2.2. In order to achieve this objective, the synthesis of a living PMMA carrying a reactive SKA group at its ω-end, PMMA–SKA, was first prepared by the *t*-Bu-P_4-catalyzed GTP of MMA in the absence of any terminating agent. The resulting living polymer chain end was then reacted with an excess amount of a benzaldehydes terminator. Importantly, the ω-end-functionalization reaction was required to be implemented immediately after the monomer consumption to suppress any side reactions, such as the back-biting reaction, which results in the cyclization of the ω-terminal trimer, to the barest minimum. The polymerization of MMA with $[MMA]_0/[SKA_{Et}]_0/[t\text{-Bu-}P_4]_0$ = 25/1/0.01 and the termination reaction with PhCHO were initially carried out in toluene at room temperature under an argon atmosphere, as listed in Table 2.4 (runs 30-33). These

polymerizations produced PMMA products with polydispersities of ca. 1.20 and molar masses in the range of 3.6–4.1 kg mol^{-1} by SEC measurements and in the range of 3.2–3.6 kg mol^{-1} by ^{1}H NMR measurements, either of which were ca. 20–50% higher than the calculated molar mass ($M_{n,cald}$) of 2.7 kg mol^{-1}. This could be attributed to the fact that the low polarity of toluene led to relatively lower initiation efficiency. It was found that the initial molar ratio of terminator to initiator ($[T]_0/[I]_0$) significantly affected the %F of the resulting polymers. A relatively high $[PhCHO]_0/[SKA_{Et}]_0$ ratio was preferred for synthesizing the PMMA-OH with a high %F. The %F increased with the increasing $[PhCHO]_0/[SKA_{Et}]_0$ ratio and a quantitative %F was eventually achieved at the $[PhCHO]_0/[SKA_{Et}]_0$ ratio of 10 (run 33). This ratio was thus applied to all the subsequent termination reactions when benzaldehyde derivatives were used as terminators.

Table 2.4. Synthesis of hydroxyl ω-end-functionalized PMMAs by *t*-Bu-P$_4$-catalyzed GTP using benzaldehyde (PhCHO) as terminator [a]

run	Catalyst	$[PhCHO]_0/[SKA_{Et}]_0$	$M_{n,calcd}$ [b] (kg mol^{-1})	$M_{n,SEC}$ [c] (kg mol^{-1})	$M_{n,NMR}$ [d] (kg mol^{-1})	M_w/M_n [c]	%F [d]
30	*t*-Bu-P$_4$	1	2.7	3.6	3.2	1.20	12.6
31	*t*-Bu-P$_4$	2	2.7	3.5	3.3	1.19	30.2
32	*t*-Bu-P$_4$	5	2.7	4.0	3.6	1.20	82.4
33	*t*-Bu-P$_4$	10	2.7	4.1	3.5	1.23	>99

[a] Ar atmosphere; room temperature; Solvent, toluene; $[MMA]_0/[SKA_{Et}]_0$, 25; $[t\text{-Bu-P}_4]_0/[SKA_{Et}]_0$, 0.01; Polymerization time, 3 min; $[PhCHO]_0/[SKA_{Et}]_0$, 10; Termination time, 12 h; MMA conversion > 99%. [b] Calculated from $([MMA]_0/[SKA_{Et}]_0)$ × (MMA conversion) × (M.W. of MMA) + (M.W. of initiator residue) + (M.W. of terminator residue) × %F. [c] Determined by SEC in THF using PMMA standards. [d] Estimated by ^{1}H NMR measurements in acetone-d_6.

In order to obtain a better molar mass control, the polymerization in THF (run 35, Table 2.5) was examined. The fine tuning of the molar mass of the resulting polymer suggested that THF was the preferred solvent for the *t*-Bu-P_4-catalyzed GTP of MMA compared to the polymerization in toluene, *i.e.*, the polymerization in THF affording a PMMA with an $M_{n,NMR}$ of 2.7 kg mol^{-1} and an M_w/M_n of 1.15, obviously allowed a much better polymerization control than that in toluene, which produced a PMMA (run 34, Table 2.5) with an $M_{n,NMR}$ of 3.7 kg mol^{-1} and an M_w/M_n of 1.23. Accordingly, THF was used as the polymerization solvent for all the *t*-Bu-P_4-catalyzed GTPs of MMA in the following sections.

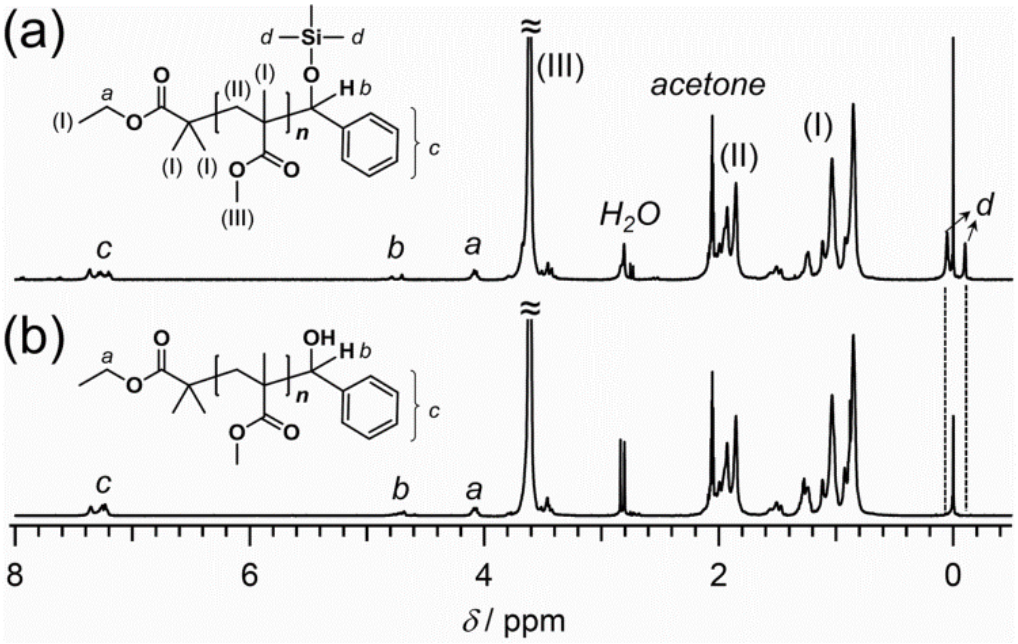

Figure 2.12. ^{1}H NMR spectra of (a) PMMA-$OSiMe_3$ obtained from Run 35 and (b) PMMA-OH obtained from Run 35 in acetone-d_6.

In the ^{1}H NMR spectrum of the PMMA terminated using PhCHO (PMMA-$OSiMe_3$, Figure 2.12a), the characteristic proton signals due to both the α- and ω-ends simultaneously appeared, *i.e.*, the methylene protons at 4.03 ppm (peak a) due to the

SKA_{Et} residue and the aromatic protons at 7.18-7.42 ppm (peak c) due to the benzaldehyde residue were clearly observed. In addition, the signals at 0.2 and -0.4 ppm (peak d) due to the trimethylsilyl group were also clearly observed even after the eventual termination by methanol. The *O-Si* bond was actually stable enough in methanol so that the trimethylsilyl group was still bonded as a protection moiety. Based on the fact that a polymer chain must possess an initiator residue at its α-end during the GTP process, the %*F* of the resulting PMMA was readily calculated by comparing the integral areas of peaks a and c, which was the reason that SKA_{Et} was used instead of SKA_{Me}.

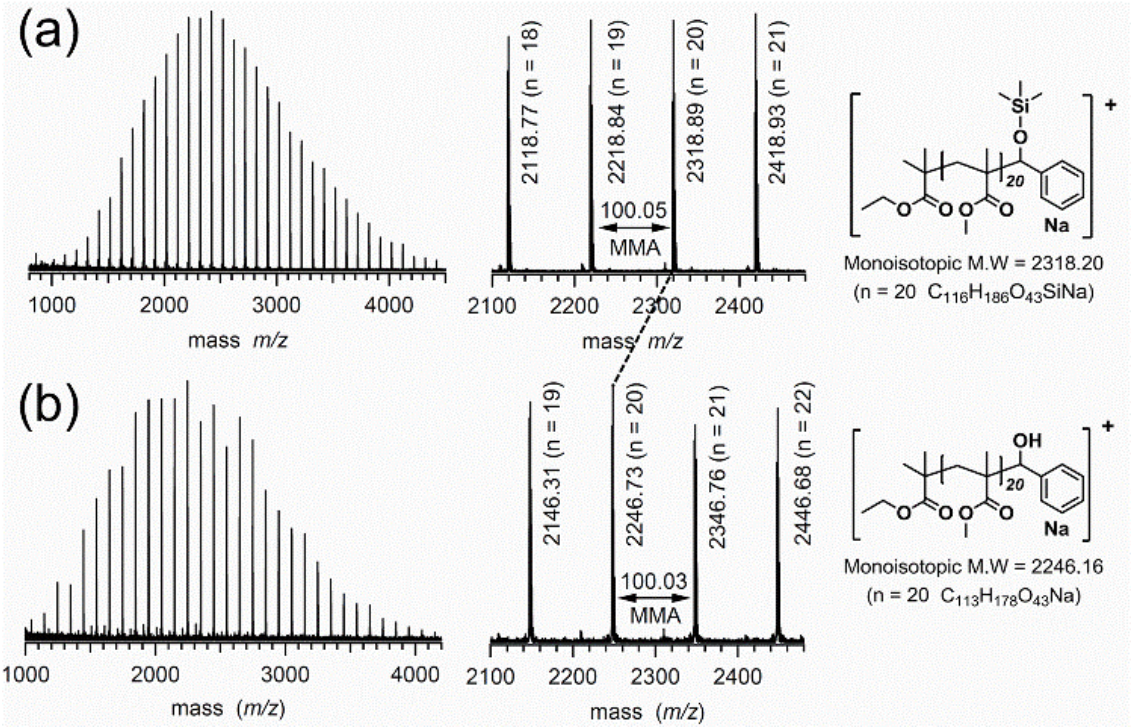

Figure 2.13. MALDI-TOF MS spectra in reflector mode of of (a) PMMA-$OSiMe_3$ obtained from Run 35 and (b) PMMA-OH obtained from Run 35.

The incorporation of a benzaldehyde moiety into the ω-end of the polymer chain was directly verified by matrix assisted laser desorption/ionization time-of-flight mass (MALDI-TOF MS) analyses. As a typical example, the MALDI-TOF MS spectrum of PMMA-$OSiMe_3$ (run 35, Figure 2.13a) showed only one population of molecular ion peaks. The distance between any two neighboring molecular ion peaks was extremely close to 100.05, which corresponded to the exact mass of 100.12 (MMA unit). In addition, the *m*/*z* values of the observed molecular ion peaks were very consistent with the calculated molar masses of the PMMAs having an SKA_{Et} residue as the α-end group and a terminator residue as the ω-end group; for example, the observed value of 2318.89 Da well agreed with the calculated value of 2318.20 for the sodium-cationized 20-mer of PMMA-$OSiMe_3$ $[EtO_2CMe_2C\text{-}MMA_{20}\text{-}CH(OSiMe_3)Ph + Na]^+$. This result strongly suggested that the termination reaction using benzaldehyde smoothly proceeded to produce structurally defect-free PMMA-$OSiMe_3$ without any side reactions after the *t*-Bu-P_4-catalyzed GTP of MMA. To obtain the hydroxyl functionality at the ω-end of PMMA, the deprotection reaction was further carried out to remove the trimethylsilyl group. This deprotection was implemented by treating PMMA-$OSiMe_3$ with 1N *aq.* HCl in methanol to produce PMMA-OH. The completion of deprotection was confirmed by ^1H NMR and MALDI-TOF MS measurements; the proton signals of trimethylsilyl group completely disappeared after processing the polymer with 1N *aq.* HCl, as shown in Figure 2.12b. In the MALDI-TOF MS spectrum of the deprotected product (PMMA-OH), as shown in Figure 2.13b, the *m*/*z* values of the observed molecular ion peaks were in good agreement with the calculated molar masses of PMMA-OHs; for example, the observed ion peak value of 2318.89 Da of the 20-mer of PMMA-$OSiMe_3$ showed an

obvious shift to 2246.73 corresponding to its deprotected 20-meric product of PMMA-OH, which has the sodium-cationized structure of $[EtO_2CMe_2C\text{-}MMA_{20}\text{-}CH(OH)Ph + Na]^+$, clearly indicating that the deprotection was very successful and the targeted structurally defect-free PMMA-OH was eventually obtained.

These results demonstrate that *t*-Bu-P_4 is an effective catalyst for the GTP of MMA along with the ω-end-functionalization of the propagating PMMA end with benzaldehydes. The author thereby investigated the catalyst effect on the %*F* of PMMAs. Apart from *t*-Bu-P_4, other organocatalysts, such as 2,8,9-triisobutyl- 2,5,8,9-tetraaza-1-phosphabicyclo[3.3.3]undecane (TiBP), trifluoromethanesulfonimide ($HNTf_2$), and 2,3,4,5,6-pentafluorophenylbis(trifluoromethanesulfonyl)methane ($C_6F_5CHTf_2$), which have been previous proven to be effective for the GTP of MMA,[18-23] were used, Table 2.5 lists the polymerization results (runs 36-36). For quantitative monomer conversion, the catalysts of TiBP, $HNTf_2$, and $C_6F_5CHTf_2$ needed 2 - 24 h even though only 3 min was sufficient for *t*-Bu-P_4. In addition, the molar mass control using these catalysts was less effective with the molar masses much higher than their respective calculated values in comparison to *t*-Bu-P_4. It is very clear that all the termination reactions using these catalysts did not achieve quantitative ω-end-functionalization, *i.e.*, TiBP, $HNTf_2$, and $C_6F_5CHTf_2$ achieved %*F*s of 65.5, 47.3 and 15.2%, respectively. These results obviously indicated that the organic base catalysts are more suitable than organic acid catalysts for the termination reaction. The ω-end-functionalization by benzaldehyde is assumed to be significantly dependent on the polymerization mechanism because the base catalysts should promote the SKA ends of the polymer to produce extremely reactive enolate anions while the SKA structures are maintained for the acid catalysts. These results

demonstrated again that *t*-Bu-P_4 is the most effective catalyst for the synthesis of the ω-end-functionalized polymers with a hydroxyl group using the GTP method. Also unlike previous conventional catalysts used to synthesize hydroxyl end-functionalized PMMA, [33] *t*-Bu-P_4 could suppress back-biting side reactions.

Table 2.5 Synthesis of hydroxyl ω-end-functionalized PMMAs by organocatalyzed GTP using different catalysts [a]

run	Catalyst	Solvent	$[MMA]_0/[SKA_{Et}]_0$	$M_{n,calcd}$ [b] (kg mol^{-1})	$M_{n,SEC}$ [c] (kg mol^{-1})	$M_{n,NMR}$ [d] (kg mol^{-1})	M_w/M_n [c]	%F [d]
34	*t*-Bu-P_4	Toluene	25	2.7	4.1	3.7	1.23	>99
35	*t*-Bu-P_4	THF	25	2.7	2.9	2.7	1.15	>99
36[e]	TiBP	THF	25	2.7	4.9	4.5	1.41	65.5
37 [f]	$HNTf_2$	CH_2Cl_2	25	2.7	4.5	4.1	1.07	47.3
38[g]	$C_6F_5CHTf_2$	CH_2Cl_2	25	2.6	4.0	3.7	1.08	15.2
39[h]	*t*-Bu-P_4	THF	50	5.2	5.9	5.2	1.17	>99
40[i]	*t*-Bu-P_4	THF	100	10.2	11.1	11.4	1.14	>99

[a] Ar atmosphere; room temperature; $[t\text{-Bu-}P_4]_0/[SKA_{Et}]_0$, 0.01; Polymerization time, 3 min; $[PhCHO]_0/[SKA_{Et}]_0$, 10; Termination time, 12 h; MMA conversion > 99%. [b] Calculated from $([MMA]_0/[SKA_{Et}]_0)$ × (MMA conversion) × (M.W. of MMA) + (M.W. of initiator residue) + (M.W. of terminator residue) × %F. [c] Determined by SEC in THF using PMMA standards. [d] Estimated by ^{1}H NMR measurements in acetone-d_6. [e] $[TiBP]_0/[SKA_{Et}]_0$, 0.02; Polymerization time, 2 h; Termination time, 24 h. [f] $[HNTf_2]_0/[SKA_{Et}]_0$, 0.05; Solvent, CH_2Cl_2; Polymerization time, 24 h; Termination time, 24 h. [g] $[C_6F_5CHTf_2]_0/[SKA_{Et}]_0$, 0.05; Polymerization time, 24 h; Termination time, 24 h. [h] $[t\text{-Bu-}P_4]_0/[SKA_{Et}]_0$, 0.02. [i] $[t\text{-Bu-}P_4]_0/[SKA_{Et}]_0$, 0.02; 0.64 equiv. of *t*-Bu-P_4 was further added to the polymerization mixture followed by the addition of PhCHO.

The author next estimated the effect of the molar mass of PMMA on the %*F* (Runs 35, 39-40). The molar mass of the synthesized polymers increased with the increasing monomer-to-initiator ratio ($[MMA]_0/[SKA_{Et}]_0$) and maintaining the terminator ratio constant at 10 while monitoring the effect that had on the %*F*. The polymerization results showed that the living nature of the GTP afforded excellent control of the molar mass and narrow polydispersity. The $M_{n,SEC}$s well agreed with their $M_{n,cald.}$s in that sense, and the polydispersities were also narrow for the polymerizations of all the $[M]_0/[I]_0$ ratios investigated. For the %*F*, the results showed that an increase in the molar mass made the end-functionalization reaction more difficult due to increased steric hindrance for the longer polymer chains. Therefore, an increased amount of the catalyst was required to achieve quantitative functionalization. The %*F* results showed that the quantitative ω-end-functionalization of PMMA by *t*-BuP_4-catalyzed GTP using benzaldehyde could be effectively achieved at even high molar masses ($M_{n,NMR}$) of 5.2 (run 39) and 11.4 kg mol^{-1} (run 40), which were directly confirmed by ^1H NMR measurements by comparing the proton signals at the α and ω-ends, as already described.

Electron-withdrawing and electron-donating substituents play significant role in organic reactions, whose introduction to a reactant in general affects the reaction rate, yield and even the reaction possibility. In this work, the author also investigated the effect of *para*-position substituent of benzaldehydes on the %*F* of PMMAs by using benzaldehydes possessing electro-withdrawing substituents, such as *p*-phenylbenzaldehyde, *p*-fluorobenzaldehyde, and *p*-trifluoromethylbenzaldehyde, and electro-donating substituent, such as *p*-anisaldehyde, on their *para*-positions. The termination results shown in Runs 41-44 firmly indicated that *para*-position substituents had little or no significant effect

on %*F* as the results obtained using *para*-substituted benzaldehyde terminators were almost the same as that obtained with the unsubstituted benzaldehyde (Run 35) under the same conditions. Nevertheless, the kinetic studies, shown in Figure 2.14, proceeded quite fast and did imply that *para*-position substituents affected the rate of the reaction with the end-functionalization reaction proceeding faster when terminators carrying an electron-withdrawing substituent like –F, whereas those carrying an electron-donating *para*-substituents like $–OCH_3$ were relatively slower compared to benzaldehydes with no substituents.

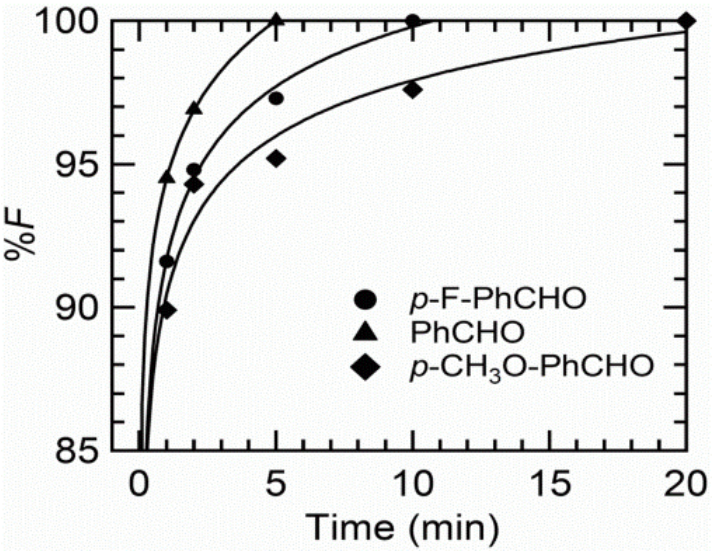

Figure 2.14. Dependence of %*F* on the reaction time of termination using benzaldehydes of (▲) *p*-F-PhCHO, (●) PhCHO, and (◆) *p*-CH_3O-PhCHO.

Table 2.6. Synthesis of ω-end-functionalized PMMAs by *t*-Bu-P_4-cayalyzed GTP using functional benzaldehyde as terminator [a]

run	Terminator (T)	$M_{n,calcd}$ [b] (kg mol^{-1})	$M_{n,SEC}$ [c] (kg mol^{-1})	$M_{n,NMR}$ [d] (kg mol^{-1})	M_w/M_n [c]	%F [d]
41	*p*-MeO-PhCHO	2.8	3.0	3.0	1.14	>99
42	*p*-Ph-PhCHO	2.8	2.8	2.8	1.17	>99
43	*p*-F-PhCHO	2.8	2.8	2.7	1.17	>99
44	*p*-CF_3-PhCHO	2.8	3.0	3.8	1.14	>99
45	*p*-H_2C=$CHCH_2O$-PhCHO	2.8	3.3	3.2	1.21	>99
46	*p*-$Me_3SiC{\equiv}CCH_2O$-PhCHO	2.8	3.5	3.3	1.17	>99
47	*p*-Et_2N-PhCHO	2.8	3.5	3.4	1.12	>99
48	*p*-*t*BuO-PhCHO	2.8	3.6	3.8	1.20	>99

[a] Ar atmosphere; room temperature; Solvent, THF; $[MMA]_0/[SKA_{Et}]_0$, 25; $[t\text{-Bu-}P_4]_0/[SKA_{Et}]_0$, 0.01; Polymerization time, 3 min; $[T]_0/[SKA_{Et}]_0$, 10; Termination time, 12 h; MMA conversion > 99%. [b] Calculated from $([MMA]_0/[SKA_{Et}]_0) \times$ (MMA conversion) × (M.W. of MMA) + (M.W. of initiator residue) + (M.W. of terminator residue) × %F. [c] Determined by SEC in THF using PMMA standards. [d] Estimated by ^{1}H NMR measurements in acetone-d_6.

The effectiveness of the ω-end-functionalization by the *t*-Bu-P_4-catalyzed GTP was also applied to synthesize ω-end-bifunctionalized PMMAs (Runs 45-48) using functional benzaldehydes as terminators. Similar to the case using *para*-substituted benzaldehyde, functional benzaldehyde terminations also provided quantitative %F. After the end-functionalization reaction, a deprotection reaction was further carried out to remove the trimethylsilyl groups with 1N *aq.* HCl, affording the hydroxyl and alkynyl, hydroxyl and butoxy, hydroxyl and allyloxy, and hydroxyl and amino -end-bifunctionalized PMMAs.

2.4 Conclusions

A set of α-end-functionalized PMMAs with hydroxyl, ethynyl, vinyl, and norbornenyl groups were obtained with targeted molar masses up to 50 000 g mol^{-1}, dispersities narrower than 1.22, and defect-free polymer structures by either Me_3SiNTf_2 or *t*-Bu-P_4-catalyzed GTPs using newly designed functional SKAs as initiators. In addition, quantitative ω-end-functionalization of PMMA by the Me_3SiNTf_2-catalyzed GTP succeeded for the first time using α-phenylacrylate terminators. The quantitative incorporation of ethynyl, hydroxyl, vinyl, norbornenyl, and bromo functionalities into either the α- or ω-end of PMMA was significantly supported by the MALDI-TOF MS measurements. The author described the precise synthesis of PMMAs functionalized with a hydroxyl group by *t*-Bu-P_4-catalyzed GTP using aromatic aldehydes as terminators. The termination reaction between a living PMMA and benzaldehyde was proved to be an efficient system for synthesizing ω-end-functionalized PMMAs with the hydroxyl group with controlled molar masses, relatively narrow polydispersities, and quantitative ω-end functionalization efficiencies. In addition, ω-end-bifunctionalized PMMAs with a hydroxyl group along with an alkynyl, a butoxy, an allyloxy, and an amino group were successfully synthesized using functional benzaldehydes. This study provides a facile method for end-functionalization by the organocatalyzed GTP procedure. These reactive functionalities at the polymer ends are of great significance for carrying out further chemical conversions into other functional moieties, such as bioactive peptides and fluorescent dyes, and to serve as polymeric precursors for constructing polymethacrylate-based complicated polymer architectures, such as block copolymers, star-shaped polymers, and graft copolymers.

2.5 References

1. D. J Lunn, E. H. Discekici, J. R. de Alaniz, W. R. Gutekunst and C. J Hawker, *J. Polym. Sci., Part A: Polym. Chem.*, **2017**, 55, 808-819.
2. F. Lo Verso and C. N. Likos, *Polymer* **2008**, *49*, 1425–1434.
3. R. A. Sperling and W. J. Parak, *Philos. Trans. R. Soc. A Math. Phys. Eng. Sci.* **2010**, *368*, 1333–1383
4. Y. Mai and A. Eisenberg, *Chem. Soc. Rev.* **2012**, *41*, 5969–5985.
5. M. Beija, M.-T. Charreyre and J. M. G. Martinho, *Prog. Polym. Sci*. **2011**, *36*, 568–602.
6. S. Dehn, R. Chapman and K. A. Jolliffe, S. Perrier, *Polym. Rev.* **2011**, *51*, 214–234.
7. Miasnikova, A. Laschewsky, *J. Polym. Sci. Part A Polym. Chem.* **2012**, *50*, 3313–3323.
8. B. J. Kim, S. Given-Beck, J. Bang, C. J. Hawker and E. J. Kramer, *Macromolecules* **2007**, *40*, 1796–1798.
9. T. D. Michl, K. E. S. Locock, N. E. Stevens, J. D. Hayball, K. Vasilev, A. Postma, Y. Qu, A. Traven, M. Haeussler, L. Meagher and H. J. Griesser, *Polym. Chem.* **2014**, *5*, 5813–5822.
10. J. Du, H. Willcock, J. P. Patterson, I. Portman and R. K. O'Reilly, *Small* **2011**, *7*, 2070–2080.
11. M.-H. Wei, B. Li, R. L. A. David, S. C. Jones, V. Sarohia, J. A. Schmitigal and J. A. Kornfield, *Science* **2015**, *350*, 72–75.

12. U. Koldemir, S. R. Puniredd, M. Wagner, S. Tongay, T. D. McCarley, G. D. Kamenov, K. Mullen, W. Pisula and J. R. Reynolds, *Macromolecules* **2015**, *48*, 6369–6377.
13. J. Kuwabara, T. Yasuda, N. Takase and T. Kanbara, *ACS Appl. Mater. Interfaces* **2016**, *8*, 1752–1758.
14. C.-M. Chen, T.-H. Jen and S.-A. Chen, *ACS Appl. Mater. Interfaces* **2015**, *7*, 20548–20555.
15. G. Gody, C. Rossner, J. Moraes, P. Vana, T. Maschmeyer and S. Perrier, *J. Am. Chem. Soc.*, **2012**, *134*, 12596−12603.
16. R. Gnaneshwar and S. Sivaram**,** *J. Polym. Sci., Part A: Polym. Chem.*, **2007**, *45*, 2514-2531.
17. K. Y. Baek, M. Kamigaito and M. Sawamoto, *J. Polym. Sci.: Part A: Polym. Chem.*, **2002**, *40*, 1937–1944
18. D. Sogah and O. Webster, *J. Polym. Sci. Polym. Lett. Ed.*, **1983**, *21*, 927-931
19. W. R. Hertler, *J. Polym. Sci., Part A: Polym. Chem.*, **1991**, *29*, 869-873.
20. M. K. Mishra and S. Kobayashi, *Plast. Eng. (N.Y)*, **1999,** *53*, 350-376.
21. O. W. Webster, W. R. Hertler, D. Y. Sogah, W. B. Farnham and T. V.Rajanbabu, *J. Am. Chem. Soc.* **1983**, *105*, 5706-5708.
22. A. H. E. Müller, G. Litvinenko and D-Y. Yan, *Macromolecules* **1996**, *29*, 2346-2353.
23. D. Seebach, *Angew. Chem. Int. Ed. Engl.* **1988**, *27*, 1624-1654.
24. R. P. Quirk and G. P. Bidinger, *Polym. Bull.* **1989**, *22*, 63-70.

25. D. Y. Sogah, W. R. Hertler, O. W. Webster and G. M. Cohen, *Macromolecules* **1987**, *20*, 1473.

26. O. W. Webster and T. Heitz, *Makromol Chem* **1991**,*192*, 2463.

27. R. Asami, Y. Kondo and M. Takaki, *ACS Polym. Prepr., 1986, 27,* 186–187.

28. G. M. Cohen, *ACS Polym. Prepr.*, **1988**, *29*, 46.

29. W. R. Hertler, D. Y. Sogah and F. P. Boettcher, *Macromolecules*, **1990**, *23*, 1264–1268.

30. R. Quirk and J. Ren, *Polym. Int.*, **1993**, *32*, 205–212.

31. Y. Miura, T. Satoh, A. Narumi, O. Nishizawa, Y. Okamoto and T. Kakuchi, *J. Polym. Sci. Part A: Polym. Chem.* **2006**, *44*, 1436–1446.

32. K. Takada, K. Fuchise, N. Kubota, T. Ito, Y. G. Chen, T. Satoh and T. Kakuchi, *Macromolecules* **2014**, *47*, 5514-5525

Chapter 3

Organocatalytic Synthesis of Star-shaped Poly(methyl methacrylate)s Functionalized with Hydroxyl Groups by Arm- and Core-first Group Transfer Polymerizations

3.1 Introduction

The properties of polymers depend on their composition and structure or architecture. Therefore, the precise synthesis of complex architectures of polymers to control properties is a very important field of study in polymer chemistry. Star-shaped polymers are well-known to exhibit a low hydrodynamic volume and low viscosity in solution and these properties differ significantly in comparison with their linear equivalents.[1] It is generally accepted that the number and length of the arms have extremely significant influence on the properties of the star-shaped polymers.[2] A star-shaped polymer consists of at least three linear polymeric chains of comparable lengths radiating from one single multifunctional branched point, usually called the core or the central nodule, and which can itself be polymeric.[3] In a star-shaped polymer the core radius should be much smaller than the dimension, *e.g.*, the root-mean square end-to-end distance of the arm. If the core size is much larger, such an entity can be considered as a "nanoparticle", as its property will be dominated by the cross-linked nanometer-sized core. The main feature of star-shaped polymers, which makes them different from their linear analogues with identical molar mass (M_n), is their compact structure (smaller hydrodynamic volume and radius of gyration, and therefore lower viscosity) and multiple functionality that are useful in various applications. Star-shaped polymers are called homo-stars when all arms have the same chemical structure. On the contrary, those having arms with different chemical ingredients are hetero-stars. Arms may be built of homo-, co-, or even terpolymers, therefore the final properties of the resulting star-shaped polymers (*e.g.*, star-block and hetero-star copolymers) may be adjusted by choosing the respective chemical structure of an arm and core, depending on the required application.[4] A unique feature of a star-

shaped polymer is that it has a densely packed core and a less-compact outer shell. This nature might make a star-shaped polymer an interesting object when it is a thermoresponsive polymer.[5]

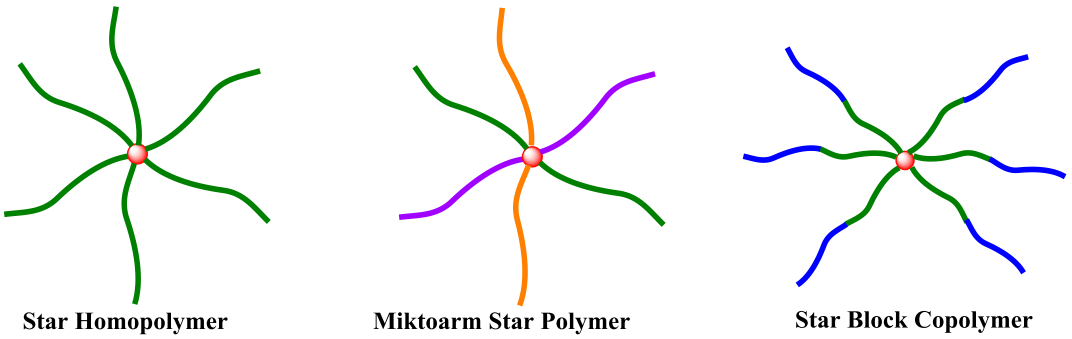

Figure 3.1. A schematic diagram of the three types of star-shaped polymers

Interest in the synthesis of star polymers, which began in the 1950s with living anionic polymerization, has increased in recent years due to the development of controlled/living radical polymerization (CRP).[6-9] Star polymers are synthesized via CRP using two strategies: core-first [10-20] and arm-first.[24-28] The core-first method involves the use of a multifunctional initiator, and the number of arms per star polymer is determined by the number of initiating functionalities on each initiator. The initiating sites on the star polymers can be further used for chain extension with a second monomer to form star block copolymers.[29-31] On the other hand, the arm-first method involves the synthesis of preformed linear arms and can be subdivided into two categories according to the features of the star formation procedure. The first is linear chain coupling with a multifunctional terminator or "grafting onto" a multifunctional core. The second one is chain extension of the linear arm precursor with a multivinyl cross-linking agent. In the former case, the

number of arms per star is determined by the functionality of the terminator, and the resulting star polymer no longer contains any initiating sites. However, because of the slow reaction between the polymer chain end and the multifunctional terminator, this method suffers from low coupling efficiency. Often a product obtained from such a reaction is a mixture of stars with different numbers of arms.[32] In the second case, the core of the star polymer is a cross-linked microgel, and the number of arms per star macromolecule is an average value. The initiating sites in the cross-linked core are still "living" and therefore can initiate polymerization of another monomer and produce miktoarm star copolymers via the "in-out" method.[12,32-36] The latter method using a multivinyl cross-linker is much simpler for synthesis of star polymers than the former one using a multifunctional terminator. Actually, the term "arm-first method" often refers to the latter approach. Star polymers prepared using this strategy contain multiple arms per molecule, and each arm and initiating site in the star molecule are potentially available for further modification and/or functionalization.

Our group has focused on studying and improving the scope and efficiency of group transfer polymerization by using metal-free organocatalysts. We have successfully reported the synthesis of star-shaped poly(methyl methacrylate)s by both the core and arm-first methods. [2,37] As a continuation of that previous work, in this chapter the author describes the precise synthesis of star-shaped poly(methyl methacrylate)s functionalized with hydroxyl groups through the core-first and arm-first methods by *t*-Bu-P_4-catalyzed GTP.

Scheme 3.1. Synthesis of Hydroxyl-functionalized Linear, Three-, Six- and Twelve-Armed Star-Shaped PMMAs (PMMA-OH, $(PMMA\text{-}OH)_3$, $(PMMA\text{-}OH)_6$ and $(PMMA\text{-}OH)_{12}$ respectively) by *t*-Bu-P_4-Catalyzed GTP of MMA Using SKA_{Et}, $(SKA)_3$, $(SKA)_6$, and $(SKA)_{12}$ as Initiators.

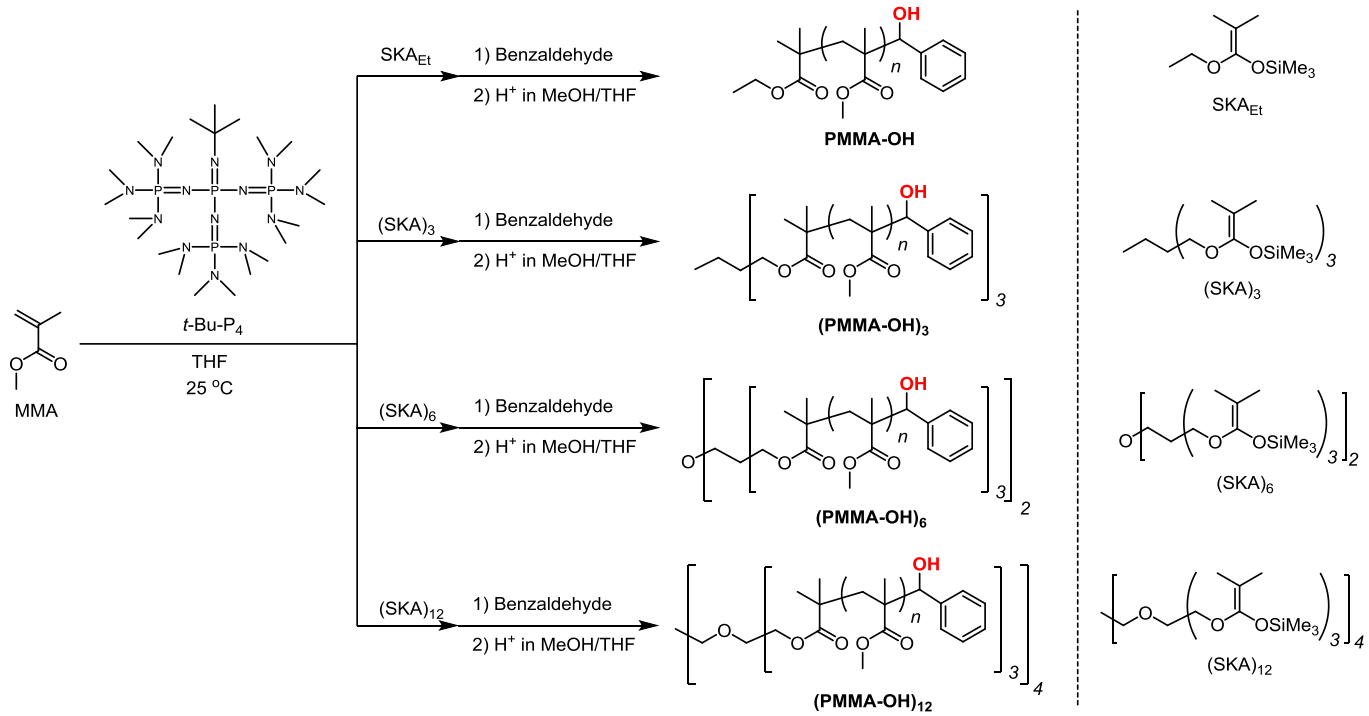

In the synthesis of star-shaped PMMAs functionalized with hydroxyl groups by GTP based on the core-first method the author describes the synthesis of the three-, six- and twelve-armed hydroxyl-functionalized star-shaped PMMAs $(PMMA\text{-}OH)_3$, $(PMMA\text{-}OH)_6$, and $(PMMA\text{-}OH)_{12}$, respectively by the *t*-Bu-P_4-catalyzed GTP using the silyl enolate initiators $(SKA)_3$, $(SKA)_6$, and $(SKA)_{12}$, respectively and benzaldehydes as the terminator as shown in Scheme 3.1. In the synthesis of star-shaped PMMAs functionalized with hydroxyl groups by GTP based on the arm-first method the author describes the synthesis of two- and three-armed hydroxyl-functionalized star-shaped PMMAs $PMMA_2\text{-}OH_2$ and $PMMA_3\text{-}OH_3$ by *t*-Bu-P_4-catalyzed GTP using multi-

aldehydic terephthaldehyde and benzene-1,3,5-tricarbaldehyde for the electrophilic termination of pre-synthesized PMMA arms as shown in Scheme 3.2.

Scheme 3.2. Synthesis of two- and three-arm PMMAs functionalized with two and three hydroxyl groups by organocatalyzed GTP of MMA using terepthalaldehyde and benzene-1,3,5-tricarbaldehyde, respectively as terminators.

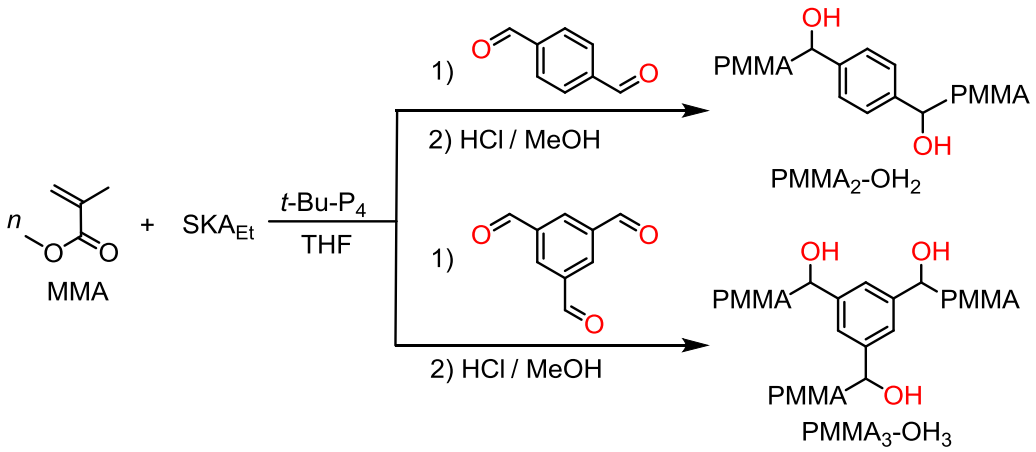

3.2 Experimental Section

Materials

Methyl methacrylate (MMA, >99.8%) and benzaldehyde (>98%) were purchased from Tokyo Kasei Kogyo Co., Ltd., (TCI) and used after distillation over CaH_2 under reduced pressure. L-Lactide (LLA) was also purchased from TCI and purified by recrystallization from dry toluene twice. *N*-(trimethylsilyl)bis(trifluoromethanesulfonyl)-imide (Me_3SiNTf_2, >95.0%) was also purchased from TCI and used as received. 1-*tert*-Butyl-4,4,4-tris(dimethylamino)-2,2-bis[tris(dimethylamino)-phosphoranylidenamino]-$2\Lambda^5,4\Lambda^5$-catenadi(phosphazene) (*t*-Bu-P_4, 1.0 mol L^{-1} in *n*-hexane) was purchased from Sigma-Aldrich Chemicals Co., and used as received. 1-Ethoxy-1-(trimethylsiloxy)-2-methylprop-1-ene (SKA_{Et}) was synthesized according to a previously reported procedure.[35] Its detailed synthesis is described in Chapter 2. The detailed syntheses of $(SKA)_3$, $(SKA)_6$ and $(SKA)_{12}$ were reported in our previous study.[30] Dry toluene (>99.5%; water content, <0.001%) was purchased from Kanto Chemical Co., Inc., and passed through the dry solvent system, MBRAUN MB SPS, prior to use. Tetrahydrofuran (THF > 99.5%; water content, <0.001%) purchased from Kanto Chemical Co., Inc., was distilled from sodium benzophenone prior to use. Dichloromethane (>99.5%; water content, <0.001%) was also purchased from Kanto Chemical Co., Inc., and distilled over CaH_2 under an argon atmosphere prior to use. All other reagents unless otherwise stated were used as received without further purification.

Measurements

^{1}H (400 MHz) and ^{13}C NMR (100 MHz) spectra were recorded on a JEOL JNM-ECS400. The polymerization solution was prepared in an MBRAUN stainless steel glove-box equipped with a gas purification system (molecular sieves and copper catalyst) under a dry argon atmosphere (H_2O, O_2 <1 ppm). The moisture and oxygen contents in the glove-box were monitored by using an MB-MO-SE 1 and an MB-OX-SE 1, respectively. Size exclusion chromatography (SEC) measurements for the end functionalized PMMAs were performed at 40 °C using a Jasco GPC-900 system equipped with a reflective index (RI) detector and two Shodex KF-804 L columns (linear, 8 mm × 300 mm) in THF at the flow rate of 1.0 mL min^{-1}. The molar mass ($M_{n,SEC}$) and polydispersity (M_w/M_n) of the resulting PMMAs were determined by SEC based on PMMA standards with their M_w (M_w/M_n)s of 1.25 × 10^3 kg mol^{-1} (1.07), 6.59 × 10^2 kg mol^{-1} (1.02), 3.003 × 10^2 kg mol^{-1} (1.02), 1.385 × 10^2 kg mol^{-1} (1.05), 60.15 kg mol^{-1} (1.03), 30.53 kg mol^{-1} (1.02), 11.55 kg mol^{-1} (1.04), 4.90 kg mol^{-1} (1.10), 2.87 kg mol^{-1} (1.06), and 1.43 kgmol^{-1} (1.15). Preparative SEC was performed in $CHCl_3$ (3.5 ml min^{-1}) at 23 °C using a JAI LC-9201 equipped with a JAI JAIGEL-2H column (20 mm × 600 mm; exclusion limit, 5 ×10^3), a JAI JAIGEL-3H column (20 mm × 600 mm; exclusion limit, 7 × 10^4) and a JAI RI-50s refractive index detector. The differential scanning calorimetry (DSC) was performed using a Bruker AXS TG-DTA 3100SA equipped with a Bruker AXS CU9440. Typically, the sample (4–5 mg) was heated to 160 °C at the heating rate of 10 °C min^{-1}, cooled to -40 °C at the cooling rate of 40 °C min^{-1}, then heated again to 200 °C at the heating rate of 10 °C min^{-1}. The glass transition temperature (T_g) was determined during the second heating scan.

Core-first synthesis of star-shaped PMMAs functionalized with hydroxyl groups

A typical procedure for the polymerization of 3-arm star PMMA with hydroxyl groups $(PMMA\text{-}OH)_3$ was carried out under the condition of $[MMA]_0/[(SKA)_3]_0/[t\text{-}Bu\text{-}P_4]_0/[PhCHO]_0$ = 90/1/0.02/30 as follows: a stock solution (200 μL) of $(SKA)_3$ (40.0 μmol, 0.20 mol L^{-1}) in THF and a stock solution (16 μL) of *t*-Bu-P_4 (0.80 μmol, 0.05 mol L^{-1}) in THF in a test tube were stirred for a few minutes, and then a stock solution (3.6 mL) of MMA (3.6 mmol, 1.0 mol L^{-1}) in THF was added within about 5 min. The polymerization was terminated by adding benzaldehyde (126 μL, 1.2 mmol) to the polymerization solution immediately afterwards and the ω-end-functionalization reaction was allowed to proceed for 6 h. Aliquots were taken out from the reaction mixture before termination to determine the conversion of MMA by ^1H NMR measurements. The polymer product was purified by precipitation in *n*-hexane after quenching the reaction with methanol to give a white solid powder; conversion > 99%. Yield, 336 mg (93.4%); $M_{n,SEC}$ = 6.7 kg mol^{-1}, M_w/M_n = 1.08. A deprotection reaction was then carried out to remove the trimethylsilyl group by reacting the polymer with 1 N HCl in MeOH/THF for 30 min to quantitatively obtain $(PMMA\text{-}OH)_3$. The synthesis of $(PMMA\text{-}OH)_6$ and $(PMMA\text{-}OH)_{12}$ were carried out using a similar procedure with $(SKA)_6$ and $(SKA)_{12}$ as the core initiators respectively.

Arm-first synthesis of two-arm PMMA functionalized with two hydroxyl groups and three-arm PMMA with three hydroxyl groups using terepthalaldehyde and benzene-1,3,5-carbaldehyde respectively.

A typical procedure for the synthesis of two-arm PMMA functionalized with two hydroxyl groups is described as follows: SKA_{Et} (160 μL, 80 μmol; 0.50 mol L^{-1} in toluene), a *t*-Bu-P_4 stock solution (16 μL, 0.80 μmol; 0.05 mol L^{-1} in THF), and THF (0.50 mL) were added to a test tube at room temperature under an argon atmosphere, followed by the dropwise addition of MMA (213 μL, 2.0 mmol) in THF (2.0 mL). The polymerization was terminated by adding terephthalaldehyde (4.3 mg, 32 μmol) to the polymerization solution immediately afterwards and the ω-end-functionalization reaction was allowed to proceed for 12 h. Aliquots were taken out from the reaction mixture before termination to determine the conversion of MMA by ^1H NMR measurements. The polymer product was isolated by precipitation in *n*-hexane after quenching the reaction with methanol. A deprotection reaction was then carried out to remove the trimethylsilyl group by reacting the polymer with 1N HCl in MeOH/THF for 30 minutes. The resulting polymer was then purified by preparative SEC using $CHCl_3$ as an eluent to afford $PMMA_2$-OH_2 as a white solid. Yield, 135 mg (67.5%); $M_{n,SEC}$ = 6.0 kg mol^{-1}, M_w/M_n = 1.08. The synthesis of $PMMA_3$-OH_3 using benzene-1, 3 , 5-tricarbaldehyde was carried out by a similar procedure.

3.3 Results and Discussion

In the previous chapter, author described the precise synthesis of PMMAs functionalized with a hydroxyl group by *t*-Bu-P_4-catalyzed GTP using aromatic aldehydes as terminators. Building on the success of that work, the author proceeded to synthesize star-shaped PMMAs functionalized with hydroxyl groups by *t*-Bu-P_4-catalyzed GTP by the core-first and the arm-first methods.

3.3.1. Synthesis of ω-end hydroxyl functionalized star-shaped PMMA via the Core-first method by *t*-Bu-P_4-catalyzed GTP using $(SKA)_3$, $(SKA)_6$ and $(SKA)_{12}$ as initiators.

In another previous work, we reported the design and synthesis of initiators possessing multiple numbers of silyl enolate groups, such as $(SKA)_3$, $(SKA)_4$, and $(SKA)_6$ for the synthesis of the three-, four-, and six-armed star-shaped PMMAs $(PMMA)_3$, $(PMMA)_4$, and $(PMMA)_6$, respectively.[13] In this work, for the core-first synthesis of the star-shaped PMMAs by GTP, $(SKA)_3$, $(SKA)_6$ and $(SKA)_{12}$ were used to synthesize three-, six- and twelve-armed star-shaped PMMAs, $(PMMA)_3$, $(PMMA)_6$ and $(PMMA)_{12}$, carrying reactive SKA groups at their chain ends respectively. These reactive SKAs at their chain ends were then functionalized by reacting it with excess benzaldehyde to synthesize $(PMMA\text{-}OH)_3$, $(PMMA\text{-}OH)_6$ and $(PMMA\text{-}OH)_{12}$ respectively as shown in Scheme 1. For the synthesis of three-, six- and twelve-armed PMMAs $(PMMA)_3$, $(PMMA)_6$, and $(PMMA)_{12}$, polymerizations were performed with $[MMA]_0/[(SKA)_3]_0 = 90$, $[MMA]_0/[(SKA)_6]_0 = 180$ and $[MMA]_0/[(SKA)_{12}]_0 = 360$, respectively, to make it 30 MMA units per arm in all obtained star-shaped PMMAs. For the functionalization reactions, the ratio between the initiator and terminator was 10 per arm to achieve

quantitative functionalization.

Table 3.1. Synthesis of hydroxyl-functionalized star-shaped PMMA by *t*-BuP_4-catalyzed GTP [a]

run	Initiator (I)	$[MMA]_0/[I]_0/[P_4]_0/[PhCHO]_0$	$M_{n,theo.}$ [b] ($kgmol^{-1}$)	$M_{n,SEC}$ [c] ($kgmol^{-1}$)	$M_{n,NMR}$ [d] ($kgmol^{-1}$)	M_w/M_n [c]	%F [d]
1	$(SKA)_3$	90/1/0.02/30	9.3	6.7	9.2	1.08	>99
2	$(SKA)_6$	180/1/0.03/60	19.3	11.8	17.8	1.03	>99
3	$(SKA)_{12}$	360/1/0.05/120	38.7	20.0	39.3	1.04	>99

[a] Ar atmosphere; temperature, r.t.; $[MMA]_0$ = 1.0 mol L^{-1}; MMA conversion (conv.) determined by ^{1}H NMR in acetone-d_6, >99 %; polymerization time, 5 min; functionalization time; 6 h. Shape of SEC trace was monomodal. [b] Calculated from $([MMA]_0/[I]_0)$ × (Conv.) × (M.W. of MMA) + (M.W. of initiator residue) + (n × M.W of PhCHO). [c] Determined by SEC with RI detector in THF. [d] Calculated from ^{1}H NMR spectrum in acetone-d_6.

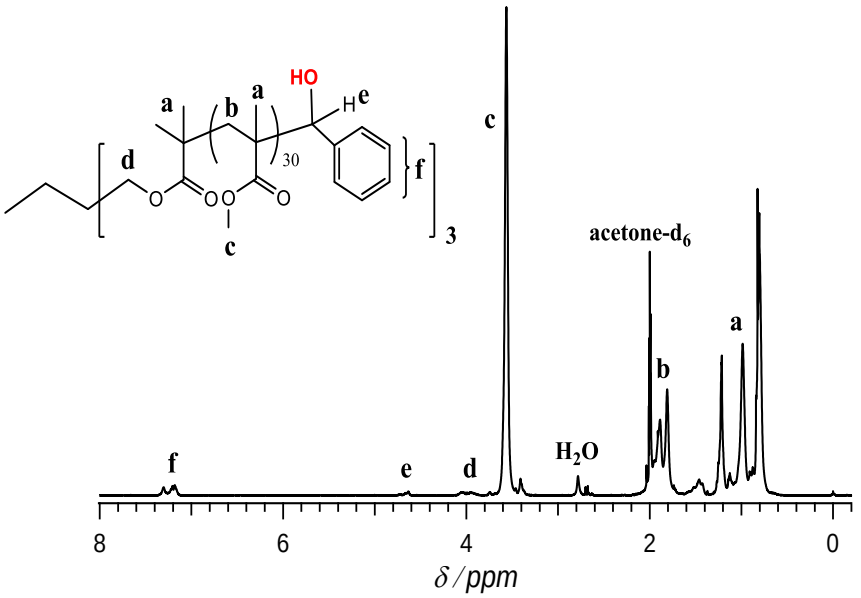

Figure 3.2. ^{1}H NMR spectrum of the hydroxyl end-functionalized 3-arm star-shaped PMMA in acetone-d_6 (400 MHz).

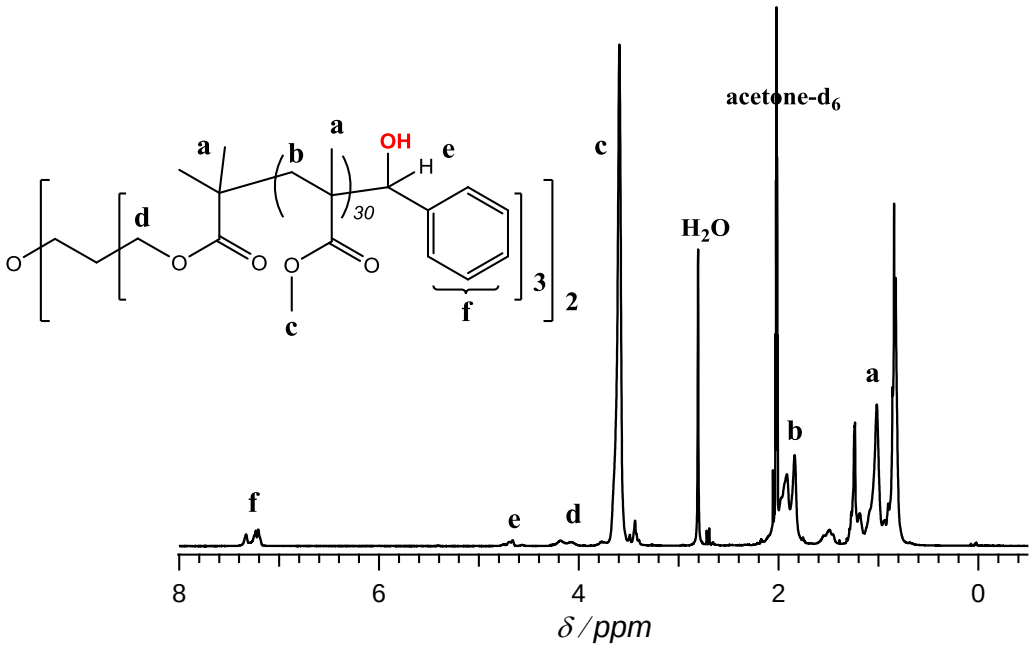

Figure 3.3. ^{1}H NMR spectrum of hydroxyl end-functionalized 6-arm star-shaped PMMA in acetone-d_6 (400 MHz).

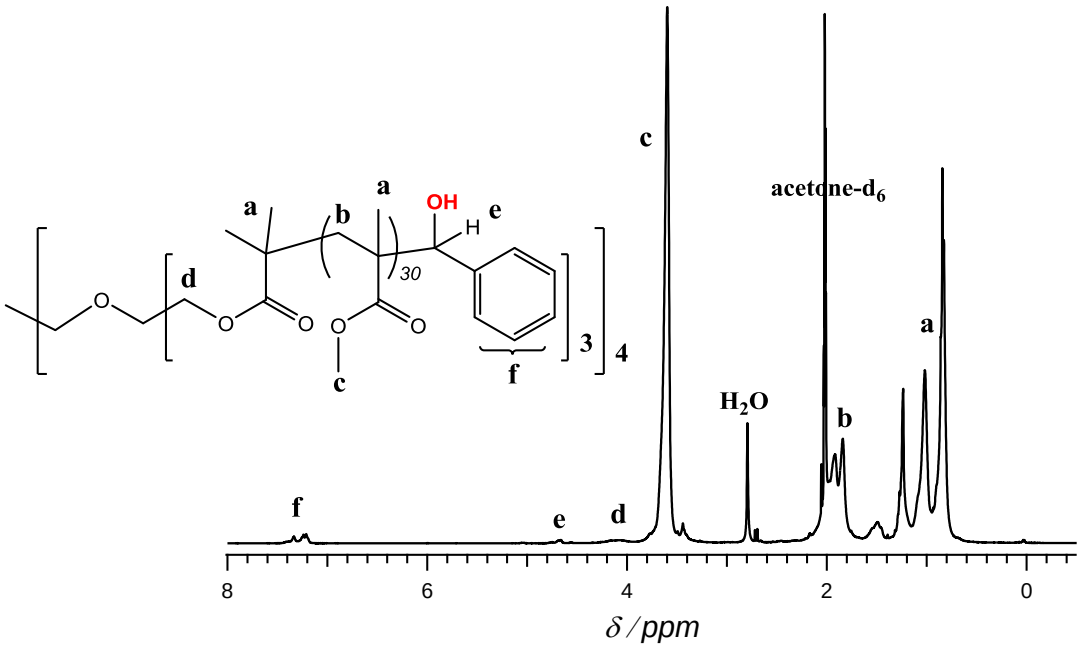

Figure 3.4. ^{1}H NMR spectrum of hydroxyl end-functionalized 12-arm star-shaped PMMA in acetone-d_6 (400 MHz).

The ^{1}H NMR spectra of the obtained hydroxyl-functionalized star-shaped PMMAs showed characteristic peaks for the initiator core, the MMA arms and the phenyl and hydroxyl groups at the chain ends as shown for example in the ^{1}H NMR spectrum of hydroxyl-functionalized three arm PMMA $(PMMA\text{-}OH)_3$ in Figure 3.1. These results provided evidence for homogeneous growth of each PMMA arm during the polymerization, which strongly led to the conclusion that the precise synthesis of the three-, six-, and twelve-armed PMMAs with well-defined star-shaped structures carrying a hydroxyl group at each chain end were achieved by the *t*-Bu-P_4-catalyzed GTP based on the core-first method.

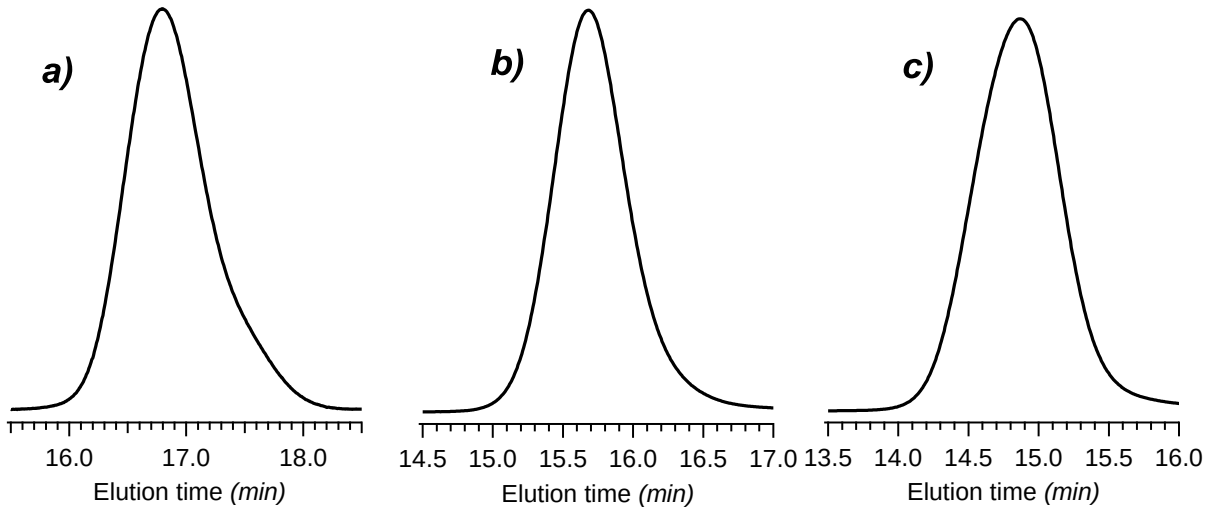

Figure 3.5. SEC traces of (a) $(PMMA_{30}\text{-}OH)_3$ (run 1) (b) $(PMMA_{30}\text{-}OH)_6$ (run 2) (c) $(PMMA_{30}\text{-}OH)_{12}$ (run 3)

All SEC traces of the obtained star PMMAs were unimodal and had narrow molecular weight distributions. Run 1-3 (Table 3.1) summarizes the polymerization results. The number-average molecular weights ($M_{n(SEC)}$s) of the obtained hydroxyl-functionalized star PMMAs estimated by size exclusion chromatography with a refractive index (RI) detector using a linear PMMA calibration showed a slight deviation from their theoretical number-average molecular weights ($M_{n,Theor}$.s) The deviation became larger as the number of arms increased. The deviation could be attributed to the different hydrodynamic volume between the star-shaped PMMAs and the linear PMMA used as a calibration. The absolute molecular weight was calculated by ^{1}H NMR with their theoretical molecular weights.

3.3.2. Synthesis of two- and three-arm PMMAs functionalized with hydroxyl groups by the arm-first method

The propagating end of polymers in GTP is stable and electronically neutral, which is advantageous for the synthesis of star-shaped polymers in comparison to other controlled/living polymerization systems. Unlike in living radical polymerization systems, GTP is not prone to intermolecular termination reactions that normally involve two propagating polymers species. Although there are several reports for the core-first synthesis of star-shaped polymers by GTP using multi-functionalized initiators,[35,43] there is no report for the arm-first synthesis of star-shaped polymers by GTP using terminators to the best of our knowledge. Thus, two- and three-arm PMMAs functionalized with hydroxyl groups were synthesized by *t*-Bu-P_4-catalyzed GTP using terminators with two and three aldehyde groups, such as terepthalaldehyde and benzene-1,3,5-tricarbaldehyde, respectively, as shown in Scheme 3.2.

Table 3.2. Synthesis of hydroxyl functionalized two- and three-arm PMMAs by *t*-Bu-P_4-catalyzed GTP using multifunctional benzaldehydes as terminators [a]

run	$[M]_0/[I]_0$	Terminator (T)	$[T]_0/[I]_0$	$M_{n,calcd}$ [b] (kg mol^{-1})	$M_{n,SEC}$ [c] (kg mol^{-1})	$M_{n,NMR}$ [d] (kg mol^{-1})	M_w/M_n [c]
4a	25	--	--	2.6	2.9	3.2	1.18
4b	--	$Ph(CHO)_2$	0.45	5.8	6.0	6.4	1.08
5a	25	--	--	2.6	3.2	2.9	1.12
5b	--	$Ph(CHO)_3$	0.30	9.6	11.6	10.8	1.05

[a] Ar atmosphere; room temperature; I, SKA_{Et} ; M, MMA; [*t*-Bu-P_4]/$[I]_0$, 0.01; Polymerization time, 3 min; Termination time, 12 h; MMA conversion >99%. [b] Calculated from ($[M]_0/[I]_0$) × (MMA conversion) × (M.W. of MMA) + (M.W. of initiator residue) + (M.W. of terminator residue) × %*F*. [c] Determined by SEC in THF using PMMA standards. [d] Calculated by ^{1}H NMR measurements in acetone-d_6.

Table 3.2 summarizes the polymerization results. For this arm-first method, we first synthesized a linear living PMMA as the arm by *t*-Bu-P_4-catalyzed GTP and then the terminators with multiple aldehyde groups were added as the core to the prior synthesized arms. When carrying out the termination reaction, the initiator ratios in double and triple excess to that of the appropriate terminators were required to synthesize the two- and three-arm polymers, respectively. The results obtained from the SEC(RI) measurements showed that the SEC trace in Figure 3.5 shifted to the high molar mass region after the termination using the terepthalaldehyde and benzene-1,3,5-tricarbaldehyde and the molar masses of the acquired polymers were exactly two and three times those of the pre-synthesized linear PMMA arms to produce the two- and three-arm PMMAs, respectively, which were also directly confirmed by the ^{1}H NMR calculations of the molar masses, as listed in Table 3.2 (runs 4b and 5b). These results indicated that all the obtained polymers

consisted of a core unit derived from the terminators and the PMMA arms; *i.e.*, two- and three-arm PMMAs.

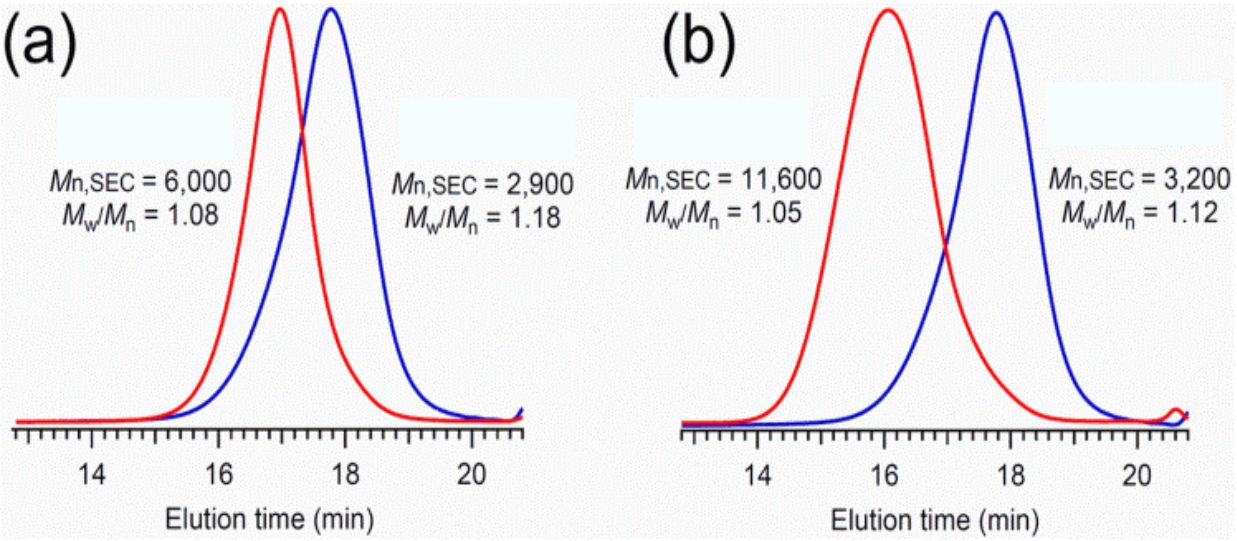

Figure 3.6. SEC traces of (a) hydroxyl-functionalized two-arm PMMA (red) and its precursor (blue) and (b) hydroxyl-functionalized three-arm PMMA (red) and its precursor (blue).

3.4 Conclusions

In this chapter, the author described the precise synthesis of star-shaped PMMAs functionalized with hydroxyl groups by *t*-Bu-P_4-catalyzed GTP via the core-first method using multifunctional SKA initiators as the core and benzaldehyde as the terminators. The termination reaction between the living star PMMA chain ends and benzaldehyde was proved to be an effective method for synthesizing hydroxyl-functionalized PMMAs with controlled molar masses and quantitative hydroxyl group functionalities. In this chapter, the author also established the arm-first method for the synthesis of two- and three-arm PMMAs with hydroxyl groups existing in the core, which is the first report about this kind of synthesis in GTP chemistry to the best of the knowledge of the author.

3.5 References

1. M. K. Mishra and S. Kobayashi, *Plast. Eng. (N.Y)*, **1999,** *53*, 350-376.
2. Y. Chen, K. Fuchise, A. Narumi, S. Kawaguchi, T. Satoh and T. Kakuchi, *Macromolecules* **2011**, *44*, 9091–9098.
3. S. Bywater , *Adv. Polym. Sci.*, **1979***; 30*, 89–116.
4. G. Lapienis, *Prog. Polym. Sci.*, **2009**, *34* , 852–892
5. T. A. Orofino, F. Wenger, *J. Phys. Chem*., **1963**, *67*, 566–575.
6. K. Matyjaszewski and T. P. Davis, *Eds.; Handbook of Radical Polymerization*, Wiley: Hoboken, NJ, **2002.**
7. J. Chiefari, Y. K. Chong, F. Ercole, J. Krstina, J. Jeffery, T. P. T. Le, R. T. A. Mayadunne, G. F. Meijs, C. L. Moad, G. Moad, E. Rizzardo and S. H. Thang, *Macromolecules* **1998**, *31*, 5559-5567.
8. C. J. Hawker, A. W. Bosman and E. Harth, *Chem. Rev.* **2001**, *101*, 3661-3705.
9. K. A. Davis and K. Matyjaszewski, *Adv. Polym. Sci.* **2002**, *159*, 2-10.
10. J.-S. Wang, D. Greszta and K. Matyjaszewski, *Polym. Mater. Sci. Eng.***1995**, *73*, 416-424.
11. K. Matyjaszewski, P. J. Miller, J. Pyun, G. Kickelbick and S. Diamanti, *Macromolecules* **1999**, *32*, 6526-6534.
12. K. Matyjaszewski, *Polym. Int.* **2003**, *52*, 1559-1568.
13. S. Angot, K. S. Murthy, D. Taton and Y. Gnanou, *Macromolecules* **1998**, *31*, 7218-7226.
14. J. Ueda, M. Kamigaito and M. Sawamoto, *Macromolecules* **1998**, *31*, 6762-6770.
15. C. J. Hawker, *Angew. Chem., Int. Ed. Engl.* **1995**, *34*, 1456-1462.

16. R. T. A. Mayadunne, J. Jeffery, G. Moad and E. Rizzardo, *Macromolecules* **2003**, *36*, 1505-1512.

17. V. Coessens, J. Pyun, P. J. Miller, S. G. Gaynor and K. Matyjaszewski, *Macromol. Rapid Commun.* **2000**, *21*, 103-106.

18. K. Matyjaszewski, P. J. Miller, E. Fossum and Y. Nakagawa, *Appl. Organomet. Chem.* **1998**, *12*, 667-675.

19. K. Matyjaszewski, P. J. Miller, G. Kickelbick, Y. Nakagawa, S. Diamanti and C. Pacis, *ACS Symp. Ser.* **2000**, *729*, 270-276.

20. K. Matyjaszewski, S. Qin, J. R. Boyce, D. Shirvanyants and S. S. Sheiko, *Macromolecules* **2003**, *36*, 1843-1850.

21. A. W. Bosman, A. Heumann, G. Klaerner, D. Benoit, J. M. J. Frechet and C. J. Hawker, *J. Am. Chem. Soc.* **2001**, *123*, 6461-6467.

22. A. J. Pasquale and T. E. Long, *J. Polym. Sci., Part A: Polym. Chem.* **2001**, *39*, 216-223.

23. G. Moad, R. T. A. Mayadunne, E. Rizzardo, M. Skidmore and S. H. Thang, *Macromol. Symp.* **2003**, *192*, 1-12.

24. T. Tsoukatos, S. Pispas and N. Hadjichristidis, *J. Polym. Sci., Part A: Polym. Chem.* **2001**, *39*, 320-327.

25. D. Held and A. H. E. Muller, *Macromol. Symp.* **2000**, *157*, 225-232.

26. K. A. Davis, B. Charleux and K. Matyjaszewski, *J. Polym. Sci., Part A: Polym. Chem.* **2000**, *38*, 2274-2280.

27. M. Li, N. M. Jahed, K. Min and K. Matyjaszewski, *Macromolecules* **2004**, *37*, 2434-2441.

28. K. Min, H. Gao and K. Matyjaszewski, *J. Am. Chem. Soc.* **2005**, *127*, 3825-3834.

29. M. Morton, T. E. Helminiak, S. D. Gadkary and F. Bueche, *J. Polym. Sci.* **1962**, *57*, 471-474.

30. N. Hadjichristidis, *J. Polym. Sci., Part A: Polym. Chem.* **1999**, *37*, 857-866.

31. H. Gao, N. V. Tsarevsky and K.Matyjaszewski, *Macromolecules* **2005**, *38*, 5995-6002.

32. G. Lapienis and S. Penczek, *Macromolecules* **2000**, *33*, 6630-6638.

33. G. Lapienis and S. Penczek, *J. Polym. Sci., Part A: Polym. Chem.* **2004**, *42*, 1576-1581.

34. J.-S. Wang and K. Matyjaszewski, *J. Am. Chem. Soc.* **1995**, *117*, 5614-5620.

35. K. Matyjaszewski and J. Xia, *Chem. Rev.* **2001**, *101*, 2921-2930.

36. M. Kamigaito, T.Ando and M. Sawamoto, *Chem. Rev.* **2001**, *101*, 3689-3732.

37. Y. Chen, K. Takada, K. Fuchise, T. Satoh and T. Kakuchi, J. *Polym. Sci., Part A: Polym. Chem.*, **2012**, *50*, 3277–3285.

Chapter 4

Synthesis of Star-shaped Poly(methyl methacrylate)-block-Poly(L-lactide)s

4.1 Introduction

The most significant advances in polymer chemistry in recent years has been based on employing concepts and tools in organic chemistry to construct structures with macromolecular architectures at the molecular level.[1] Synthesis of new materials with improved properties and applications is still an intense and challenging area for polymer science and the advent of modern synthetic methods has paved the way for new opportunities in the preparation of well-defined polymeric materials.[2,3,4] Among these materials, end-functionalized polymers are receiving considerable attention due to their wide applications, such as compatibilizing agents for polymer processing, macromolecular surfactants, surface modifiers, and carriers in drug delivery systems.[5-8,9] To achieve the synthesis of end-functionalized polymers, polymer chemists have widely adopted various synthetic techniques typically employed in the synthesis of small organic molecules.[3]

End-functionalized polymers are mostly synthesized using controlled/living polymerizations methods, such as living radical and anionic polymerizations,[10-12,13] *i.e.*, the α-, ω-, and α,ω-end functionalization are achieved using functional initiators, terminators, and both, respectively. For quantitative α- and ω-end functionalization, quantitative initiation by functional initiators is required for the introduction of functional groups at the α-end of polymers, as well as to maintain the livingness of polymers prior to quantitative termination at the ω-end of polymers. For preparing the desired type of polymer main-chain and targeted end-functional groups, it is important to choose a suitable living polymerization method along with the functional initiators and terminators that are appropriately designed and synthesized in consideration of the selected living

polymerization type.[14-15] Among the various living polymerizations, living anionic polymerization is a versatile method of introducing functional groups into the α-, and ω-ends of polymers compared to living radical polymerization method. Thus, we have focused on the group transfer polymerization (GTP) of acrylic monomers, one of the important living anionic polymerizations methods, which proceeds through numerous iterations of the Mukaiyama-Michael reaction between the propagating polymer chain end and a monomer.[16]

Scheme 4.1. Synthesis of AB block and A_2B_2 and A_3B_3 miktoarm star polymers consisting of PMMA and PDLA by combining GTP of MMA, ω-end-functionalization of PMMA using benzaldehyde as terminator, and ROP of DLA.

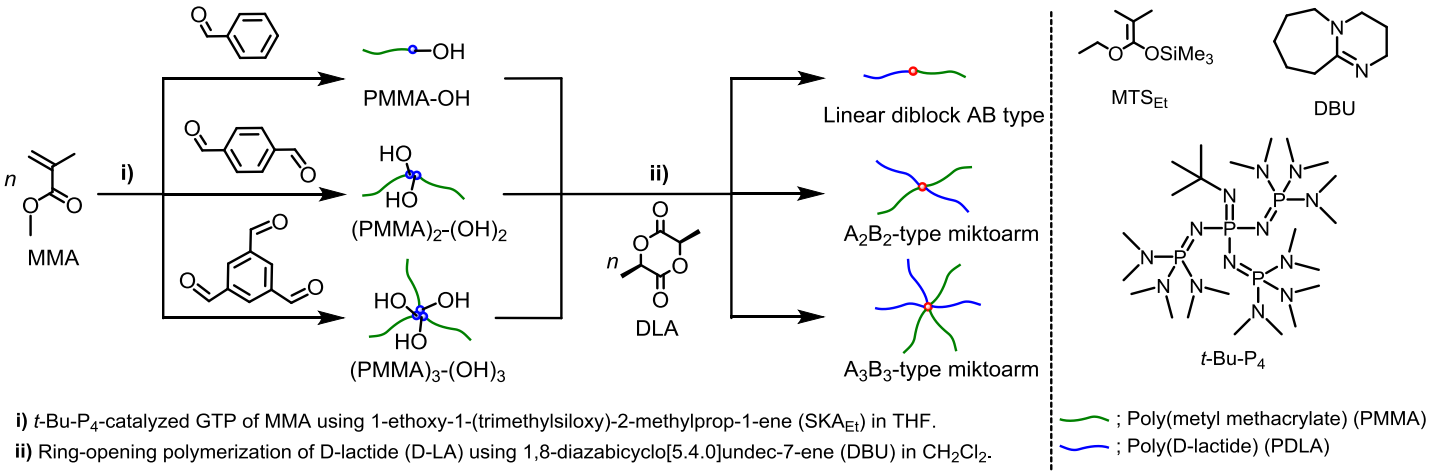

Scheme 4.2. Synthesis of PMMA-*b*-PLLA block copolymer and (PMMA-*b*-PLLA)$_3$, (PMMA-*b*-PLLA)$_6$ and (PMMA-*b*-PLLA)$_{12}$ star block copolymers via DBU-catalyzed ROP of LLA using PMMA-OH, (PMMA-OH)$_3$, (PMMA-OH)$_6$ and (PMMA-OH)$_{12}$, respectively.

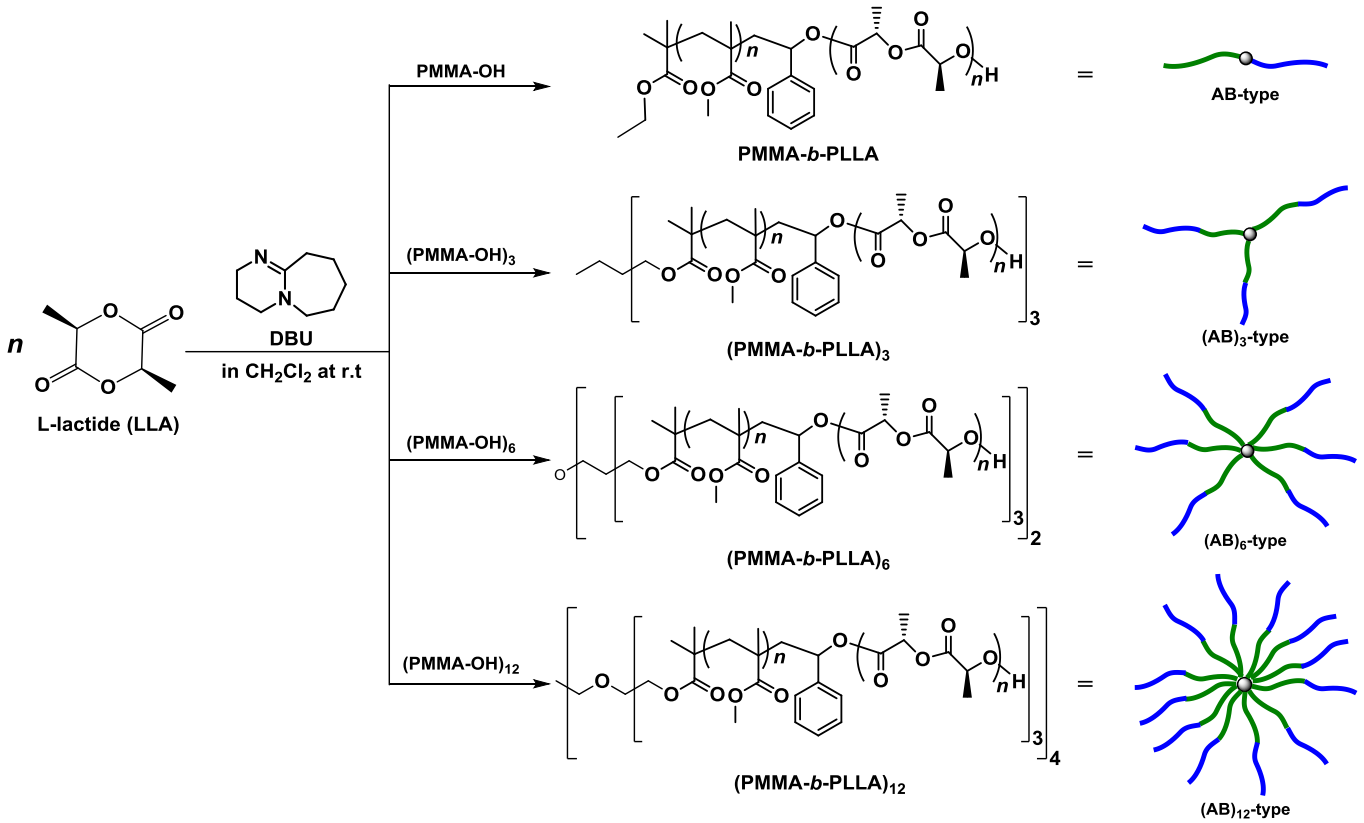

End-functionalized polymers are very important in polymer chemistry because, they are used as precursors for preparing structurally complex macromolecular architectures and intelligent network structures.[10] Synthesis of polymeric materials having complex architectures has gained significance since the advent of various methods of living polymerization. This is because polymers having complex architectures possess interesting and unique properties, which differs from that of linear polymers. For example, polymers with branched structures, such as star-shaped, dendritic, and hyperbranched

polymers, are known to exhibit a low hydrodynamic volume and low viscosity in solution, which is significantly different in comparison to their linear equivalents.[37] Star-shaped polymers are the most prominent among these complex architectures. Star block copolymers are star-shaped polymers which contain multiple linear block copolymer arms connected to a central core.[38-40] Star block copolymers have many unique properties because they combine the special features of both block copolymers with tuneable block composition and lengths, and star polymers, with compact structure and multifunctionality, into one entity.[41-44] Another reason star block copolymers have gained such prominence in recent times is their numerous potential applications as engine oil additives, coatings, lithographic or biomedical devices such as drug delivery vehicles and as unimolecular containers for nanomaterials.[45-49]

Miktoarm star polymers have attracted considerable attention in recent times because the different chemical compositions of the arms in miktoarm star molecules lead to very interesting microphase separations in bulk, in solution, and at different interfaces. The segregated compartments in the aggregates, such as micelles, could in turn provide distinct chemical environments to store various kinds of drug molecules, fragrance compounds, and gene therapy agents. Until recent times, most of the miktoarm star copolymers were synthesized by the living anionic polymerization method. However, ATRP, RAFT polymerization, ROP as well as GTP is rapidly changing this situation because of the broad variety of applicable monomers and conducive experimental conditions.[50]

The synthesis of star-shaped end-functionalized polymers using the arm-first method leads to miktoarm star polymers while the synthesis of star-shaped end-functionalized polymers using the core-first method leads to star block copolymers. The synthesis of miktoarm star polymers and star block copolymer generally requires a three-step process when the arm-first or core-first method is employed respectively. Organocatalyzed group transfer polymerization (GTP) is used for the preparation of star-shaped PMMAs with reactive end-groups in step one. In the second step, benzaldehyde terminator reacts with these reactive end-groups to synthesize hydroxyl-functionalized star-shaped PMMAs. In the third step, the previously synthesized hydroxyl-functionalized star-shaped PMMAs are used as macroinitiators (MI) for the ring opening polymerization (ROP) of Lactide to synthesize miktoarm star polymers or star block copolymers. The steps one and two are performed as a one-pot synthesis making this an efficient method for the synthesis of miktoarm star polymers and star block copolymers.

In this chapter, the author describes the convenient synthesis of AB block and A_2B_2 and A_3B_3 miktoarm star polymers using the PMMAs with the hydroxyl groups for the ring-opening polymerization of D-lactide, as shown in Scheme 4.1. As well as the convenient synthesis of AB linear block and $(AB)_3$, $(AB)_6$ and $(AB)_{12}$ star block copolymers using the PMMA macroinitiators with hydroxyl groups to initiate the ring opening polymerization of L-lactide Scheme 4.2 and the analysis of the thermal properties of the obtained linear and star block copolymers.

4.2 Experimental Section

Materials

Methyl methacrylate (MMA, >99.8%), benzaldehyde (PhCHO, >98%), was purchased from Tokyo Chemical Industries Co., Ltd., (TCI) and used after distillation over CaH_2 under reduced pressure. D-Lactide (DLA) and L-Lactide (LLA) were also purchased from TCI and purified by recrystallization from dry toluene (twice). 1-*tert*-Butyl-4,4,4-tris(dimethylamino)-2,2-bis[tris(dimethylamino)-phosphoranylidenamino]-2Λ^5,4Λ^5-catenadi(phosphazene) (*t*-Bu-P_4, 1.0 mol L^{-1} in *n*-hexane) was purchased from Sigma-Aldrich Chemicals Co., and used as received. 1-Ethoxy-1-(trimethylsiloxy)-2-methylprop-1-ene (SKA_{Et}) was synthesized according to a previously reported procedure .[36-37] Details of its synthesis is provided in Chapter 2. Dry toluene (> 99.5%; water content, < 0.001%) was purchased from Kanto Chemical Co., Inc., and passed through the dry solvent system, MBRAUN MB SPS, prior to use. Tetrahydrofuran (THF > 99.5%; water content, < 0.001%) purchased from Kanto Chemical Co., Inc., was distilled from sodium benzophenone prior to use. All other reagents unless otherwise stated were used as received without further purification.

Measurements

^{1}H (400 MHz) and ^{13}C NMR (100 MHz) spectra were recorded by a JEOL JNM-ECS400. The polymerization solution was prepared in an MBRAUN stainless steel glove-box equipped with a gas purification system (molecular sieves and copper catalyst) in a dry argon atmosphere (H_2O, O_2 <1 ppm). The moisture and oxygen contents in the glove-box were monitored by an MB-MO-SE 1 and an MB-OX-SE 1, respectively. Size exclusion chromatography (SEC) measurements for the end-functionalized PMMAs were performed at 40 °C using a Jasco GPC-900 system equipped with a reflective index (RI) detector and two Shodex KF-804 L columns (linear, 8 mm × 300 mm) in THF at the flow rate of 1.0 mL min^{-1}. The molar mass ($M_{n,SEC}$) and polydispersity (M_w/M_n) of the resulting PMMAs were determined by SEC based on PMMA standards with their M_w (M_w/M_n)s of 1.25×10^3 kg mol^{-1} (1.07), 6.59×10^2 kg mol^{-1} (1.02), 3.003×10^2 kg mol^{-1} (1.02), 1.385×10^2 kg mol^{-1} (1.05), 60.15 kg mol^{-1} (1.03), 30.53 kg mol^{-1} (1.02), and 11.55 kg mol^{-1} (1.04), 4.90 kg mol^{-1} (1.10), 2.87 kg mol^{-1} (1.06), and 1.43 kg mol^{-1} (1.15). Preparative SEC was performed in $CHCl_3$ (3.5 mL min^{-1}) at 23 °C using a JAI LC-9201 equipped with a JAI JAIGEL-2H column (20 mm × 600 mm; exclusion limit, 5×10^3), a JAI JAIGEL-3H column (20 mm × 600 mm; exclusion limit, 7×10^4) and a JAI RI-50s refractive index detector. The differential scanning calorimetry (DSC) was performed using a Bruker AXS TG-DTA 3100SA equipped with a Bruker AXS CU9440. Typically, the sample (4–5 mg) was heated to 160 °C at the heating rate of 10 °C min^{-1}, cooled to -40 °C at the cooling rate of 40 °C min^{-1}, then heated again to 200 °C at the heating rate of 10 °C min^{-1}. The glass transition temperature (T_g) was determined during the second heating scan.

Synthesis of PMMA-PDLA miktoarm star polymers using PMMAs functionalized with hydroxyl groups.

A typical procedure for the synthesis of A_2B_2 miktoarm star polymers using $PMMA_2$-OH_2 for the ROP of DLA[42] under the conditions of $[DLA]_0/[PMMA_2\text{-}OH_2]_0/[DBU]_0 = 150/1/2$ is described as follows: $PMMA_2$-OH_2 (66 mg, 6.6 kg mol^{-1}, 10 μmol), DLA (216 mg, 1.5 mmol) and CH_2Cl_2 (1.5 mL) were added to a test tube followed by the addition of DBU (20 μL, 20 μmol; 1.0 mol L^{-1} in CH_2Cl_2) under an argon atmosphere. The polymerization was allowed to proceed at room temperature for 20 min. after which it was quenched by the addition of excess benzoic acid. The mixture was then purified by reprecipitation from CH_2Cl_2 into cold MeOH to give $PMMA_2$-$PDLA_2$ as a white solid. The product was further purified by preparative SEC using $CHCl_3$ as the eluent. Yield, 140 mg (65%); $M_{n\ SEC}$ = 27.6 kg mol^{-1}, M_w/M_n = 1.17. The synthesis of the AB block and A_3B_3 miktoarm star polymers was carried out by a similar procedure using PMMA-OH and $PMMA_3$-OH_3, respectively as macroinitiators.

Synthesis of PMMA-*b*-PLLA star block copolymers using PMMA macroinitiators functionalized with hydroxyl groups

A typical procedure for the synthesis of $(AB)_3$ star block copolymers using $(PMMA\text{-}OH)_3$ for the ROP of LLA under the conditions of $[LLA]_0/[(PMMA\text{-}OH)_3]_0/[DBU]_0$ = 90/1/0.5 is described as follows: $(PMMA\text{-}OH)_3$ (100 mg, 6.7 kg mol^{-1}, 15 μmol), LLA (194 mg, 1.34 mmol) and CH_2Cl_2 (1.5 mL) were added to a test tube followed by the addition of DBU (15 μL, 7.5 μmol; 0.5 mol L^{-1} in CH_2Cl_2) under an argon atmosphere. The polymerization was allowed to proceed at room temperature for 20 min after which it was quenched by the addition of excess benzoic acid. The mixture was then purified by reprecipitation from CH_2Cl_2 into cold MeOH to give $(PMMA\text{-}b\text{-}PLLA)_3$ as a white solid. The product was further purified by preparative SEC using $CHCl_3$ as the eluent. Yield, 140 mg (72.1%); $M_{n\ SEC}$ = 23.7 kg mol^{-1}, M_w/M_n = 1.14. The synthesis of the AB linear block, $(AB)_6$ and $(AB)_{12}$ star block copolymers were carried out by a similar procedure using PMMA-OH, $(PMMA\text{-}OH)_6$ and $(PMMA\text{-}OH)_{12}$, respectively, as macroinitiators.

4.3 Results and Discussion

Miktoarm star polymers and star block copolymers have are among the most unique polymer architectures because the different chemical composition of their arms leads to very interesting microphase separations in bulk, in solution, and at different interfaces. The synthesis of star-shaped end-functionalized polymers using the arm-first method leads to miktoarm copolymers while the synthesis of star-shaped end-functionalized polymers using the core-first method leads to star block copolymers. The synthesis miktoarm and star block copolymer generally requires a three-step process when the arm-first or core-first method is employed respectively. Organocatalyzed group transfer polymerization (GTP) is used for the preparation of star-shaped PMMAs with reactive end-groups in step one. In the second step, benzaldehyde terminator reacts with these reactive end-groups to synthesize hydroxyl-functionalized star-shaped PMMAs. In the third step, the previously synthesized hydroxyl-functionalized star-shaped PMMAs are used as macroinitiators (MI) for the ring opening polymerization (ROP) of Lactide to synthesize miktoarm star polymers or star block copolymers. The steps one and two are performed as a one-pot synthesis making this an efficient method for the synthesis of miktoarm star polymers and star block copolymers.

4.3.1 Synthesis of PMMA-PDLA linear block and miktoarm star polymers.

Having demonstrated the effectiveness of GTP for the synthesis of linear and two- and three-arm PMMAs end-functionalized with hydroxyl groups by the termination reactions with benzaldehydes in Chapter 3, the author proceeded to demonstrate the applicability of the hydroxyl functionalities by employing the hydroxyl end-functional groups to initiate the ring opening polymerization (ROP) of D-lactide (DLA), as shown in Scheme 4.3.

Scheme 4.3 Synthesis of PMMA-*b*-PDLA diblock copolymer and $PMMA_2$-$PDLA_2$ and $PMMA_3$-$PDLA_3$ miktoarm star polymers via DBU-catalyzed ROP of DLA using PMMA-OH, $PMMA_2$-OH_2, and $PMMA_3$-OH_3, respectively.

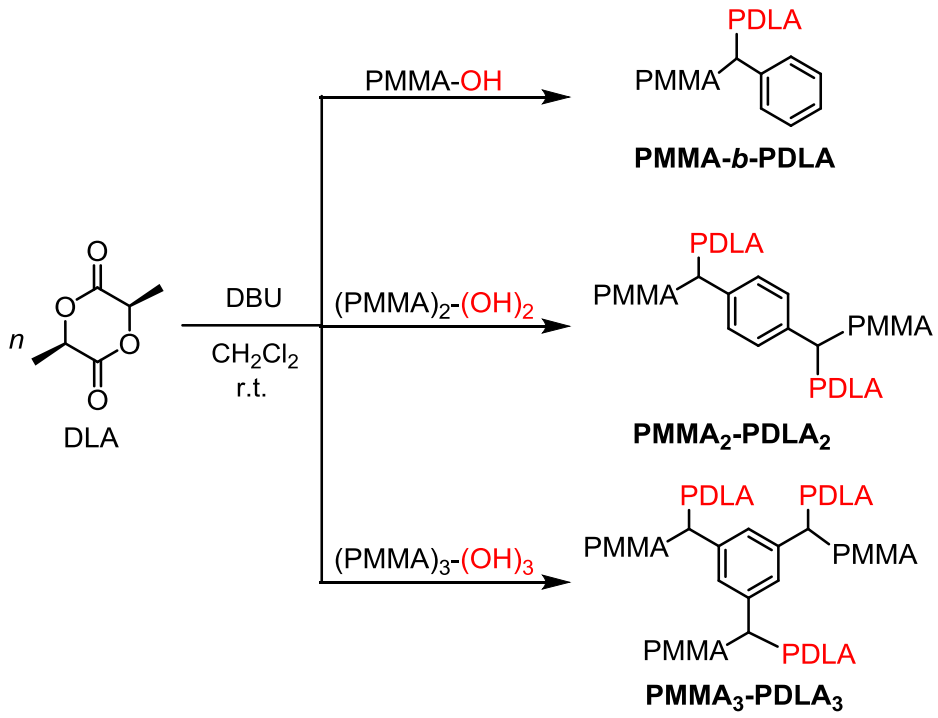

The polymerization results are listed in Table 4.1 The hydroxyl group ω-end-functionalized PMMA (PMMA-OH; $M_{n,SEC}$ = 3.2 kg mol^{-1}, M_w/M_n = 1.20) and two- ($PMMA_2$-OH_2; $M_{n,SEC}$ = 6.6 kg mol^{-1}, M_w/M_n = 1.17) and three-arm ($PMMA_3$-OH_3; $M_{n,SEC}$ = 11.6 kg mol^{-1}, M_w/M_n = 1.05) PMMAs were used to initiate the ROP of DLA in CH_2Cl_2 to produce the expected diblock copolymer (AB type), four-arm (A_2B_2 type) and six-arm (A_3B_3 type) miktoarm star polymers respectively.

The molar ratio of DLA to the hydroxyl group was fixed at a value of 75 in order to keep each AB arm having a total degree of polymerization (DP) of 100. The DBU catalyst was used because a previous report [42] had shown it to be the best catalyst for the ROP of hydroxyl initiated lactide monomers. The quantity of catalyst was appropriately tuned in light of the macroinitiator used. All the ROPs of DLA (runs 1-3) afforded high DLA conversions (90 – 94%). After purification by preparative SEC, the $M_{n,SEC}$ (kg mol^{-1}) (M_w/M_n)s of the final polymer products of PMMA-*b*-PDLA (run 10), $PMMA_2$-$PDLA_2$ (run 11), and $PMMA_3$-$PDLA_3$ (run 12) were 18.9 (1.08), 27.6 (1.17), and 40.5 (1.21), respectively.

Table 4.1 Synthesis of AB diblock, A_2B_2 and A_3B_3 miktoarm star polymers by DBU-catalyzed ROP of DLA using PMMAs functionalized with hydroxyl groups as macroinitiators.

run	Polymers	Macroinitiator (MI) ($M_{n,SEC}$ (kg mol^{-1}), M_w/M_n)	$[DLA]_0/[MI]_0/[DBU]_0$	Conv. [b] (%)	$M_{n,theo.}$ [c] (kg mol^{-1})	$M_{n,SEC}$ [d] (kg mol^{-1})	M_w/M_n [d]
1	PMMA-*b*-PDLA	PMMA-OH (3.2, 1.20)	75/1/0.5	94	13.8	18.9	1.08
2	$PMMA_2$-$PDLA_2$	$PMMA_2$-OH_2 (6.6, 1.17)	150/1/2	90	26.0	27.6	1.17
3	$PMMA_3$-$PDLA_3$	$PMMA_3$-OH_3(11.6, 1.05)	225/1/3	93	38.3	40.5	1.21

[a] Ar atmosphere; solvent, CH_2Cl_2; temperature; r.t.; $[DLA]_0$ = 1.0 mol L^{-1}; polymerization time; 20 min. [b] Estimated by ^{1}H NMR measurements. [c] Calculated from $([DLA]_0/[I]_0) \times$ (DLA Conv.) × (M.W. of DLA) + (M.W. of MI). [d] Estimated by SEC in THF using PMMA standards.

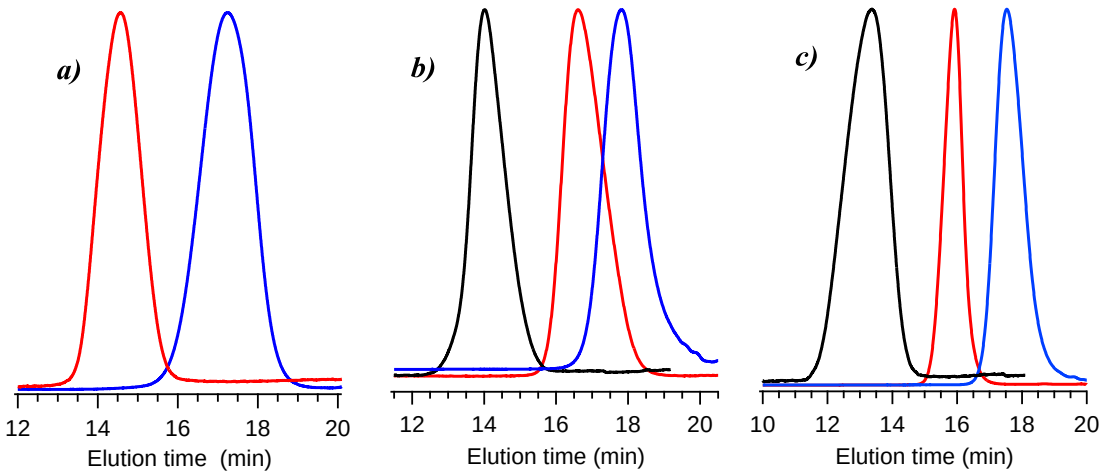

Figure 4.1 SEC traces of (a) PMMA-*b*-PDLA (black line) and its precursor of PMMA-OH (red line), (b) $PMMA_2$-$PDLA_2$ (black line) and its precursors of $PMMA_2$-OH_2 and a PMMA arm (red and blue lines, respectively), and (c) $PMMA_3$-$PDLA_3$ and its precursors of $PMMA_3$-OH_3 and a PMMA arm (red and blue lines, respectively).

The results obtained from the SEC (RI) measurements showed that the SEC trace in Figure 4.1 clearly shifted to the high molar mass region from the pre-terminated PMMA to the hydroxyl-functionalized macroinitiator to its respective corresponding diblock copolymer or miktoarm star polymer, respectively. In addition, a typical ^1H NMR measurement of PMMA-*b*-PDLA in Figure 4.2 simultaneously showed the proton signals from the PMMA main chain (peaks B and C) and PDLA main chain (peaks a and b). The same results were also obtained for $PMMA_2$-$PDLA_2$ and $PMMA_3$-$PDLA_3$. These results strongly indicated that all the obtained polymers consisted of a core unit derived from the benzaldehyde terminators and two types of chemically different polymer arms.

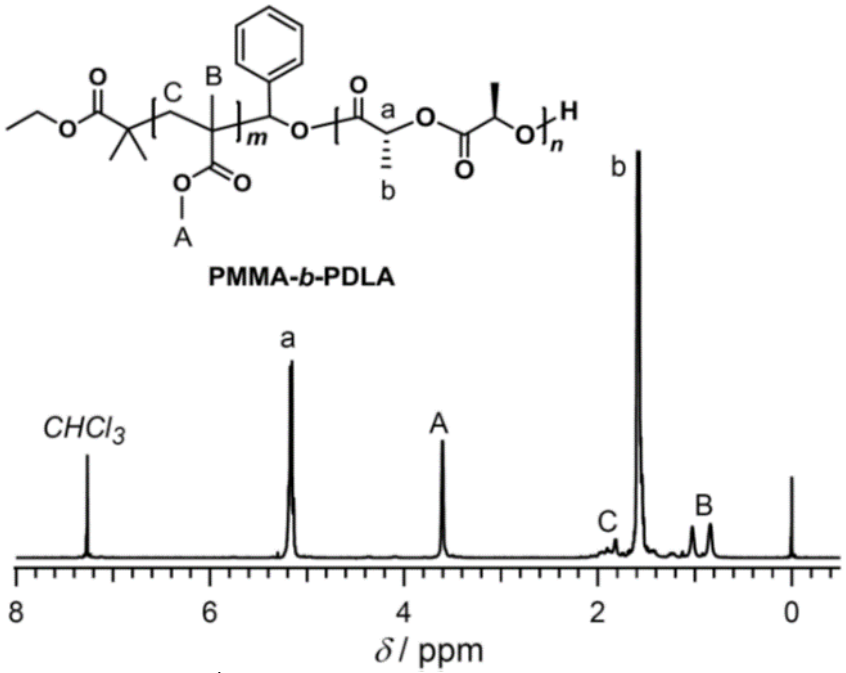

Figure 4.2 A typical ^{1}H NMR spectrum of PMMA-*b*-PDLA in $CDCl_3$.

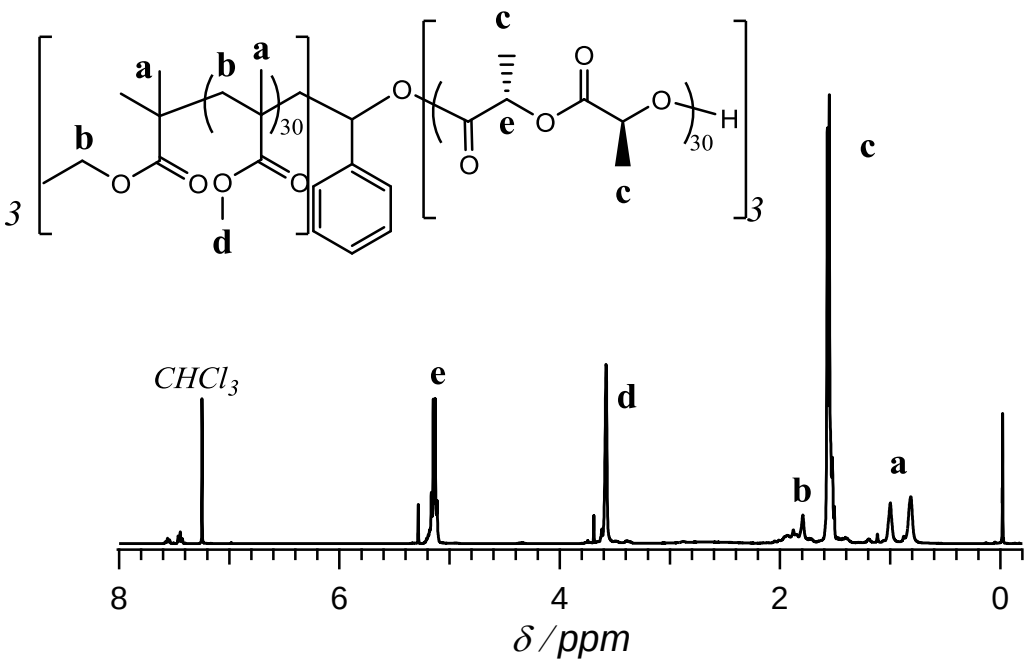

Figure 4.3 ^{1}H NMR spectrum of $PMMA_3$-$PLLA_3$ mikotarm star polymer in $CDCl_3$ (400 MHz).

4.3.2 Synthesis of PMMA-*b*-PLLA linear and star block copolymers

Having successfully synthesized miktoarm polymers using hydroxyl-functionalized PMMAs prepared via the arm-first method, the author proceeded to establish an effective synthetic route for the synthesis of linear and star block copolymers.

Table 4.2. Synthesis of linear and star diblock copolymers using hydroxyl functionalized PMMAs as macroinitiators.[a]

run	Diblock copolymers	Macroinitiators	$[LLA]_0/[MI]_0/[DBU]_0$ [b]	Conv. [c] (%)	$M_{n,theo.}$ [d] ($kgmol^{-1}$)	$M_{n,SEC}$ [e] ($kgmol^{-1}$)	$M_{n,NMR}$ [c] ($kgmol^{-1}$)	M_w/M_n
4	$PMMA_{39}$-*b*-$PLLA_{37}$	$PMMA_{37}$-OH	30/1/0.5	98.7	8.5	13.4	9.2	1.09
5	$(PMMA_{31}$-*b*-$PLLA_{29})_3$	$(PMMA_{30}$-$OH)_3$	90/1/1	99	18.5	23.7	18.9	1.14
6	$(PMMA_{30}$-*b*-$PLLA_{15})_6$	$(PMMA_{30}$-$OH)_6$	90/1/1	98.8	22.8	25.9	24.5	1.10
7	$(PMMA_{30}$-*b*-$PLLA_{34})_6$	$(PMMA_{30}$-$OH)_6$	180/1/2	97.6	35.3	36.4	38.5	1.15
8	$(PMMA_{30}$-*b*-$PLLA_{57})_6$	$(PMMA_{30}$-$OH)_6$	360/1/5	97.8	62.6	69.3	66.7	1.17
9	$(PMMA_{30}$-*b*-$PLLA_{28})_{12}$	$(PMMA_{30}$-$OH)_{12}$	360/1/5	95.4	70.1	80.4	85.8	1.17

[a] Ar atmosphere; solvent, CH_2Cl_2; temperature; room temperature; [b] $[LLA]_0$ = 0.7 mol L^{-1};.[c] Estimated by the ^1H NMR spectrum. [d] Calculated from $([LLA]_0/[I]_0) \times$ (LLA conversion) × (M.W. of LLA) + (M.W. of macroinitiator). [e] Estimated by SEC in THF using PMMA standards.

In Chapter 3, the author showed that organocatalyzed GTP was an efficient method for the synthesis of linear and star-shaped PMMAs functionalized with hydroxyl groups by the termination reactions with benzaldehydes via the core-first method. In this chapter, the author proceeded to demonstrate the applicability of the hydroxyl functionalities by employing the hydroxyl end-functional groups to initiate the ring-opening polymerization (ROP) of L-lactide (LLA), as shown in Scheme 4.2 to synthesize linear and star block copolymers. The ω-end-hydroxyl functionalized linear ($PMMA_{30}$-OH; $M_{n,\,SEC}$ = 4.0 kg mol^{-1}, M_w/M_n = 1.12), three-arm star $(PMMA_{31}$-$OH)_3$; $M_{n,\,SEC}$ = 6.7 kg mol^{-1}, M_w/M_n =

1.08) , six-arm star ($PMMA_{30}$-OH)$_6$; $M_{n,\,SEC}$ = 11.8 kg mol^{-1}, M_w/M_n = 1.03) and twelve-arm star ($PMMA_{33}$-OH)$_{12}$; $M_{n,\,SEC}$ = 20.0 kg mol^{-1}, M_w/M_n = 1.04) PMMAs were used to initiate the ROP of LLA in CH_2Cl_2 to produce the expected AB-type linear block copolymer, $(AB)_3$-type three-arm, $(AB)_6$-type six-arm and $(AB)_{12}$-type twelve-arm star block copolymers, respectively.

The molar ratio of LLA to the hydroxyl group was fixed at 30 in order to give each arm an identical number of MMA and LLA monomer units in each block except in the $(AB)_6$-type in which an LLA to hydroxyl group ratio of 15 and 60 (run 6 and 8, Table 4.2) was synthesized to determine the effect of $[LLA]_0/[OH]_0$ on the LLA conversion. The DBU catalyst was used because the author`s previous synthesis of miktoarm copolymers had shown it to be the best catalyst for the ROP of hydroxyl initiated lactide monomers. The amount of catalyst used was appropriately tuned to the monomer macroinitiator ratio ($[LLA]_0/[MI]_0$ Table 4.2). All the ROPs of LLA (run 4-9) afforded high LLA conversions (96.5-99.0 %).The results obtained from the SEC(RI) measurements showed that the SEC trace in Figure. 4.4 clearly shifted to the high molar mass region from the hydroxyl-functionalized linear or star PMMA macroinitiator to its corresponding linear or star block copolymer. In addition, a typical ^{1}H NMR measurement of (PMMA-*b*-PLLA)$_3$ in Fig. 4.6 simultaneously showed the proton signals from the PMMA main chain (peaks a, b and d) and PLLA main chain (peaks c and e). The same results were also obtained for the linear block copolymer PMMA-*b*-PLLA and the star block copolymers (PMMA-*b*-PLLA)$_6$ and (PMMA-*b*-PLLA)$_{12}$. These results strongly indicated that all the obtained polymers consisted of a core unit derived from the initiator and a block made up of two types of chemically different polymer in each arm.

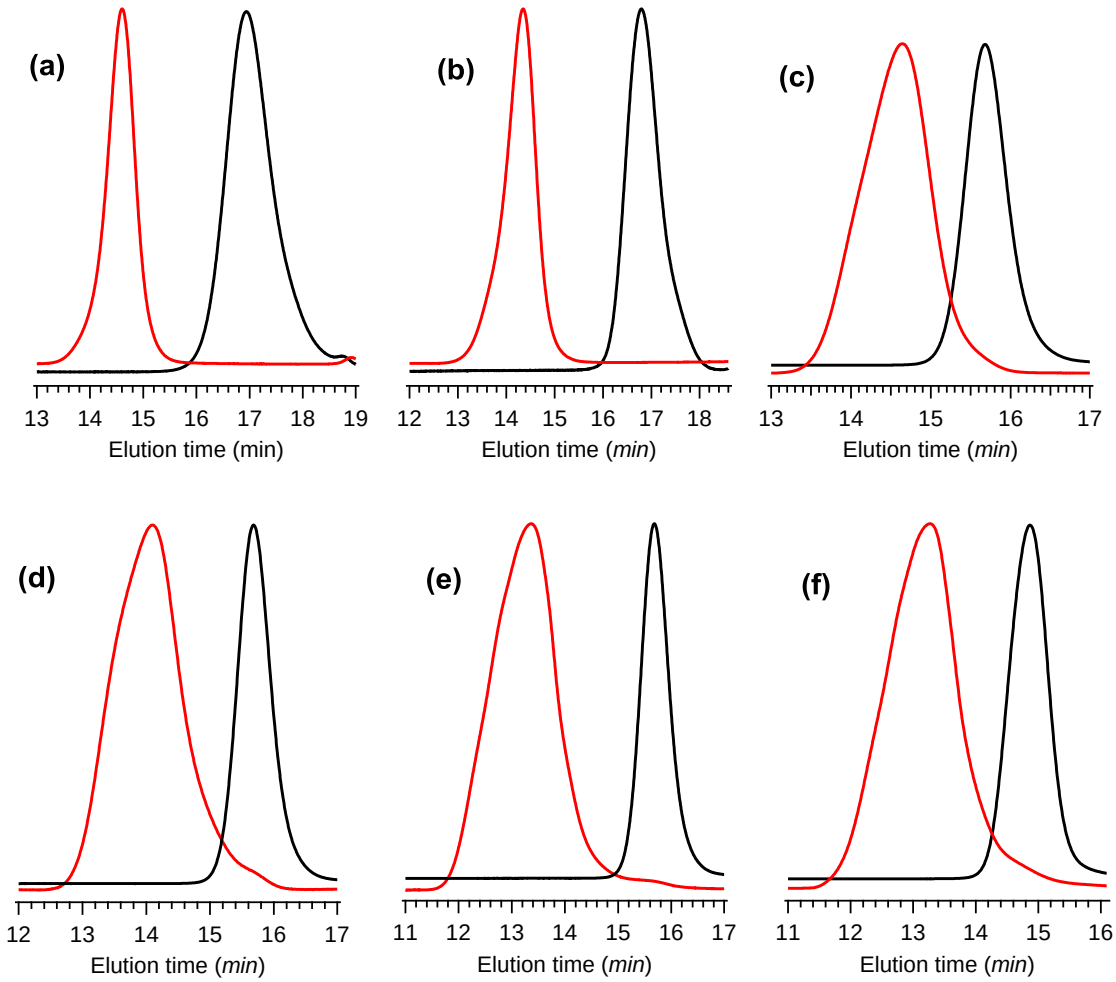

Figure 4.4 SEC traces of (a) $PMMA_{30}$-*b*-$PLLA_{30}$ (black line) and its precursor of $PMMA_{30}$-OH (red line), (b) $(PMMA_{30}$-*b*-$PLLA_{30})_3$ (black line) and its precursors of $(PMMA_{30}$-$OH)_3$ (red line), (c) $(PMMA_{30}$-*b*-$PLLA_{15})_6$ (black line) and its precursors of $(PMMA_{30}$-$OH)_6$ (red line), (d) $(PMMA_{30}$-*b*-$PLLA_{30})_6$ (black line) and its precursors of $(PMMA_{30}$-$OH)_6$ (red line), (e) $(PMMA_{30}$-*b*-$PLLA_{60})_6$ (black line) and its precursors of $(PMMA_{30}$-$OH)_6$ (red line) and (f) $(PMMA_{30}$-*b*-$PLLA_{30})_{12}$ (black line) and its precursors of $(PMMA_{30}$-$OH)_{12}$ (red line)

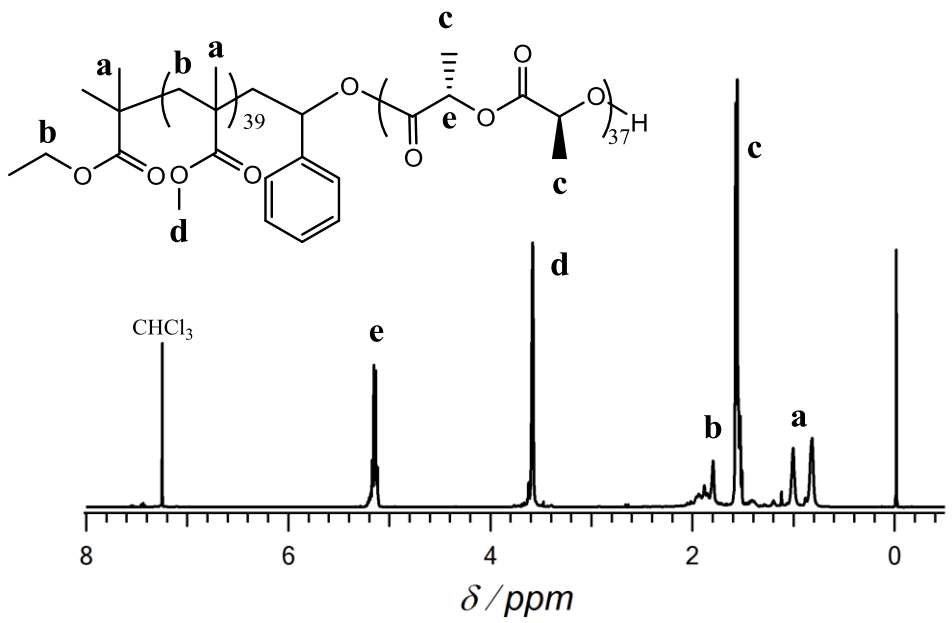

Figure 4.5 ^{1}H NMR spectrum of $PMMA_{39}$-*b*-$PLLA_{37}$ in $CDCl_3$ (400 MHz).

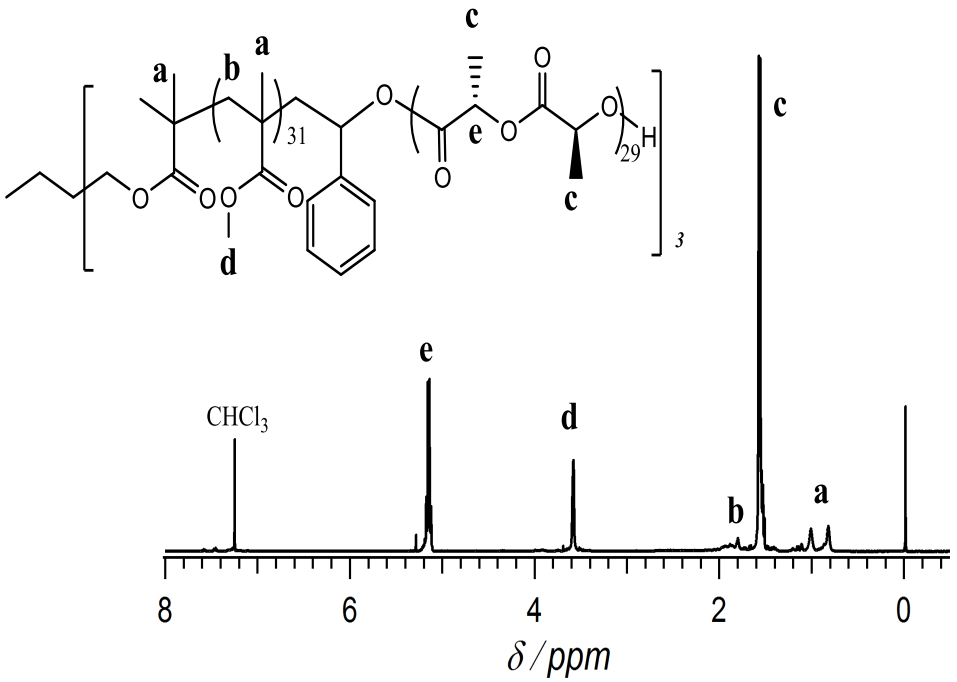

Figure 4.6 ^{1}H NMR spectrum of $(PMMA_{31}$-*b*-$PLLA_{29})_3$ in $CDCl_3$ (400 MHz).

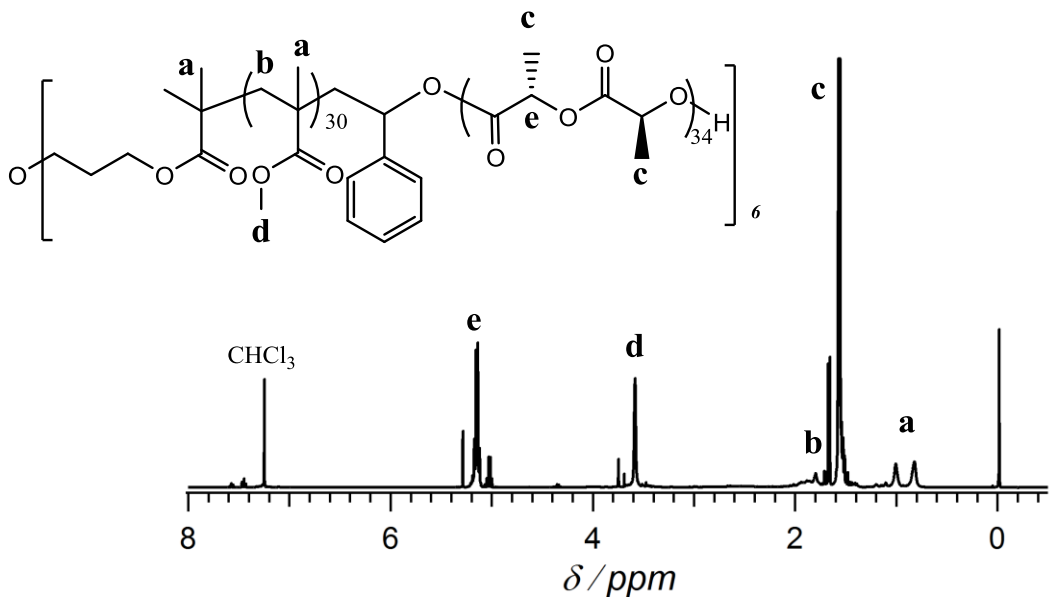

Figure 4.7 ^{1}H NMR spectrum of $(PMMA_{30}\text{-}b\text{-}PLLA_{34})_6$ in $CDCl_3$ (400 MHz).

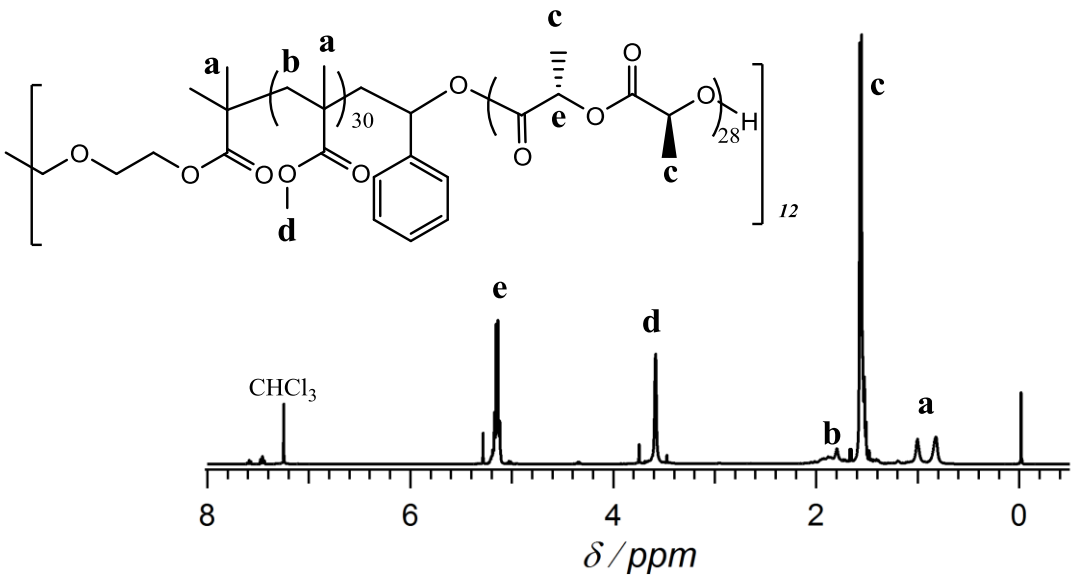

Figure 4.8 ^{1}H NMR spectrum of $(PMMA_{30}\text{-}b\text{-}PLLA_{30})_{12}$ in $CDCl_3$ (400 MHz).

4.3.3 Thermal properties of hydroxyl-functionalized PMMA macroinitiators and their block copolymers.

Table 4.3. Glass transition temperature analysis of linear and star block copolymers and their hydroxyl-functionalized linear and star PMMA precursors

Polymer	$M_{n,NMR}$ (kgmol^{-1})	T_g (°C)
$PMMA_{30}$-OH	3.9	67
$(PMMA_{30}\text{-}OH)_3$	9.2	87
Arm-first $(PMMA_{30})_3\text{-}OH_3$	10.2	93
$(PMMA_{30}\text{-}OH)_6$	17.8	104
$(PMMA_{30}\text{-}OH)_{12}$	39.3	114
$PMMA_{30}$-*b*-$PLLA_{30}$	9.2	49
$(PMMA_{30}\text{-}b\text{-}PLLA_{30})_3$	18.9	47
Miktoarm$(PMMA_{34})_3\text{-}(PLLA_{36})_3$	26.2	49
$(PMMA_{30}\text{-}b\text{-}PLLA_{30})_6$	38.5	51
$(PMMA_{30}\text{-}b\text{-}PLLA_{28})_{12}$	85.8	50

PMMA and PLLA exhibit different thermal properties and it is also a well-known fact that molecular weight has an effect on glass transition temperatures (T_g) of polymers [44-47] and the fact that in a previous work, [36] we reported that the number of arms also had an effect on the T_g of PMMA so we decided to investigate the thermal properties of hydroxyl functionalized star PMMAs and their subsequently produced star diblock copolymers by DSC. As shown in Table 4.3, the T_g observed for the hydroxyl-functionalized star-shaped PMMA showed that an increase in the number of arms which caused an increase in molecular weight prompted an increase in T_g. $(PMMA\text{-}OH)_3$, $(PMMA\text{-}OH)_6$ and $(PMMA\text{-}OH)_{12}$ had T_gs of 87, 104 and 114 °C, respectively. We compared the T_g of core-first synthesized $(PMMA\text{-}OH)_3$ and that of arm-first $PMMA_3\text{-}OH_3$ synthesized using

multi-aldehydic benzene-1,3,5-tricarbaldehyde to terminate PMMA.[20] The three arm hydroxyl-functionalized PMMA by the arm-first method $PMMA_3$-OH_3 ($M_{n,NMR}$ = 10.2 kg mol^{-1}) was found to have a higher T_g of 93 °C compared to the core-first synthesized $(PMMA\text{-}OH)_3$ ($M_{n,NMR}$ = 9.2 kg mol^{-1}) which had a T_g of 87 °C. The difference in T_g between these star PMMAs with the same number of arms may be due to the slightly higher molecular weight of the arm-first synthesized star PMMA and also due to the different end groups of the arm-first synthesized star PMMA and the core-first synthesized star PMMA. The arm-first synthesized 3-arm hydroxyl-functionalized PMMA has non-polar alkyl end groups whiles its core-first synthesized counterpart has polar hydroxyl end groups. This affects the free volumes of the two polymers causing them to have different T_gs.

For the thermal properties of the linear and star block copolymers, their T_gs reduced significantly in comparison with their hydroxyl-functionalized precursors with a different trend in terms of T_g`s relation to molecular weight. Only one T_g was observed for all the diblock copolymers. This may be due to the fact that the PMMA-*b*-PLLA diblock copolymers obtained are not phase separated since phase separated copolymers sometimes show to two T_gs. According the free volume theory; an increase in chain ends increases the free volume and thus lowers the T_g.[51] This was true of the observed T_gs of the PMMA-*b*-PLLA diblock copolymers as shown in Figure 4.11. The observed T_gs were between 47-51°C which implies the domination of the T_g of PLLA in the PMMA-*b*-PLLA diblock copolymers since the T_gs are close to the T_g of PLLA homopolymer with a small molecular weight. For the PMMA-*b*-PLLA diblock copolymers, the lowering of T_g due to the free volume effect is cancelled by the raising of T_g due to the molecular weight effect.

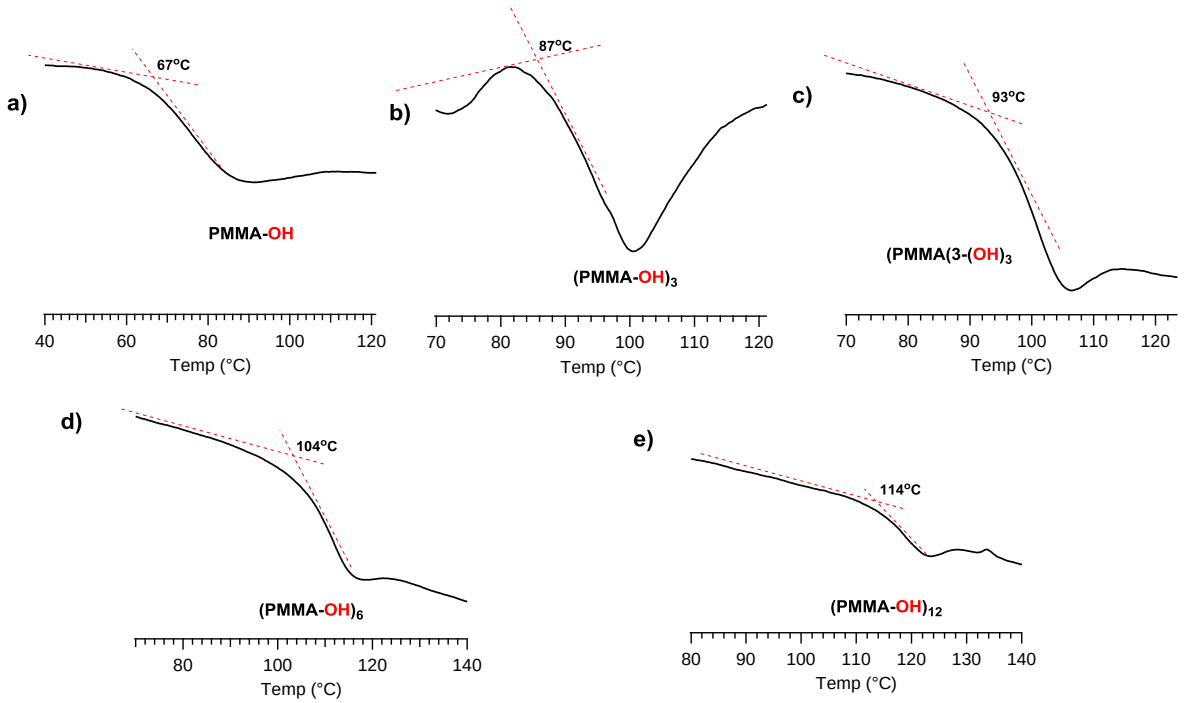

Figure 4.9 DSC thermograms of linear and star-shaped hydroxyl-functionalized PMMA

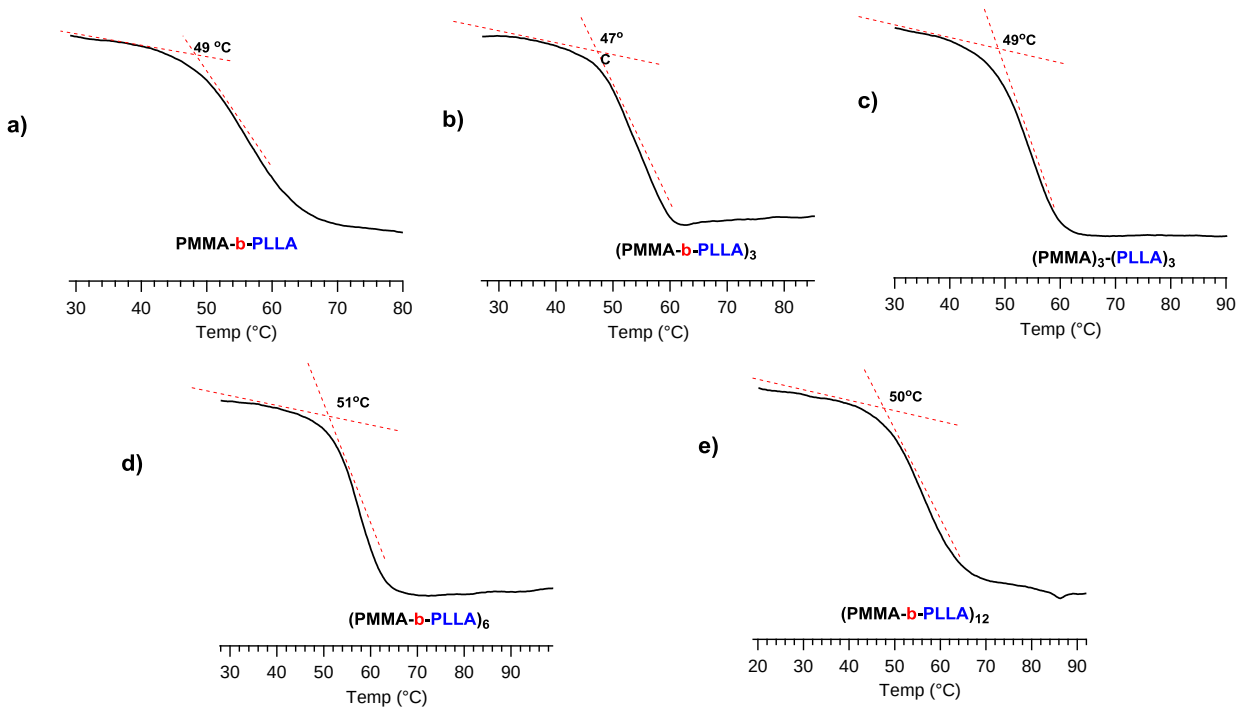

Figure 4.10 DSC thermograms of linear, star block copolymers and miktoarm star polymers.

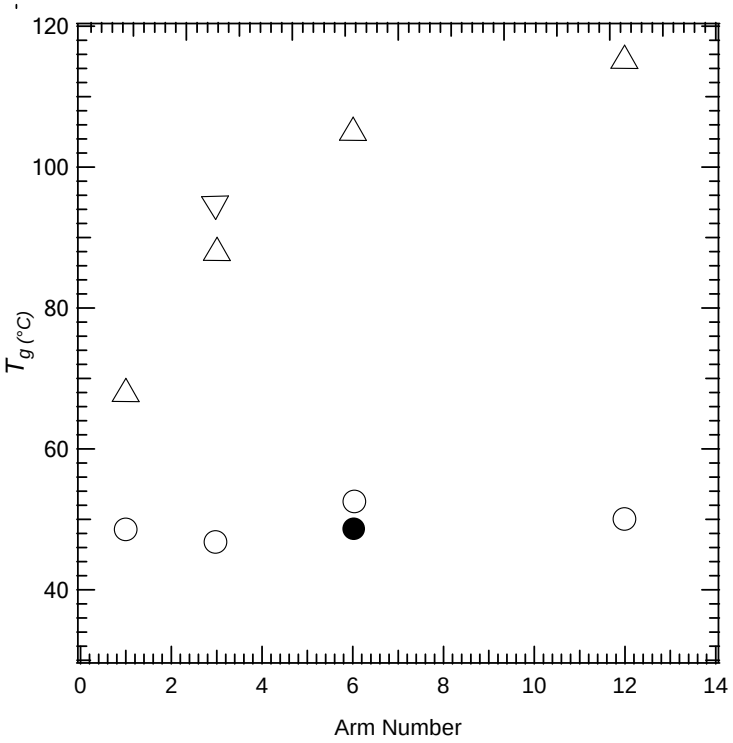

Figure 4.11 Relation between T_g versus arm numbers for core-first synthesized hydroxyl-functionalized PMMAs (Δ), arm-first synthesized hydroxyl-functionalized PMMA (∇), linear and star block copolymers (○) and miktoarm star polymer (●).

4.4 Conclusions

The preparation of the miktoarm star polymers was achieved using the multi-arm PMMAs functionalized with hydroxyl groups synthesized by organocatalyzed GTP the arm-first method as macroinitiators. The preparation of star block copolymers was also achieved using the multi-arm PMMAs functionalized with hydroxyl groups synthesized by organocatalyzed GTP the core-first method as macroinitiators. The author finally investigated and elucidated the thermal properties of the block copolymers prepared as well as that of their hydroxyl-functionalized precursors. The glass transition temperature (T_g) of the hydroxyl-functionalized PMMAs increased with increasing arm numbers (increasing MW) whiles the T_g of the block copolymers were did not show much changes with increasing molecular weight. The DSC thermograms showed only one T_g for the block copolymers implying no phase separation took place between the polymer blocks. The molecular weight effect was prominent in determining the T_gs of the hydroxyl-functionalized PMMAs whiles the free volume effect was dominant in determining the T_gs of the star block copolymers and miktoarm star polymers.

4.5 References

1. G. Gody, C. Rossner, J. Moraes, P. Vana, T. Maschmeyer and S. Perrier, *J. Am. Chem. Soc.*, **2012**, *134*, 12596-12603.
2. A. C. Balazs, T. Emrick and T. P. Russell, *Science* **2006**, *314*, 1107-1110.
3. C. B. Kowollik and A. Inglis, *J. Macromol. Chem. Phys*., **2009**, *210*, 987-992.
4. C. J. Hawker and K. L. Wooley, *Science* **2005**, *309*, 1200-1205.
5. G. Pasut and F. M. Veronese, *Prog. Polym. Sci.*, **2007**, *32*, 933-961.
6. B. Le. Droumaguet and J. Nicholas, *Polym. Chem.*, **2010**, *1*, 563-598.
7. M. Beija, J. D. Marty and M. Destarac, *Prog. Polym. Sci.*, **2011**, *36*, 845-886.
8. C. Boyer, M. H. Stenzel and T. P. Davis, *J. Polym. Sci., Part A: Polym. Chem.*, **2011,** *49*, 551-595.
9. A. O. Patil, D. N. Schulz and M. Novak, *Functional Polymers: Modern Synthetic Methods and Novel Structures*, ACS Symposium Series 704, American Chemical Society, Washington DC, **1998**
10. R. Gnaneshwar and S. Sivaram, *J. Polym. Sci., Part A: Polym. Chem.*, **2007**, *45*, 2514-2531.
11. K. Matyjaszewski and J. Xia, *Chem. Rev.* **2001**, *101*, 2921-2990.
12. V. Coessens, T. Pintauer and K. Matyjaszewski, *Prog. Polym. Sci.* **2001,** *26*, 337-377.
13. R. T. Mayadune, E. Rizzardo, J. Chiefari, Y. K. Chong, G. Moad and S. H. Thang, *Macromolecules* **1999**, *32*, 6977-6980.
14. A. Hirao, M. Hayashi, S. Loykulnant, K. Sugiyama, S. W. Ryu, N. Haraguchi, A. Matsuo and T. Higashihara, *Prog. Polym. Sci.*, **2005**, *30*, 111-182.

15. K. Y. Baek, M. Kamigaito and M. Sawamoto, *J. Polym. Sci.: Part A: Polym. Chem.*, **2002**, *40*, 1937-1944.

16. T. Mukaiyama, *Angew. Chem. Int. Ed.*, **2004**, *43*, 5590-5614.

17. D. Sogah, W. Hertler, O. Webster and G. Cohen, *Macromolecules* **1987**, *20*, 1473-1486

18. D. Sogah and O. Webster, *J. Polym. Sci. Polym. Lett. Ed.*, **1983**, *21*, 927-931.

19. M. T. Reetz, R. Ostarek, K. E. Piejko, D. Arlt and B. Bömer, *Angew. Chem. Int. Ed. Engl. Ed.*, **1986**, *25*, 1108-1109.

20. W. P. Shen, W. D. Zhu, M. F. Yang and L. Wang, *Makromol. Chem.*, **1989**, *190*, 3061-3066.

21. W. R. Hertler, *J. Polym. Sci., Part A: Polym. Chem.*, **1991**, *29*, 869-873.

22. R. Asami, Y. Kondo and M. Takaki, *ACS Polym. Prepr.*, **1986**, *27*, 186-187.

23. G. M. Cohen, *ACS Polym. Prepr.*, **1988**, *29*, 46.

24. W. R. Hertler, D. Y. Sogah and F. P. Boettcher, *Macromolecules* **1990**, *23*, 1264-1268.

25. O. Webster, W. R. Hertler, D. Y. Sogah, W. B. Farnham and T. V. RajanBabu, *J. Am. Chem. Soc.*, **1983**, *105*, 5706-5708.

26. R. Quirk and J. Ren, *Polym. Int.* **1993**, *32*, 205-212.

27. J. Raynaud, Y. Gnanou and D. Taton, *Macromolecules* **2009,** *42*, 5996-4000.

28. M. D. Sholten, J. L. Hedrick and R. M. Waymouth, *Macromolecules* **2008,** *41*, 7399-7404.

29. Y. Zhang, E. and Y.-X. Chen, *Macromolecules* **2008**, *41*, 36-42

30. Y.-G. Chen, K. Fuchise, A. Narumi, S. Kawaguchi, T. Satoh and T. Kakuchi, *Macromolecules* **2011**, *44*, 9091-9098.

31. Y.-G. Chen, K. Takada, K. Fuchise, T. Satoh, and T. Kakuchi, *J. Polym. Sci., Part A: Polym. Chem.,* **2012**, *50*, 3277-3285.

32. T. Kakuchi, Y.-G. Chen, J. Kitakado, K. Mori, K. Fuchise and T. Satoh, *Macromolecules* **2011**, *44*, 4641-4647.

33. K. Takada, K. Fuchise, Y.-G. Chen, T. Satoh, and T. Kakuchi, *J. Polym. Sci., Part A: Polym. Chem.,* **2012**, *50*, 3560-3566.

34. R. Kakuchi, K. Chiba, K. Fuchise, R. Sakai, T. Satoh, and T. Kakuchi, *Macromolecules* **2009**, *42*, 8747-8750.

35. Y.-G. Chen, K. Takada, N. Kubota, O. T. Eric, T. Ito, T. Isono, T. Satoh, and T. Kakuchi, *Polym. Chem.* **2015**, *5*, **1830-1837**.

36. K. Takada, K. Fuchise, N. Kubota, T. Ito, Y.-G. Chen, T. Satoh, and T. Kakuchi, *Macromolecules* **2014**, *47*, **5514-5525**.

37. M. K. Mishra and S. Kobayashi, Eds. Star and hyperbranched polymers; Marcel Dekker, Inc.: New York and Basel, 1999.

38. A. Blencowe, J. F. Tan, T. K. Goh and G. G. Qiao, *Polymer* **2009**, *50*, 5−32.

39. N. Hadjichristidis, M. Pitsikalis, S. Pispas and H. Iatrou, *Chem. Rev.* **2001**, *101*, 3747−3792.

40. K. Inoue, *Prog. Polym. Sci.* **2000**, *25*, 453−571.

41. L. A. Connal, P. A. Gurr, G. G. Qiao and D. H. Solomon, *J. Mater. Chem.* **2005**, *15*, 1286−1292.

42. G. Kreutzer, C. Ternat, T. Q. Nguyen, C. J. Plummer, J.-A. E. Manson, V. Castelletto, I. W. Hamley, F. Sun, S. S. Sheiko and A. Herrmann, *Macromolecules*, **2006**, *39*, 4507−4516.

43. J. M. Ren, T. G. McKenzie, Q. Fu, E. H. H. Wong, J. Xu, Z. An, S. Shanmugam, T. P. Davis, C. Boyer and G. G. Qiao, *Chem. Rev*. **2016**, *116*, 6743−6836.

44. C. Zhang, X. Wang, K. Min, D. Lee, C. Wei, H. Schulhauser and H. Gao, *Macromol. Rapid Commun.* **2014**, *35*, 221−227

45. F. Wang, T. K. Bronich, A. V. Kabanov, R. D. Rauh and J. Roovers, *Bioconjugate Chem.* **2005**, *16*, 397−405.

46. Y. Deng, S. Zhang, G. Lu and X. Huang, *Polym. Chem.* **2013**, *4*, 1289−1299.

47. H. Gao, *Macromol. Rapid Commun.* **2012**, ***33***, 722−734.

48. T. Ooya, J. Lee and K. Park, *J. Controlled Release*, **2003,** *93*, 121−127.

49. T. Mukaiyama, *Angew. Chem. Int. Ed.* **2004**, *43*, 5590-5614

50. T. Isono, Y. Kondo, I. Otsuka, Y. Nishiyama, R. Borsali, T. Kakuchi and T. Satoh, *Macromolecules* **2013**, *46*, 8509-8518.

51. Md. D. Hossain, D. Lu, Z. Jia, and M. J. Monteiro, *ACS Macro Lett.* **2014**, *3*, 1254−1257

Chapter 5

Conclusions

In this thesis, the author described the *Organocatalyzed Synthesis of End-functional Poly(methacrylate)s using Group Transfer Polymerization.* Throughout the study, the author has been conscious of the metal-free concept and devoted his efforts to developing environment-friendly organocatalysts for polymer synthesis all the time. The study affords important achievements mainly in three areas as follows:

1. The organocatalyzed GTP of defect-free α- and ω-end-functionalized Poly (methyl methacrylate) has been established for the first time. The α-end functionalization of PMMA was achieved using functional initiators and ω-end functionalization of PMMA catalyzed by the low nucleophilic strong organic Lewis acid (Me_3SiNTf_2) and phosphazene base (*t*-BuP_4) catalysts respectively. These metal-free catalysts showed high catalytic activity to produce quantitative end-functionalization of PMMA and also the advantages to avoid side reactions that have been usually observed in previous attempts to synthesize end-functionalized PMMAs using conventional metal catalysts.
2. The author established a simple core-first phosphazene base-catalyzed GTP method for the synthesis of hydroxyl-functionalized star-shaped poly (methyl methacrylate)s that possess a controlled molecular weight, narrow molecular weight distribution, and quantitative hydroxyl-functionalization. A simple arm-first method for the synthesis of hydroxyl-functionalized star-shaped PMMAs by phosphazene base-catalyzed GTP was also established. To the best of the author's knowledge, this is the first study to achieve the perfect synthesis of hydroxyl-functionalized star-shaped PMMAs.

3. The applicability of the obtained hydroxyl-functionalized star-shaped PMMAs was demonstrated by successfully using them as precursors for the synthesis of star block copolymers and miktoarm star polymers. To serve as further proof of the successful synthesis of hydroxyl-functionalized star-shaped PMMAs, the hydroxyl groups were used to initiate the ROP of lactide monomers to synthesize star block copolymers and miktoarm star polymers.
4. The thermal properties of the polymers synthesized in this thesis were elucidated through their glass transition temperatures (T_gs)

In conclusion, the original work in this thesis is expected to provide a new methodology in polymer functionalization, synthesis of complicated polymer architectures and to produce metal-free advanced materials.

A summary of this thesis is as follows:

Chapter 2 "Establish a Synthesis Method for Defect-free α and ω-end-functionalized PMMAs"

α-end-functionalized PMMAs with hydroxyl, ethynyl, vinyl, and norbornenyl groups were obtained with targeted molar masses, narrow dispersities and defect-free polymer structures by either Me_3SiNTf_2 or *t*-Bu-P_4-catalyzed GTPs using newly designed functional SKAs as initiators. In addition, quantitative ω-end-functionalization of PMMA by the Me_3SiNTf_2-catalyzed GTP succeeded for the first time using α-phenylacrylate terminators. The quantitative incorporation of ethynyl, hydroxyl, vinyl, norbornenyl, and bromo functionalities into either the α- or ω-end of PMMA was significantly supported by the MALDI-TOF MS measurements. The author described the precise synthesis of PMMAs functionalized with a hydroxyl group by *t*-Bu-P_4-catalyzed GTP using aromatic

aldehydes as terminators. The termination reaction between a living PMMA and benzaldehyde was proved to be an efficient system for synthesizing ω-end-functionalized PMMAs with the hydroxyl group with controlled molar masses, relatively narrow polydispersities, and quantitative ω-end functionalization efficiencies. This study provides a facile method for end-functionalization by the organocatalyzed GTP procedure. These reactive functionalities at the polymer ends are of great significance for carrying out further chemical conversions into other functional moieties, such as bioactive peptides and fluorescent dyes, and to serve as polymeric precursors for constructing polymethacrylate-based complicated polymer architectures, such as block copolymers, star-shaped polymers, and graft copolymers.

Chapter 3 "Establish a Synthesis Method for Defect-free Hydroxyl-functionalized Star-shaped PMMAs"

The author then described the precise synthesis of star-shaped PMMAs functionalized with hydroxyl groups by *t*-Bu-P_4-catalyzed GTP via the core-first method using multifunctional SKA initiators as the core and benzaldehyde as the terminators. The termination reaction between the living star PMMA chain ends and benzaldehyde was proved to be an effective method for synthesizing hydroxyl-functionalized PMMAs with controlled molar masses and quantitative hydroxyl group functionalities. The arm-first method for the synthesis of two- and three-arm PMMAs with hydroxyl groups existing in the core was also established. This is the first report about this kind of synthesis in GTP chemistry to the best of the knowledge of the author.

Chapter 4 "Demonstrate the Usefulness of the Hydroxyl-functionalized Star-shaped PMMAs to Synthesize Miktoarm Star Polymers and Star Block Copolymers"

Finally, the preparation of the miktoarm star copolymers was achieved using the multi-arm PMMAs functionalized with hydroxyl groups synthesized by organocatalyzed GTP the arm-first method as macroinitiators. The preparation of star block copolymers was also achieved using the multi-arm PMMAs functionalized with hydroxyl groups synthesized by organocatalyzed GTP via the core-first method as macroinitiators. The author also investigated and elucidated the thermal properties of the block copolymers obtained as well as that of their hydroxyl-functionalized precursors. It was discovered that T_gs of the block copolymers were much lower than that of their hydroxyl-functionalized precursors, much closer to the T_g of a small molecular weight PLLA homopolymer and no phase separation occurred at their glass transition temperature. The main determining factor for their T_gs was the free volumes. For the precursors their T_gs increased with their molecular weight and their arm numbers.

In conclusion, the author has successfully established the organocatalyzed GTP methodology for the end-functionalization of Poly (methyl methacrylate)s using low nucleophilic superbase (*t*-Bu-P_4) and a strong Lewis acid (Me_3SiNTf_2). The *t*-Bu-P_4-catalyzed GTPs was used to synthesize hydroxyl-functionalized star-shaped poly (methyl methacrylate)s with quantitative hydroxyl-functionalization. The applicability of the obtained hydroxyl-functionalized star-shaped PMMAs was demonstrated by successfully using them as precursors for the synthesis of star block copolymers and miktoarm star polymers.

The achievements mentioned in this thesis are expected to further explore the perspective for the synthesis of well-controlled polymers with complicated structures and to afford a fresh concept for organocatalyzed polymerization methodologies in polymer synthesis. The metal-free concept for the synthesis of polymers in this thesis is also expected to contribute to an environment-friendly society by the author.